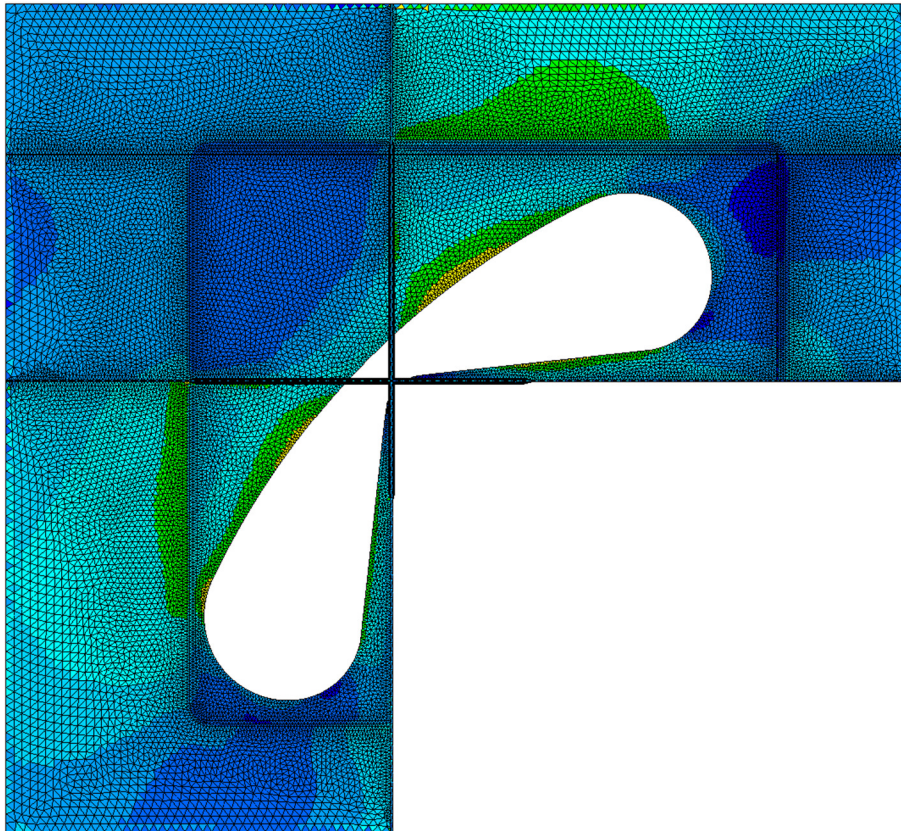


CHALMERS



Structural analysis of node cut-outs in a semi-submersible offshore platform

Master's Thesis in the International Master's Programme Naval Architecture and Ocean Engineering

DANIEL KARLSSON AND MÅRTEN FORSER

Department of Shipping and Marine Technology
Division of Marine Technology
CHALMERS UNIVERSITY OF TECHNOLOGY
Gothenburg, Sweden 2015
Master's thesis 2015:X-15/337

MASTER'S THESIS IN THE INTERNATIONAL MASTER'S PROGRAMME IN
NAVAL ARCHITECTURE AND OCEAN ENGINEERING

Structural analysis of node cut-outs in a semi-
submersible offshore platform

DANIEL KARLSSON AND MÅRTEN FORSER

Department of Shipping and Marine Technology
Division of Marine Technology
CHALMERS UNIVERSITY OF TECHNOLOGY
Gothenburg, Sweden 2015

Structural analysis of node cut-outs in a semi-submersible offshore platform
DANIEL KARLSSON AND MÅRTEN FORSER

© DANIEL KARLSSON AND MÅRTEN FORSER, 2015

Master's Thesis 2015:X-15/337
ISSN 1652-8557
Department of Shipping and Marine Technology
Division of Marine Technology
Chalmers University of Technology
SE-412 96 Gothenburg
Sweden
Telephone: + 46 (0)31-772 1000

Cover:
Node cut-out geometry analysed for yield stresses.

Chalmers Reproservice
Gothenburg, Sweden 2015

Structural analysis of node cut-outs in a semi-submersible offshore platform
Master's Thesis in the International Master's Programme in Naval Architecture and
Ocean Engineering
DANIEL KARLSSON AND MÅRTEN FORSER
Department of Shipping and Marine Technology
Division of Marine
Chalmers University of Technology

ABSTRACT

The connection between column and deck-box on a semi-submersible platform is often subjected to high stress concentrations that can be governing for the structural strength. One common design used to withstand the high stresses is a cast integral in high tensile material, which is both heavy and expensive to manufacture, which is why an alternative cut-out design is investigated. This thesis aims at analysing the current node connection, with a finite element analysis (FEA), with regard to yield stresses, buckling, fatigue damage, weight and cost in order to propose an alternative cut-out design using the same criteria. The cast integral, which is analysed as a reference case and used for comparison of designs, is of a typical design used by GVA Consultants AB.

The alternative cut-out design is first studied in a simplified two-dimensional (2D) case, developed with applied loads and boundary conditions following recommendations from the classification society DNV-GL. Different geometrical cut-out shapes used in other applications are tested and evaluated. The cut-out design with the lowest yield stresses is implemented and further evaluated in a case study of a complete semi-submersible production platform. The cut-out design is investigated with a parametric study for the complete loading condition, which is defined from previous calculations performed by GVA. The cut-out is analysed with both the simplified fatigue assessment and with a stochastic approach, in order to investigate differences and inaccuracies in the methods.

The parametric study shows that the use of a cut-out design may be advantageous in the centre bulkhead connection between the column and the deck-box. The adjacent geometry is of simple character and the cut-out does not affect the overall structural design. The cut-out is found to be a feasible alternative to the cast integral, with yield stresses and fatigue damage in the same range. Further refinements of the cut-out design could, however, decrease both yield stresses and fatigue damage, which is why the cut-out is recommended in future work.

The suggested cut-out solution leads to a decrease of 4.5 % in weight for a reference structure. For the same reference structure the production cost is estimated to decrease by 9.5 %, hence, the cut-out design is recommended for the centre bulkhead connection. However, it is concluded that the cut-out design is only developed for one specific semi-submersible platform in specific load conditions, for which reason further analysis and adjustments are needed for other applications and structures.

Key words: butterfly cut-out, cast integral, cut-out, node, semi-submersible, stress concentration, stress redistribution, stress relief.

Strukturell inverkan av en utskärning i en "semi-submersible" oljeplattform
Examensarbete inom Naval Architecture and Ocean Engineering
DANIEL KARLSSON AND MÅRTEN FORSER
Institutionen för Sjöfart och marin teknik
Avdelningen för Marin teknik
Chalmers tekniska högskola

SAMMANFATTNING

En "semi-submersible" oljeplattform utsätts för extrema laster och anslutningen mellan däckslåda och kolumn är ett känsligt område för både flytspänningar och utmattning. De höga spänningskoncentrationer som uppstår där kan ofta vara dimensionerande för hela strukturen. En vanligt förekommande design i dessa höga spänningsområden är ett gjutstycke i höghållfasthets stål. Detta gjutstycke är ofta dyrt att tillverka och montera, samt har en hög vikt, vilket påverkar den lastbärande kapaciteten och därmed också effektiviteten av plattformen. En alternativ design med en utskärning är därför analyserad och utvärderad i detta arbete. En jämförelse mellan gjutstycke och den presenterade utskärningen med avseende på flytspänningar, buckling, utmattning, vikt och kostnad är genomförd med hjälp av en finit element analys. Det analyserade gjutstycket är en typisk design som används av GVA Consultants AB.

Den alternativa utskärningen undersöks först i ett förenklat tvådimensionellt fall, med laster och randvillkor rekommenderade av klassällskapet DNV-GL. Olika designer som bland annat används i andra applikationer undersöks och utvärderas. Den design med lägst flytspänningar utvärderas vidare genom att implementeras i strukturen på en given oljeplattform designad av GVA. Designen på utskärningen utvärderas med verkliga lastfall i ULS/FLS och ytterligare förbättringar av designen undersöks. Utskärningen analyseras också med avseende på utmattning med både en förenklad och en stokastisk utmattningsanalys för att verifiera resultaten av den förenklade analysen.

Analysen visar att implementering av en utskärning i det mittersta skottet mellan kolumn och däckslåda kan vara fördelaktig. Den enkla geometrin gör det möjligt att använda en utskärning vilken kan förbättra strukturen i avseende på både flytspänningar och utmattning. Nivån på både flytspänningar och ackumulerad utmattningsskada är lika för de båda lösningarna, men ytterligare förbättringar av utskärningen kan minska både spänningsnivå och utmattningsskada. Utskärningen är således den rekommenderade designen för framtida implementering.

Den alternativa lösningen sänker vikten med 4.5 % jämfört med gjutstycket för vald referensstruktur samt sänker tillverkningskostnaden med 9.5 %. Utskärningen är dock endast utvecklad och utvärderad för den specifika oljeplattformen och med specifika laster. Därmed behövs en vidare analys och justeringar för att säkerställa funktion samt applicerbarhet även i andra strukturer och andra oljeplattformar.

Nyckelord: gjutstycke, oljeplattform, spänningsreduktion, spänningskoncentration, spänningsfördelning, utmattning, utskärning.

Contents

ABSTRACT	I
SAMMANFATTNING	II
CONTENTS	III
PREFACE	V
NOTATIONS AND ABBREVIATIONS	VII
1 INTRODUCTION	1
1.1 Objective	3
1.2 Methodology	3
1.3 Limitations	5
1.3.1 Normalisation of calculated stresses	6
1.4 Thesis outline	6
2 DESIGN CRITERIA AND ASSESSMENT	7
2.1 Loads and boundary conditions	8
2.2 The Ultimate Limit State design criterion	11
2.2.1 The Working Stress Design (WSD) method	12
2.2.2 Buckling analysis	13
2.3 The Fatigue Limit State design criterion	17
2.3.1 Scaling of allowable stress range	18
2.3.2 The hot spot method	18
2.3.3 Thickness effect	20
2.3.4 Simplified fatigue assessment	20
2.3.5 Stochastic fatigue analysis	22
3 ANALYSIS OF REFERENCE CASE - A CAST INTEGRAL	23
3.1 Geometry and mesh	24
3.2 ULS assessment	27
3.2.1 Yield criterion	27
3.2.2 Buckling analysis	29
3.3 FLS assessment	29
4 INVESTIGATION OF POSSIBLE CUT-OUT DESIGNS	33
4.1 Consequences following a cut-out design	33
4.2 Parametric study of a 2D geometry	34

5	ANALYSIS AND ASSESSMENT OF A CUT-OUT DESIGN	39
5.1	Geometry and mesh	39
5.2	Parametric study of the cut-out geometry	42
5.3	ULS assessment	45
5.3.1	Yield criterion	45
5.3.2	Buckling analysis	47
5.4	FLS assessment	48
6	DESIGN COMPARISON	52
6.1	Concept evaluation	52
6.2	Cost and weight analysis	52
7	DISCUSSION	56
8	CONCLUSIONS	58
9	FUTURE WORK	59
10	REFERENCES	61
	APPENDIX A - SUB-MODELLING AND COMPUTER SOFTWARE	A1
	APPENDIX B - CUT-OUT DESIGN	B1

Preface

This thesis is a part of the requirements for the master's degree in Naval Architecture and Ocean Engineering at Chalmers University of Technology, Gothenburg, and has been carried out at the structural analysis department at GVA Consultants AB, Gothenburg, between January and June of 2015. The work has been supervised by the Division of Marine Technology, Department of Shipping and Marine Technology, Chalmers University of Technology, Gothenburg.

We would like to acknowledge and thank our examiner and supervisor, Professor Jonas Ringsberg at the Department of Shipping and Marine Technology, for his excellent guidance and support throughout the work of this thesis. His efforts and ability to find time in a busy schedule made possible the carrying out of this thesis.

This project has been carried out in cooperation with GVA in Gothenburg. At first we would like to sincerely thank our supervisor Erik Olsson for providing time and knowledge for guidance and consultation throughout the work. Without Erik's continuous supervision and efforts for our understanding and learning it would have been impossible to accomplish this work. We would like to thank Kjell Vågfelt for the opportunity to write this thesis at GVA. We would also like to acknowledge all the engineers at GVA for their guidance and time for answering our many questions.

Finally, it should be noted that the stress plots and data presented in this thesis, due to confidentiality, are normalised (see Section 1.3.1 for clarification) and therefore only show the relationship between the investigated cast integral and the proposed cut-out design. It should also be noted that references made to GVA reports are subject of confidentiality and inquiries about these reports can be placed to the GVA headquarters in Gothenburg.

Gothenburg, June 2015

Daniel Karlsson and Mårten Forser

Notations and abbreviations

C_C	Total manufacturing cost, [USD]
C_L	Labour cost per hour, [USD/hour]
C_M	Material cost, [USD/ton]
D	Cumulative damage, Palmgren-Miner
E	Young's modulus, [GPa]
H_T	Man-hour per ton, [hour/ton]
L_{design}	Required fatigue life, [year]
N_0	Number of cycles
N_{30}	Number of cycles for 30-years
N_{100}	Number of cycles for 100-years
SCF	Stress concentration factor
R	Cut-out radius, [mm]
S_i	Stress 38 mm inside the cast measured from the surface
S_0	Hot spot stress on the surface
S_1	Stress range for the breakingpoint of the two curves in the S-N curve
W_S	Weight structural steel, [ton]
a	Length of plate, [mm]
b	Width of plate, [mm]
c_i	Interaction factor
m	Number of buckled half-waves in longitudinal direction
n	Number of half-waves in transverse direction
q	Weibull scale parameter
h	Weibull shape parameter
r	Ratio of minimum stress divided by maximum stress
k	Plate buckling factor
k_t	Thickness exponent
k_∞	Initial plate buckling factor for combined axial and shear force
t	Plate thickness, [mm]
t_e	Effective thickness, [mm]
t_{actual}	Thickness at the weld toe, [mm]

Γ	Complementary incomplete gamma function
$\Delta\sigma$	Maximum stress range in the number of cycles
β	Coefficient depending on structure, failure mode and slenderness
β_{aspect}	Aspect ratio for buckling, a/b
γ	Incomplete gamma function
η_p	Maximum permissible usage factor
η_0	Basic usage factor
ν	Poisson's number
ρ_s	Steel density, [kg/m ³]
σ_c	Critical stress, [MPa]
$\sigma_{c,corr}$	Johnson-Ostenfeld correction
$\sigma_{MvonMises}$	Membrane von Mises stress, [MPa]
σ_{nom}	Stress for a specific area, [MPa]
σ_p	Permissible stress
$\sigma_{vonMises}$	von Mises stress, [MPa]
$\sigma_{x,Rd}$	Design resistance in longitudinal compression stress, [MPa]
σ_y	Yield stress of the material, [MPa]
$\sigma_{y,Rd}$	Design resistance in transverse compression stress, [MPa]
τ	Shear stress, [MPa]
τ_{Rd}	Design resistance shear stress, [MPa]
DFF	Design fatigue factor
DNV	DET NORSKE VERITAS
DNV-GL	DET NORSKE VERITAS – Germanischer Lloyd
FEA	Finite element analysis
FEM	Finite element method
FLS	Fatigue Limit State
GVA	GVA Consultants AB
LRFD	Load and Resistance Factor Design
SCF	Stress concentration factor
ULS	Ultimate Limit State
WSD	Working Stress Design
2D	Two-dimensional
3D	Three-dimensional

1 Introduction

The offshore exploration market is today growing at a fast pace as a consequence of the diminishing resources onshore (Sandler Research, 2015). With the increased offshore production follow increasing depths and harsh environments, putting high demands on the constructed structures for this field of interest. One of the most used structures is the semi-submersible platform which consists of a deck connected via columns (vertical legs) to horizontal pontoons, see Figure 1.1. The columns have the purpose of providing the structure with floatation and stability when the hull is partly submerged during operation, see Figure 1.2. The columns also provide a decreased water-plane area and a better stability for the structure. The semi-submersible platform is often used for water depths exceeding 600 m, called deep-water operations (Chakrabarti, 2005).

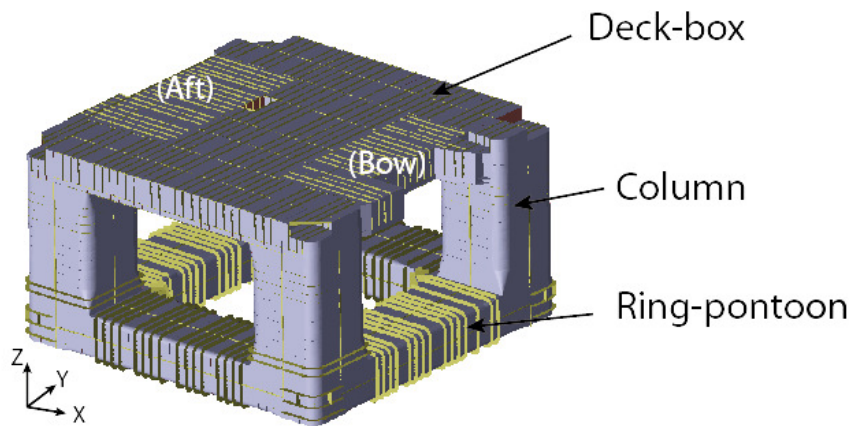


Figure 1.1 Schematic drawing of a semi-submersible production platform.

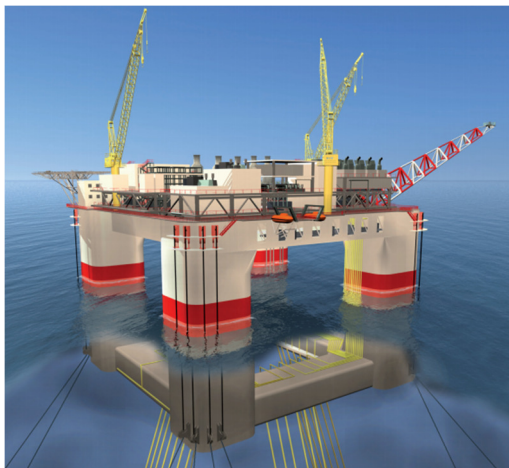


Figure 1.2 GVA 33000 semi-submersible production unit in a submerged condition.

Some of the most sensitive areas for high stresses and fatigue damage are the connections between columns/deck-box and columns/pontoons, see Figure 1.3 (Zhang et al., 2009). The environmental loads acting on the columns and pontoons are in these connections transferred to the deck-box. In a similar way, loads applied on the deck-box, such as equipment, machinery, living quarters, etc., are transferred to the column and pontoon via the connection, resulting in high stress and strain concentrations.

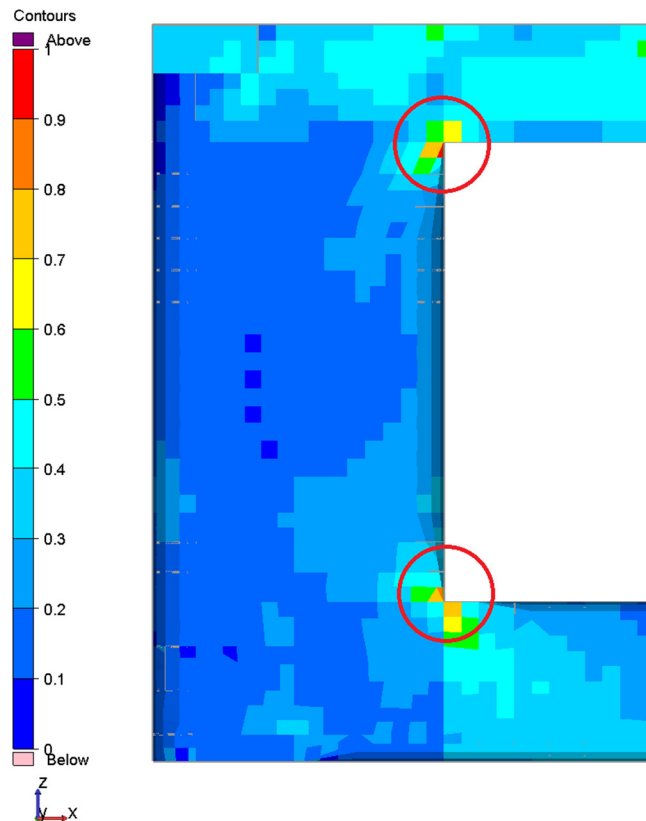


Figure 1.3 Contour plot of the major von Mises stress in the column/deck-box/pontoon intersection; sideview of Figure 1.1. Note that the stress values have been normalised according to the principle presented in Section 1.3.1.

High stress/strain concentrations are in common structures mitigated using a design to stiffen and increase the structural strength of the connection. One commonly used design is the cast integral made of high tensile steel material, see Figure 1.4.

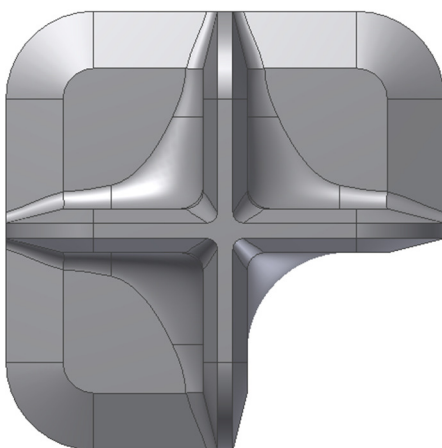


Figure 1.4 Side view of a commonly used cast integral in semi-submersibles.

Furthermore, the complexity of the design, weight, manufacturing and cost of the cast integrals are factors taken into consideration in the making of semi-submersibles. Hence, a study and comparison of alternative connection types can be useful from a

structural point of view as well as an economic one (Zhang et al., 2010). Weight reduction of the structure is considered a governing parameter, resulting in a higher load carrying capacity and an increase in efficiency of the semi-submersible, and is therefore also the subject of investigation.

A possible alternative to the commonly used cast integral is a cut-out design in the connecting plates to decrease the stiffness of the structure and therefore redistribute the stresses and lower the stress concentrations. The cut-out methodology is commonly used in other applications and can also be used for a semi-submersible, but a comparison between the cast integral and cut-out design appears to be lacking.

1.1 Objective

The objective of this thesis is to propose and assess feasible alternative cut-out designs instead of the current cast integral design in the connection between the column and deck-box of a GVA-designed semi-submersible platform. The suggested cut-out design shall only introduce local change to the structure in order to maintain the overall strength of the semi-submersible. The assessment criteria for comparison of the designs are yield stresses and fatigue damage together with weight and cost comparisons.

The tasks and aims of this thesis can be summarized as follows.

- Analyse an existing reference design of a cast integral with regard to safety against yielding, fulfilment of design criterion for fatigue life, weight and cost analyses.
- Investigate an alternative solution using a node cut-out in the centre bulkhead connection between column and deck-box. Analysis of structural stability, yield stresses and critical fatigue damage with only local structural changes.
- Compare the suggested designs and evaluate yield stresses and fatigue damage in the Ultimate Limit State (ULS) and Fatigue Limit State (FLS).
- Compare cost and weight of the alternative cut-out design and cast integral and suggest the most promising solution for future implementations.

1.2 Methodology

The aim of this thesis is the comparison between the cast integral and cut-out design in the connection between column and deck-box. The geometry chosen for investigation is the centre bulkhead connection, which is often subjected to high stresses and fatigue damage (DNV, 2012). The different loads acting on a semi-submersible, see Section 2.1, and different assessment criteria are first investigated in a literature study.

In order to evaluate the connection between column and deck-box with regards to different designs, the method of work is iterative. The analysis procedure is presented in Figure 1.5. A structural model of a semi-submersible with applied loads is obtained from previous GVA calculations and used for a case study. The model and loads are used in the investigation of both the cast integral and the alternative cut-out design. The load analysis together with the structural global finite element model (FE-model) of the semi-submersible is created by GVA and the investigated designs are applied in local sub-models of the specific node connection. The same global model, which creates boundary conditions for the local design, is used for both the cast integral and the cut-out design.

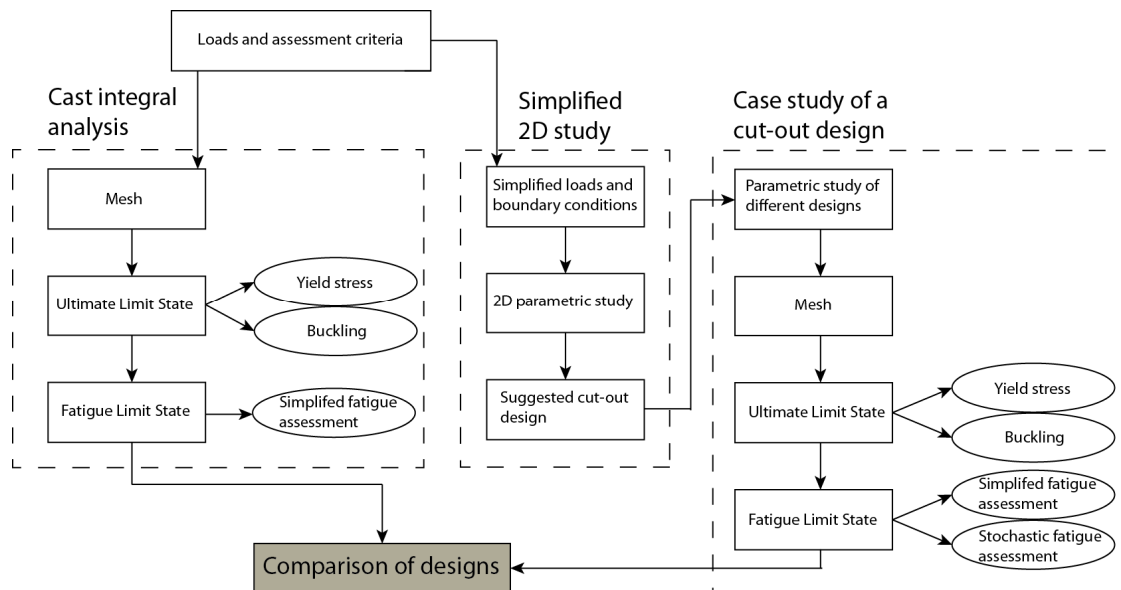


Figure 1.5 Analysis procedure used in the thesis.

The cast integral is investigated for yield stresses and fatigue damage using the von Mises equivalent stress criterion and the simplified fatigue assessment. The buckling criterion is considered with a simplified method. Yield stresses in the adjacent inner corner of the column are also investigated to verify the local influence of the cut-out.

The same design criteria and methods used for the cast integral are used in a simplified two-dimensional (2D) parametric study of different cut-outs. The cut-outs are based on two previously used designs in semi-submersibles and simple geometric cut-outs used in other applications. The 2D analysis is conducted to understand the relationship between load, cut-out design and response (Nygård, 2003). The simplified loading conditions are based on the recommendations from DNV-GL for semi-submersible platforms.

The cut-out design with the lowest yield stress from the 2D analysis is implemented in the complete structure to be verified. The design is modified with a parametric study to suit the different geometry in the three-dimensional (3D) case. The cut-out is first evaluated and designed against the von Mises equivalent stress and subsequently analysed for fatigue damage using both the simplified method suggested by DNV-GL and the stochastic approach using DNV Stofat. This is done to verify the validity of the simplified fatigue assessment provided by classification societies. The design is also controlled against buckling using a simplified buckling analysis.

The yield stresses in the neighbouring corner are calculated for comparison with the unmodified structure and for understanding the global influence of the introduced cut-out. The cut-out design is evaluated in the same loading condition as the cast integral in order to verify the structural strength and ensure a correct comparison. All objectives, analysis and methods follow the recommendations and rules in accordance with DNV-GL.

The final step in this thesis compares the two different designs with regard to yield stresses and fatigue damage. The total construction cost is estimated for the different designs, as well as the weight of the structure, which results in a recommendation for the choice of geometry for the centre bulkhead connection.

The loads are applied to the existing structural “global” FE-model designed with shell elements and created in the software program suite DNV SESAM. The model represents the complete structure and stresses are calculated with the linear finite element solver DNV Sestra (V.8.4-1) (DNV, 2010a). The area of interest is considered in smaller, more detailed “sub-models” created in DNV GeniE (V.6.6.8) (DNV, 2011a) and in Autodesk Inventor 2015. The loads are transferred to the sub-models through nodal displacements of the boundaries with the use of prescribed boundary conditions in DNV Submod (V.8.3) (DNV, 2004). The resulting stress responses are visualised in the post-processor DNV Xtract (V.4.2-02) (DNV, 2011b).

1.3 Limitations

The hydrodynamic analysis is not in the scope of the thesis, but taken from previous GVA analyses of the semi-submersible. All loads acting on the structure are applied on the global model which is also provided by GVA. The work is therefore limited to the creation of local sub-models and solid-models of specific parts of interest which are investigated and evaluated using ULS and FLS assessments.

The aim of the thesis is to find an alternative solution to the cast integral with a cut-out design and to compare and evaluate the different designs. The analysis and investigation is not performed to analyse the structural strength or fatigue damage of the structure, but to compare the cast integral with the cut-out design following classification rules and regulations.

The cast integral used as a reference case is a common standardized design used by GVA for the specific node connection. The overall structural design is also given from a previous project at GVA. Only one centre bulkhead connection is investigated due to symmetry and the assumption that the node with the highest stresses is governing. Hence, the cut-out will only be optimised for one node. The cut-out geometry in the case study will be evaluated for the given semi-submersible with the applied loads, which is why the cut-out might not be applicable in other semi-submersibles or in other locations.

The 2D analysis of different cut-out designs only investigates the recommended governing responses that apply for the node connection (DNV, 2012). The analysis is made for a simplified geometry and does not include transverse loads or plating.

Welds are only investigated in the fatigue damage evaluation due to the known sensitivity of fatigue damage in the weld, but does not include imperfections in the welds (International Institute of Welding, 2008). The fatigue resistance is accounted for with the use of S-N curves and principal stresses calculated with the hot-spot method, hence no welds are modelled in the finite element analysis (FEA). All finite element analysis is performed with the linear elastic solver DNV Sestra (DNV, 2010a).

The design of the node connection must fulfil the rules and recommendations from the classification society DNV-GL. The alternative cut-out design may not alter the overall structure, but rather introduce a local design that can be utilized without large structural changes. The adjacent corner will be investigated as to the effects a cut-out will induce.

The assessment criteria used is the Ultimate Limit State and the Fatigue Limit State, which are considered governing and induce the most critical stresses. The highest stresses in ULS are used as the first design criterion, and stress based high cycle fatigue damage is controlled as a secondary objective. The ULS for the proposed cut-out design and the cast integral includes both yield checks and control of buckling, while minimum

scantlings are disregarded. The corrosion margin is also excluded in all calculations. Local yielding of the structure is approved where large changes in the geometry are present and the adjacent structure may redistribute the stresses (DNV, 2012).

1.3.1 Normalization of calculated stresses

The calculated yield and principal stresses are presented in contour plots for the different designs. Due to confidentiality of the semi-submersible structure used in the calculations and the in-house design of the cast integral, the stresses in the presented contour plots are normalised. The normalization is made for different values for yield and principal stresses, see the corresponding sections for further information.

In the ULS assessment the stress plots present the highest general von Mises stresses for each element. The normalization is made with reference to the permissible von Mises stress according to Section 2.2.1.

The stress plots used in the simplified fatigue damage calculations present the highest principal stress in each element. The normalization is made in the same way for both the reference case and the suggested cut-out design for simple comparison of the designs. The stochastic fatigue plot presents the accumulated fatigue damage as a usage factor, defined as the design life divided by the calculated fatigue life.

1.4 Thesis outline

The first part of the thesis describes the background and motivation of the work with the analysed node connection. Chapter 2 describes the loads that act on the structure and how the response is interpreted with different methods, recommended practises, rules, etc., such as the simplified fatigue method and yield checks with the von Mises stress criterion. The specific column/deck-box connection is described in Chapter 3 together with an analysis of the cast integral, investigated as a reference case in this thesis. The cast integral is analysed, with regard to the method outlined in Chapter 2, for yield stresses, buckling and fatigue damage with the simplified fatigue method.

An alternative design using a cut-out is presented in Chapter 4 together with a simplified geometry and parametric study to find a suitable design for the cut-out. The chapter also discusses the different effects of a cut-out geometry.

To verify the results from the simplified study, a case-study of a semi-submersible platform with a cut-out is examined in Chapter 5. Different cut-out designs, based on the results from the simplified study, are examined with a parametric study in the complete structure with regard to yield stresses and fatigue damage. The fatigue damage on the cut-out design is also verified with a stochastic analysis for comparison with the simplified fatigue assessment.

Chapter 6 discusses the different advantages of the two different designs with regard to weight and cost, and overall results from the analyses are discussed in Chapter 7. The conclusions of the study are presented in Chapter 8 followed by recommendations for future work in Chapter 9.

2 Design criteria and assessment

The node connection is illustrated in Figure 2.1 and is defined as the intersection of beams in the structure. The purpose of the node connection is to provide structural strength and stability to the semi-submersible structure (Zhang et al., 2009). The simple beam model shows that there are eight similar connections on a typical semi-submersible production platform, but when adding more beams more node intersections are created. Due to symmetry conditions it is considered sufficient in this thesis to investigate only one column/deck-box connection where the highest stresses occur. The node of interest in this study is highlighted in the middle in Figure 2.1; the centre bulkhead connection. The adjacent inner corner connection is also investigated.

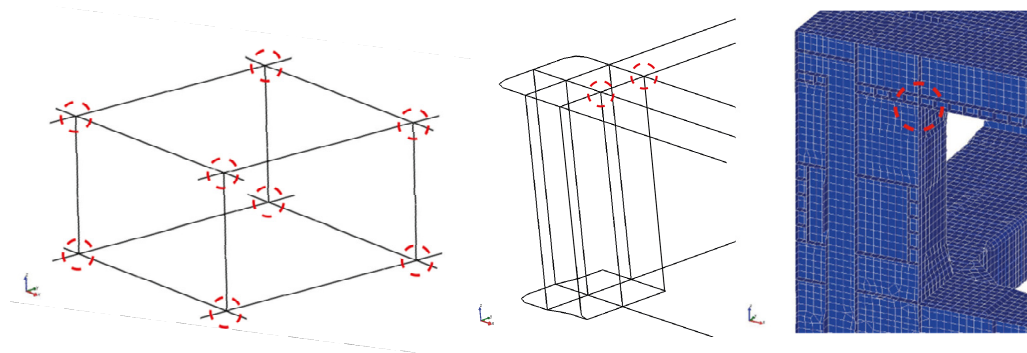


Figure 2.1 The node connection in three levels, beam model (left), expanded beam model (middle) and shell model (right).

The applied loads on the structure consist of several complex load cases; see Section 2.1, both static and cyclic loads in different limit states. The structural strength is verified by assessing yield stress, buckling and fatigue damage of the structural components in the node connection. The limit states investigated are ULS and FLS, which the structure is verified against. This can be done using one of the two structural design methods suggested by DNV-GL, the Load and Resistance Factor Design (LRFD) or the Working Stress Design (WSD) approach, see Section 2.2.1, where the latter method is chosen in this report for analyses of yielding and buckling (DNV, 2012).

The structure is verified using several different analysis methods which are described in the following sections and in Figure 2.2. The procedure and software used for the analyses of small local models (sub-model and solid model) is presented in Appendix A.

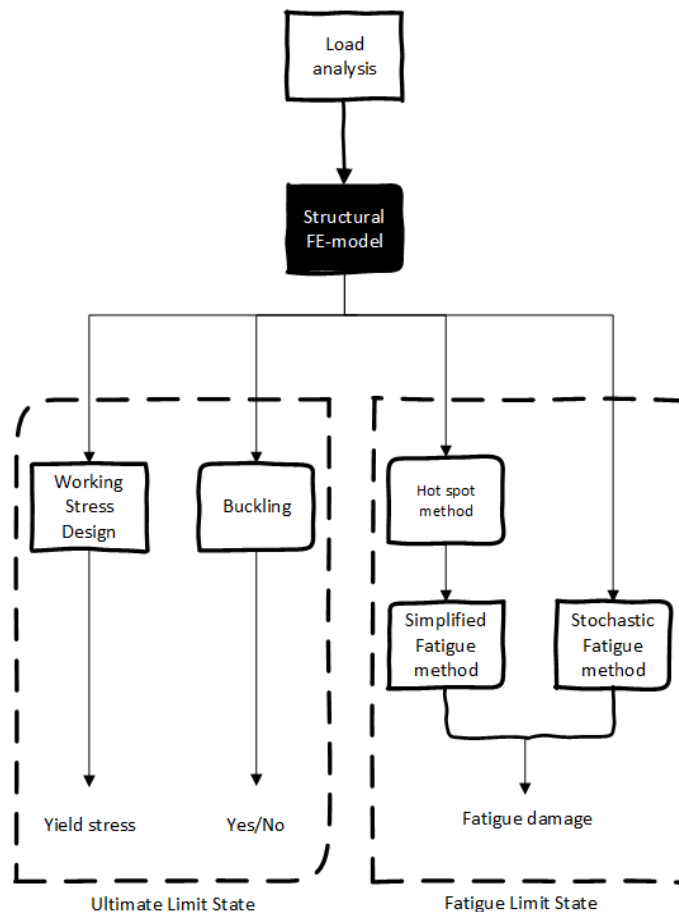


Figure 2.2 Analysis flowchart of the methods used for assessment in this thesis.

2.1 Loads and boundary conditions

A semi-submersible platform is exposed to many different and varying hydrodynamic loads from wind, waves, currents and also from applied loads on the structure (DNV, 2012). This section contains information on which forces that have been considered and how they are applied in the calculations.

The hydrodynamic analysis in this thesis is previously performed by GVA on a typical semi-submersible. The structure is evaluated for operations in the Gulf of Mexico and a fatigue life of 30 years.

The hydrodynamic simulation is performed in the frequency and time domain using linear (Airy) wave theory in DNV Wadam (DNV, 2010b). The wave loads and applied loads acting on the global FE-model are defined following the “Design wave analysis” procedure (DNV, 2012). The method is used for finding a number of different waves that represent the total spectra of waves. The Design wave analysis is considered adequate in precision of results and is a swift and easy method to implement (Lizhong, 2013). The analysis procedure is illustrated in a simplified schematic in Figure 2.3 where the load effects from wind and current are considered negligible, hence only wave induced loads and static loads are considered (DNV, 2012).

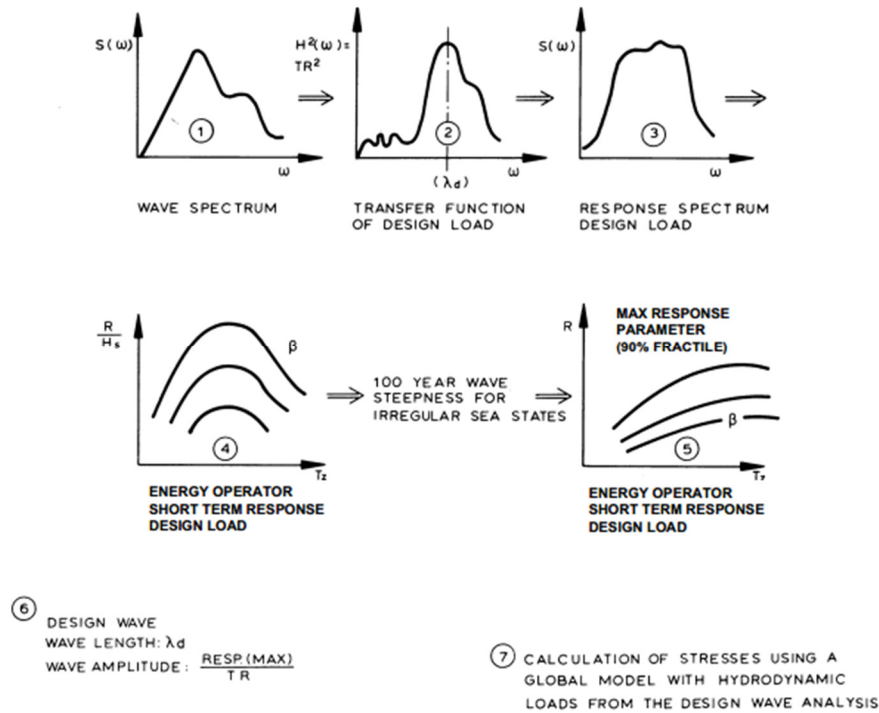


Figure 2.3 Schematic of the Design wave method (DNV, 2012).

The calculation of wave loads is made using environmental data from the specific location where the semi-submersible is supposed to operate. Identification of governing responses on the structure is performed using DNV Wadam (DNV, 2010b). The sectional loads that are investigated in both the longitudinal and transverse directions are:

- split force between the pontoons,
- torsion moments,
- shear force,
- racking force,
- heave force, and
- bending moments of the pontoons.

The global governing responses that act on semi-submersibles are shown in Figure 2.4. The responses are also valid for ring-pontoon units, when the forces are applied in both the transverse and longitudinal directions (DNV, 2012).

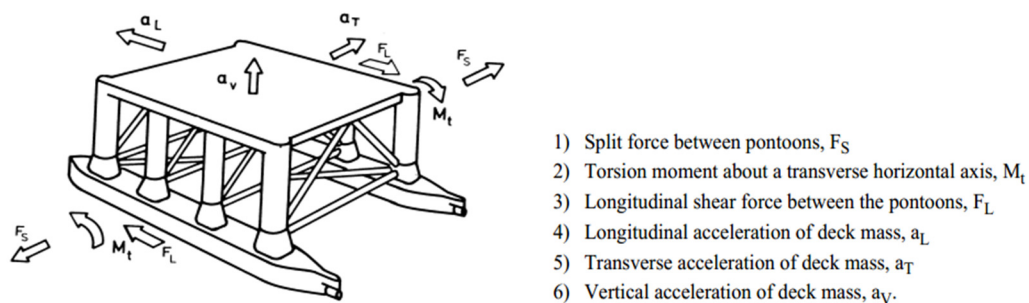


Figure 2.4 Governing hydrodynamic responses for a semi-submersible (DNV, 2012).

The maximum responses are calculated with a return period of 100 years. The 100-year hurricane is used in the calculations of the highest yield stresses and in the buckling check and the 100-year winter storm is evaluated for the fatigue condition. Both conditions are evaluated using the JONSWAP energy spectrum and 48 different wave headings and 35 wave periods are investigated. For the 100-year winter storm a cosine spreading function is used to include the effect from short-crested waves (DNV, 2012).

- 100-year hurricane
Long crested sea
JONSWAP wave energy spectrum $\gamma = 2.4$
- 100-year winter storm
Short crested sea
Cosine spreading function $\eta = 4$
JONSWAP wave energy spectrum

The individual and regular deterministic design waves that represent the global responses are used for the calculation of applied loads. This results in 61 different load cases to be investigated in the FEA of the local design.

The boundary conditions for the global structural model are applied at the bottom of the pontoons, and the structure is fixed in three different points in a total of six degrees of freedom to avoid rigid body motion, see Table 2.1 and Figure 2.5. The loads on a semi-submersible are balanced in nature due to the water pressure on the hull, mooring lines, risers, etc., which is why the model is considered statically determined and fixed restraints can be used (Lizhong, 2013).

Table 2.1 Boundary conditions applied at the bottom of the semi-submersible in Figure 2.5.

Location	Translation		
	X	Y	Z
Upper right			Fix
Upper left	Fix	Fix	Fix
Lower left	Fix		Fix
Lower right			

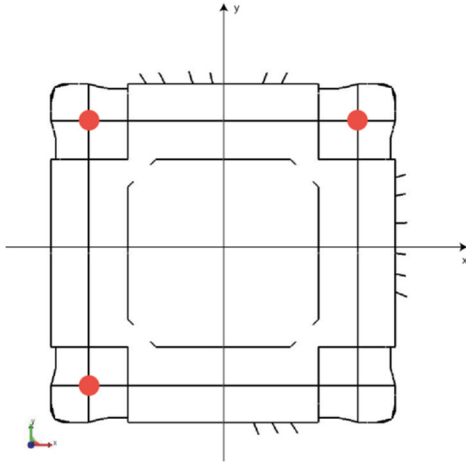


Figure 2.5 Coordinate system of the semi-submersible with highlighted points where boundary conditions are applied at the bottom of the pontoons.

The loads are transferred between different levels of models with the sub-modelling technique. Figure 2.6 show the relationship between the global model (complete semi-submersible) and the local sub-models. The method uses nodal displacement on the boundaries of the sub-model, see Appendix A for further explanation.

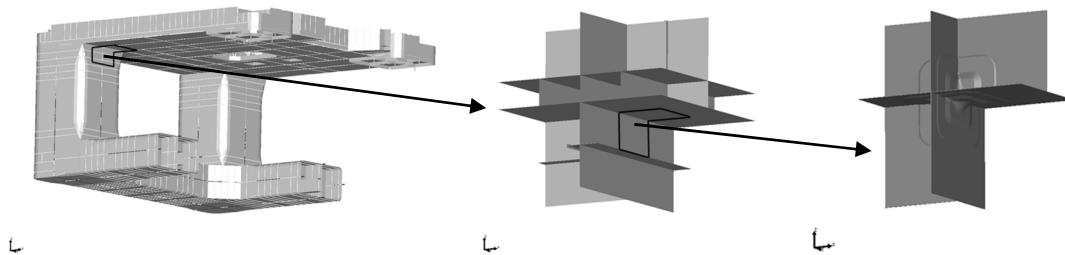


Figure 2.6 The sub-modelling technique to transfer displacements from a large global model (left), into the smaller sub-model (middle) and finally to the detailed solid model (right).

2.2 The Ultimate Limit State design criterion

The Ultimate Limit State (ULS) is the worst load condition due to local and environmental loads acting on the structure, without external damage or accidents, which induce the highest stress responses. The ULS corresponds to the maximum load carrying capacity of the semi-submersible.

The ULS can be assessed using different methods suggested by the classification societies where the LRFD method or the WSD method are two alternatives, see Section 2.2.1. Both methods are based on linear theory and give similar results, but the older WSD method does not consider resistance and load effects, such as live/dead loads or shear/bending, etc. This is assumed to have an impact on the level of conservatism in the different methods, where the WSD method tends to underestimate the allowed stress level (Saglam & Lindekrantz, 2014). The WSD method is chosen in this thesis due to both the more conservative calculations and to the load analysis already being completed and not within the scope of this investigation.

For assessment of yielding, the stresses in plated structures can be calculated using the general von Mises stress, see Equation (2.1).

$$\sigma_{vonMises} = \sqrt{\sigma_x^2 + \sigma_y^2 - \sigma_x\sigma_y + 3\tau^2} \quad (2.1)$$

2.2.1 The Working Stress Design (WSD) method

The WSD method is a suggested method by DNV-GL to design structures according to a determined safety limit. The ultimate strength of the structure can be assessed with yield stresses and buckling with the use of the WSD method (DNV, 2014a).

The WSD method adds a safety factor by multiplying the characteristic strength of the structure with a usage factor, see Equation (2.2) (DNV, 2014b). The WSD method utilizes usage factors for the different load cases, but does not consider potential load effects or resistances. The coefficient, β , depends on type of structure, failure mode and reduced slenderness. $\beta = 1$ should be used when yield stress is the dimensioning criterion in the WSD method. The usage factors are in the WSD method lumped into one reduction factor, which means that the method can be considered “more” conservative than the alternative LRFD method when the safety limit is low.

The LRFD method introduces deterministic load factors to acting loads and resistances in applied material or structures. The variation in load and resistance is thus taken into account. The LRFD method also accounts for the reduced probability that the loads will act simultaneously as their characteristic value (DNV, 2014a). The method is, however, considered time-consuming and must be implemented when loads are applied to the structure. The WSD method is thus used in the thesis due to the already performed load calculations by GVA.

$$\eta_p = \beta * \eta_0 \quad (2.2)$$

η_p = Maximum permissible usage factor

β = Coefficient depending on type of structure, failure mode and reduced slenderness.

η_0 = Basic usage factor given from Table 2.2, where b) corresponds to the ULS.

Table 2.2 Basic usage factors in the WSD method (DNV, 2012).

Basic usage factors η_0					
Loading conditions					
	a)	b)	c)	d)	e)
η_0	0.60 ¹⁾	0.80 ¹⁾	1.00	1.00	1.00
1) For units unmanned during extreme environmental conditions, the usage factor η_0 may be taken as 0.84 for loading condition b).					

The yield stress is evaluated with the von Mises equivalent stress criterion, Equation (2.1), and checked with consideration to the permissible stress, σ_p , see Equation (2.3) and (2.4).

$$\sigma_p = \sigma_y * \eta_p \quad (2.3)$$

$$\sigma_{vM} < \sigma_p \quad (2.4)$$

σ_p = Permissible stress [MPa]

σ_y = Yield stress of the material [MPa]

2.2.2 Buckling analysis

The local buckling deformation depends on the geometry and boundary conditions of the investigated structure. The direction and size of the acting loads together with potential defects in the material also affect the local buckling. However, imperfections are not regarded in this analysis.

For the buckling analysis of the cast integral, Equation (2.5) is used. The formula is valid for unstiffened plates in combined loading as illustrated in Figure 2.7 (DNV, 2010c).

$$\left(\frac{\sigma_x}{\sigma_{x,Rd}}\right)^2 + \left(\frac{\sigma_y}{\sigma_{y,Rd}}\right)^2 - c_i * \left(\frac{\sigma_x}{\sigma_{x,Rd}}\right)\left(\frac{\sigma_y}{\sigma_{y,Rd}}\right) + \left(\frac{\tau}{\tau_{Rd}}\right)^2 < 1 \quad (2.5)$$

$\sigma_{x,Rd}$ = Design resistance in longitudinal compression stress [MPa]

$\sigma_{y,Rd}$ = Design resistance in transverse compression stress [MPa]

τ_{Rd} = Design resistance shear stress [MPa]

c_i = Interaction factor obtained from Equation (2.6)

$$c_i = 1 - \frac{s}{120t}, \text{ for } \frac{s}{t} \leq 120 \quad (2.6)$$

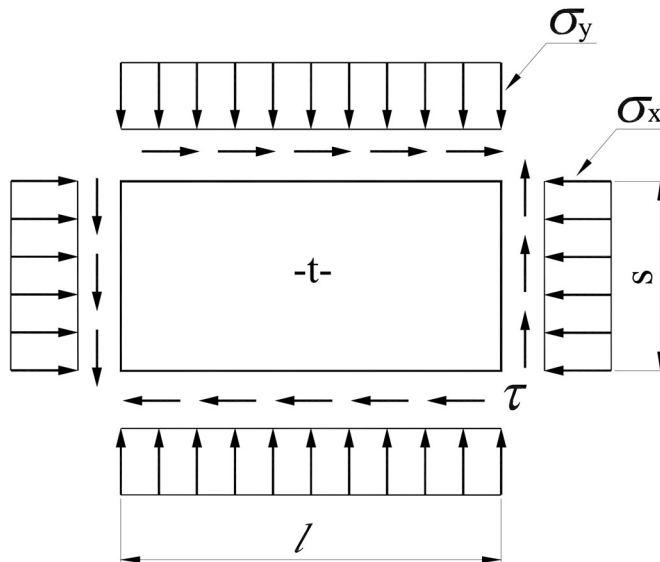


Figure 2.7 Biaxially loaded plate with shear (DNV, 2010c).

For the cut-out design a simplified buckling analysis is performed. Even if the stresses within the structure are below the yield limit for the material used, failure of the structure can occur and slender structure parts run a high risk of buckling. The critical

stress, σ_c , for buckling of plates can be calculated using Equation (2.7) (Bambach & Rasmussen, 2004).

$$\sigma_c = k \frac{\pi^2 E}{12(1-\nu^2)} \left(\frac{t}{b}\right)^2 \quad (2.7)$$

E = Young's modulus [GPa]

t = Plate thickness [mm]

b = Width of plate [mm]

ν = Poisson's number

If the critical stress from Equation (2.7) is more than half the yield stress of the material, a plasticity correction factor of the critical stress is introduced by the Johnson-Ostenfeld criterion (Ringsberg, 2011). The criterion is presented in Equation (2.8) and is used for calculating the elastic buckling capacity and accounts for the plasticity effects. Without the correction factor the critical buckling stress is overestimated.

$$\sigma_{c,corr} = \sigma_y \left(1 - \frac{\sigma_y}{4\sigma_c}\right) \quad (2.8)$$

To evaluate the cut-out design against buckling a usage factor is introduced, see Equation (2.9). The usage factor shows how close the actual stress is to the critical stress.

$$\eta = \frac{\text{Actual stress}}{\text{Critical stress}} = \frac{\sigma_{\text{applied}}}{\sigma_{\text{critical}}} < 1 \quad (2.9)$$

The factor k is often referred to as the plate buckling coefficient or simply as the plate factor. The k factor is a function of plate geometry and boundary conditions that affect the critical stress of the plate, see Equation (2.10).

$$k = \left(\frac{mb}{a} + \frac{n^2 a}{mb}\right)^2 \quad (2.10)$$

k = Plate buckling coefficient

m = Number of buckled half-waves in the longitudinal direction

n = Number of half-waves in the transverse direction

a = Length of plate [mm]

$\beta_{\text{aspect}} = a/b$, aspect ratio

For a cut-out design, the geometry and boundary conditions can be simplified to those presented in Figure 2.8, with one free edge and other edges simply supported. This is also clarified in Figure 2.9 where the cut-out can be seen.

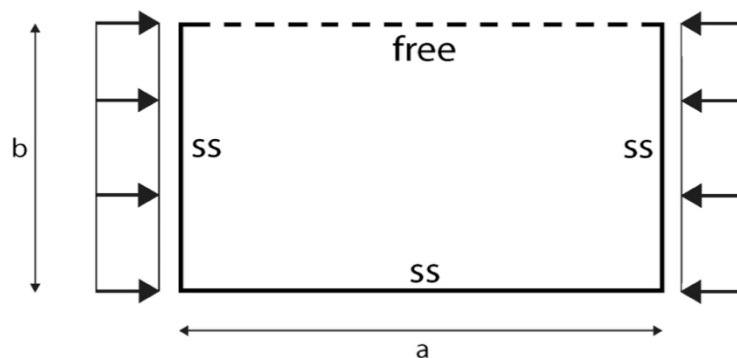


Figure 2.8 Sketch for axial compression with boundary conditions for a plate with one free edge and the others simply supported (ss).

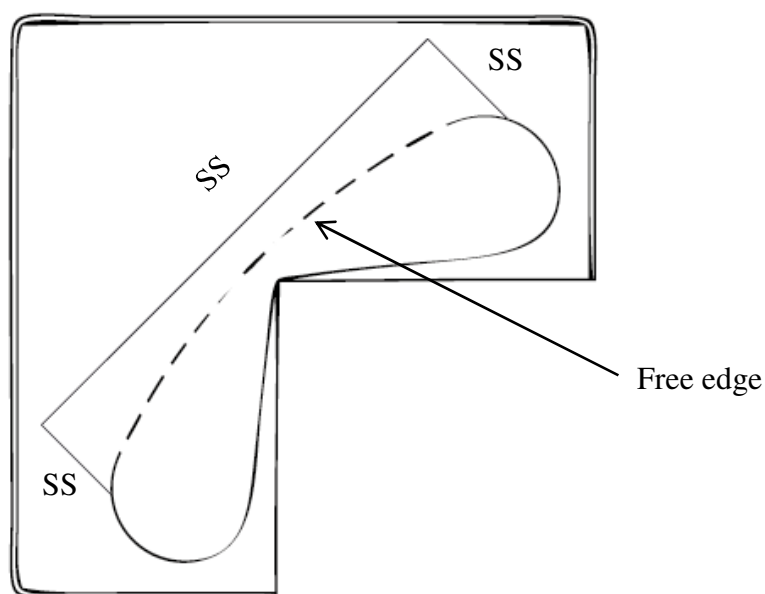


Figure 2.9 Clarification of Figure 2.8 for the simplified boundary conditions used for the buckling analysis of the cut-out design.

The plate factor for different aspect ratios with different boundary conditions and half-waves for axially compressed plates is presented and plotted in Figure 2.10 (Yu & Schafer, 2007).

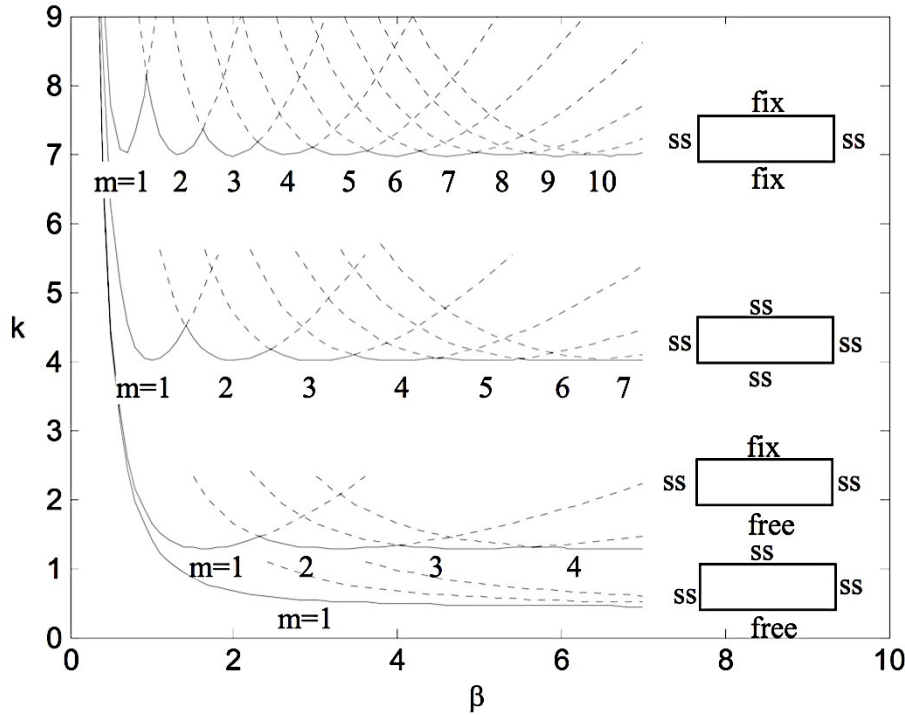


Figure 2.10 Variation of the k factor with different boundary conditions and half-waves (Yu & Schafer, 2007).

For the free edge of the cut-out design, the last case in Figure 2.10 with three edges simply supported and one free edge can be applied. For the specific case, the plate factor can be calculated with Equation (2.11) (Ringsberg, 2011).

$$k = 0.43 + \left(\frac{b}{a}\right)^2 \quad (2.11)$$

A more conservative value of the plate factor, $k = 0.42$, which is used in this assessment for a cut-out design is suggested by Bijlaard (1957). With three edges simply supported (ss) and one free edge, the plate factor, β_{aspect} , is considered constant for an aspect ratio above 3. When the aspect ratio increases the plate factor quickly turns into the constant value of 0.43 as shown in Figure 2.10.

Equation (2.12) and (2.13) can be used calculating the plate factor for the combination of axial compression and shear forces as in Figure 2.11 together with Table 2.3 (Yu & Schafer, 2007).

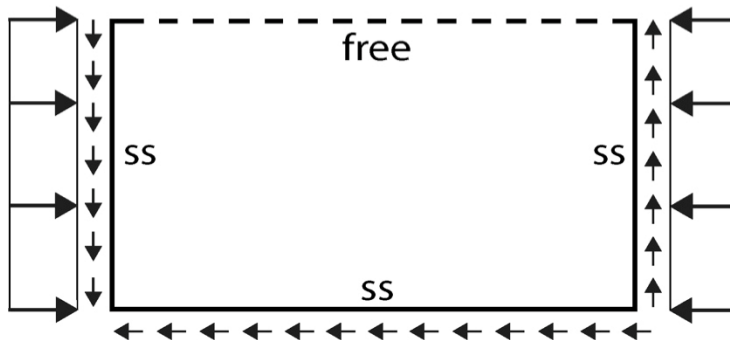


Figure 2.11 Shear forces and axial forces in the buckling criteria.

$$k = k_{\infty} + \frac{\alpha_1 r + \alpha_2}{\alpha_3 r + \alpha_4 + \beta^{\alpha_5}} \quad (2.12)$$

$$r = \frac{\sigma_{min}}{\sigma_{max}} \quad (2.13)$$

Table 2.3 Parameters for Equation (2.12) to calculate the plate factor, k (Yu & Schafer, 2007).

k_{∞}	α_1	α_2	α_3	α_4	α_5
0.42	-0.60	1.00	0	-0.60	0.95

2.3 The Fatigue Limit State design criterion

The specific design of the node connection is not only subjected to high static loads, but also to time-varying cyclic load variations during its life of operation. Consequently, a fatigue life assessment must be carried out and the node connection is recognized as a sensitive area for fatigue (DNV, 2012).

The stresses in the considered detail can be found using the nominal stress approach which is recognized as an easy and fast way of assessing the stresses for fatigue damage. Due to the somewhat changing geometries, imperfections, welds, etc., it can be hard to obtain the correct nominal stresses in the investigated detail, which is why the “Hot spot” stress approach, see Section 2.3.2, can also be used. Both methods are suggested for calculation of fatigue damage (DNV-GL, 2014). The hot spot method is recommended to be used when the nominal stress cannot be clearly defined and is therefore utilized in this thesis.

The method uses the highest principal stresses gained from the finite element analysis together with a suitable S-N curve, which is based on a 97.6% probability for survival (DNV-GL, 2014). The fatigue assessment is made for a reference life of 30 years, corresponding to 150 million load cycles using both the simplified fatigue method, see Section 2.3.4 and the stochastic method, see Section 2.3.5.

The Weibull shape parameter, h , which is used in the simplified fatigue damage calculations, can be derived using a stochastic fatigue assessment of the whole semi-submersible. The parameter is recognized as having a large influence in the calculation of fatigue life, hence it is considered critical. The shape parameter, $h = 1.1$, can be used for worldwide operations based on experience of similar structures. The value is used in the fatigue assessment in this thesis, since it is considered conservative in the current investigation (DNV, 2012).

The stochastic fatigue method is considered to be the best method for assessing fatigue damage due to the irregular wave loads, see Section 2.3.5. The simplified fatigue method suggested by DNV-GL can be used either for screening of where the stochastic fatigue method needs to be used, or by itself. Both the simplified and the stochastic fatigue analysis are stress based, meaning that Hooke’s law can be used for describing the relationship between stress and strain (Dowling, 2012).

2.3.1 Scaling of allowable stress range

The stress results from the finite element analysis are based on the return period of the 100-year winter storm. Since the fatigue assessment is calculated for 30 years of operation in this report, the results must be scaled according to Equation (2.14). The Weibull shape parameter h is in the simplified fatigue evaluation taken as 1.1 according to Section 2.1 and N_x represents the number of load cycles in x years (DNV-GL, 2014).

$$h = 1.1$$

$$N_{30} = 1.5 * 10^8 \quad [\text{cycles}]$$

$$N_{100} = 5 * 10^8 \quad [\text{cycles}]$$

$$\Delta\sigma_{30} = \Delta\sigma_{100} * \left(\frac{\log N_{30}}{\log N_{100}} \right)^{\frac{1}{h}} \quad (2.14)$$

2.3.2 The hot spot method

The hot spot stress can be seen as the geometric stress created by the considered detail. The hot spot method is suggested by DNV-GL to be used for calculations of fatigue stresses in plated offshore structures.

The fatigue resistance for welds is known to be low due to tensile residual stresses caused from the welding procedure. Welds are also sensitive to cyclic loading, which is a main concern due to the repetitive loads caused by waves (International Institute of Welding, 2008). The classification rules regard the weld sensitivity with the use of S-N curves with a reduced fatigue resistance. Welds are therefore especially investigated in the local design.

The maximum principal stress can be used instead of the nominal stress for conservative calculations of the fatigue stresses due to the difference in direction of the principal stress and the normal of the weld toe, see Figure 2.12 (DNV-GL, 2014). The fatigue crack will start to propagate inside the weld, and the notch effect of the weld toe is therefore no longer a significant factor. The maximum normal principal stress, σ_1 , for thin shell elements with 3 or 4 nodes (2D-problem) can easily be calculated (DNV, 2011b). The principal stress for solid elements (3D-problem) can be solved with a general stress theory and the eigenvalues of the complete stress tensor (Dowling, 2012).

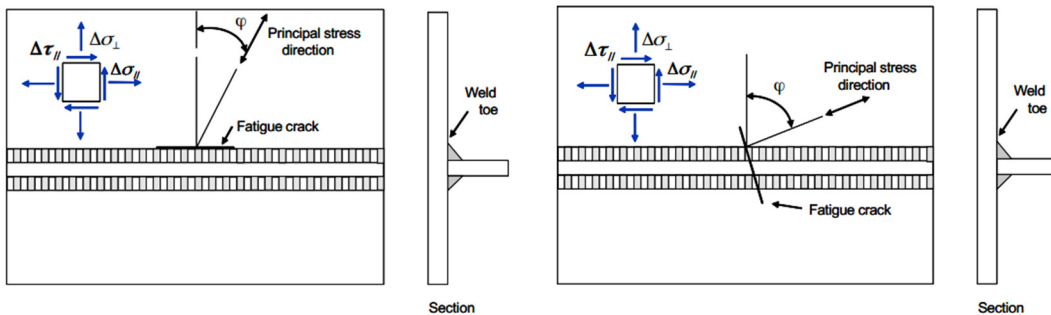


Figure 2.12 Crack growth depending on principal stress direction (DNV-GL, 2014).

The hot spot method includes the notch stress concentration factor in the S-N curve, which is why this does not need to be evaluated separately. However, the welds, due to

change in thickness of the plates and weld geometry have to be considered and the allowable stress reduced accordingly.

The notch stress is defined as the total stress at the weld toe including the geometric stress and the stress created by the weld, while the hot spot stress does not consider the weld stress. This can be done with the assumption of linear material behaviour and no misalignments of the plates (Li, 2013). S-N curves D or C2 can be utilized for plated structures using the hot spot stress method, see Figure 2.13. Similarly to the nominal stress method, requirements on the welding and geometry of the weld may approve the use of a higher S-N curve, see Figure 2.14 (DNV-GL, 2014).

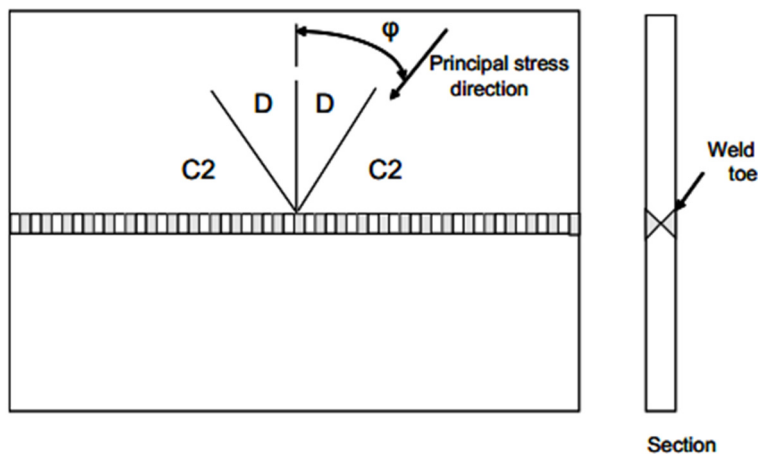


Figure 2.13 Fatigue class which can be used for plated structures depending on principal stress direction (DNV-GL, 2014).

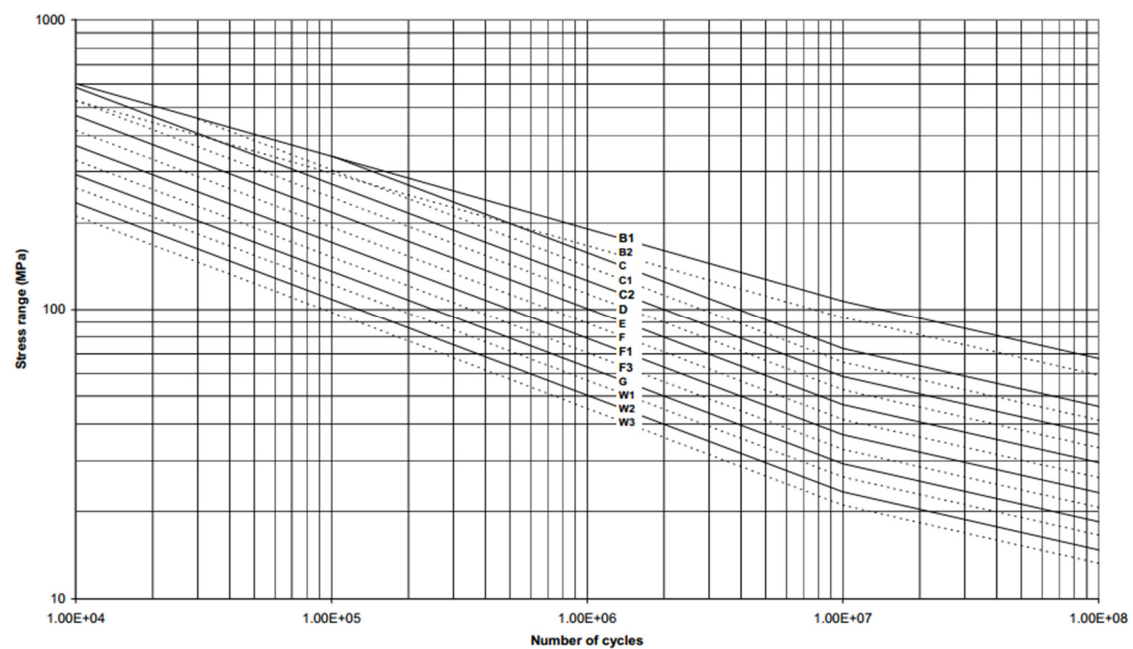


Figure 2.14 S-N curves used for structural details in air (DNV-GL, 2014).

The hot spot stress method regards the stresses on an adequate distance from the considered weld and extrapolates the stresses linearly to the actual weld hot spot, see Equation (2.15). Figure 2.15 describes the relationship between the hot spot readout points of $0.5t$ and $1.5t$ and the calculated hot spot stress. The thickness at the weld toe is here denoted as “ t ” and the surface stress is equal to the nominal stress. One of the major disadvantages of the hot spot method is the requirement of a very dense mesh (with element size $t * t$ preferred in the hot spot region) with long calculation times as the consequence (DNV-GL, 2014).

$$\sigma_{hot\ spot} = \frac{1}{2}(\sigma_{0.5t} - \sigma_{1.5t}) + \sigma_{0.5t} \quad (2.15)$$

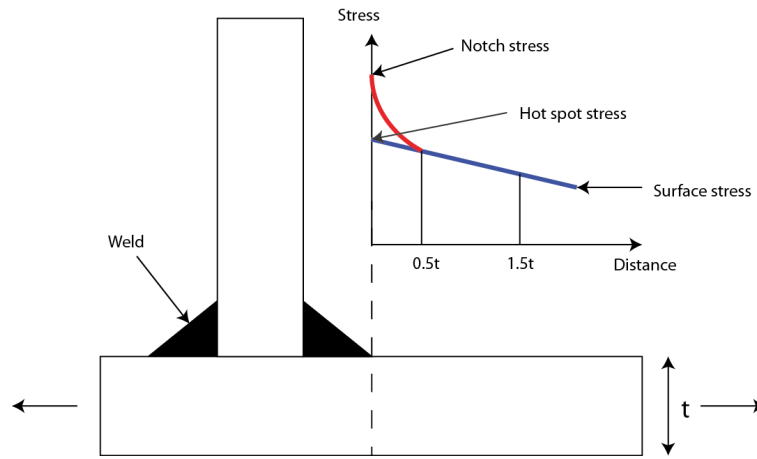


Figure 2.15 Illustration of the hot spot stress method.

2.3.3 Thickness effect

Due to the large thickness of the cast integral, it is necessary to reduce the effective thickness of the cast in the calculations. When a large stress gradient over the thickness in the integral exists, Equation (2.16) can be used for calculating the effective thickness. For cast nodes, the reference thickness of 38 mm may be used (DNV-GL, 2014).

$$t_e = t_{actual} \left(\frac{S_i}{S_0} \right)^{\frac{1}{k_t}} \quad (2.16)$$

t_e = Effective thickness [mm]

t_{actual} = Thickness at the weld toe [mm]

S_i = Stress 38 mm inside the cast measured from the surface [MPa]

S_0 = Hot spot stress on the surface [MPa]

k_t = Thickness exponent

2.3.4 Simplified fatigue assessment

The simplified fatigue assessment is used for fast calculations and assessments of the fatigue damage that can be considered as being conservative. The stress-based method uses the distribution of long-term stress ranges and utilizes a two-parameter stress distribution, for example Weibull or Rayleigh, and standard reduction factors in order

to calculate allowable stresses and fatigue life (DNV-GL, 2014). The linear analysis method is based on the assumption that the Palmgren-Miner rule for accumulated damage can be used and that the fatigue resistance is defined by S-N curves. The stress-range distribution is described by the Weibull shape parameter h and scale parameter q . The shape parameter describes the shape of the distribution, while the scale parameter governs the magnitude of stress ranges.

When utilizing the “Design wave method” for worldwide operations, the Weibull distribution parameter, h , can be taken as $h = 1.1$ in the simplified fatigue assessment, which is utilized in this thesis (DNV, 2012).

The fatigue damage, D , can be calculated directly in Equation (2.17) with the use of a two-slope or bi-linear S-N curve (DNV-GL, 2014). The choice of S-N curve is dependent on the weld classification and principal stress direction, see Section 2.3.2. The gamma function (γ) can be acquired from textbook tables and the relationship between Weibull shape and scale parameters is illustrated in Equation (2.18).

$$D = N_0 * \left[\frac{q^{m_1}}{\hat{a}_1} * \Gamma \left(1 + \frac{m_1}{h}; \left(\frac{S_1}{q} \right)^h \right) + \frac{q^{m_2}}{\hat{a}_2} * \gamma \left(1 + \frac{m_2}{h}; \left(\frac{S_1}{q} \right)^h \right) \right] \leq \eta \quad (2.17)$$

m_1, \hat{a}_1 = Parameters from the first S-N curve

m_2, \hat{a}_2 = Parameters from the second S-N curve

S_1 = Stress range for the breakingpoint of the two curves in the S-N diagram

$\Gamma(a; x)$ = Complementary incomplete gamma function

$\gamma(a; x)$ = Incomplete gamma function

$\Delta\sigma$ = Maximum stress range in the number of cycles

N_0 = Number of cycles

h = Weibull shape parameter

q = Weibull scale parameter calculated from Equation (2.18)

$$q = \frac{\Delta\sigma_0}{(\ln N_0)^{\frac{1}{h}}} \quad (2.18)$$

The S-N curve is defined by Equation (2.19) and is created from experimental data.

$$\log N = \log(\hat{a}) - m * \log(\Delta\sigma) \quad (2.19)$$

N is the number of cycles to failure, $\log \hat{a}$ is the crossing of the log-N-axis and m is here the inverse slope of the S-N curve. The S-N curves are defined from tests of the specific material and can be found in textbooks (Dowling, 2012).

The last step in the simplified fatigue analysis is to calculate the fatigue life. The Design Fatigue Factor (DFF) is applied in order to reduce the probability of fatigue damage. The factor is applied to the design fatigue life and can be expressed as in Equation (2.20), where L is the calculated fatigue life, L_{design} is the required fatigue life and D is the cumulative damage according to Palmgren-Miner. The DFF can be decided using given tables for the classification rules, and for units following the recommended 5-yearly inspection interval in sheltered waters $DFF = 1$ can be used (DNV, 2014a). This is the value used in the fatigue assessments in this thesis.

$$L = \frac{L_{design}}{D} \geq L_{design} * DFF \quad (2.20)$$

2.3.5 Stochastic fatigue analysis

The use of the simplified fatigue method is not always considered accurate and the method usually overestimates the accumulated fatigue damage. A stress-based stochastic fatigue analysis can be performed using the program DNV Stofat, which calculates the fatigue damage in the frequency domain (DNV, 2011c). The accumulated partial damage weighted over sea state and wave direction is calculated and based on the quasi-static FEA of the global model, sub-model and solid model performed in DNV Sestra (DNV, 2010a). The assessment is made using S-N curves given from tabulated values.

The analysis is based on statistical wave data from scatter diagrams for the area intended for operations. The stochastic analysis accounts for both the probability of waves and also the direction of the waves, see the procedure in Figure 2.16. However, the simultaneity of force and response is lost in the analysis, hence the method is not recommended for other than fatigue analysis (DNV, 2012).

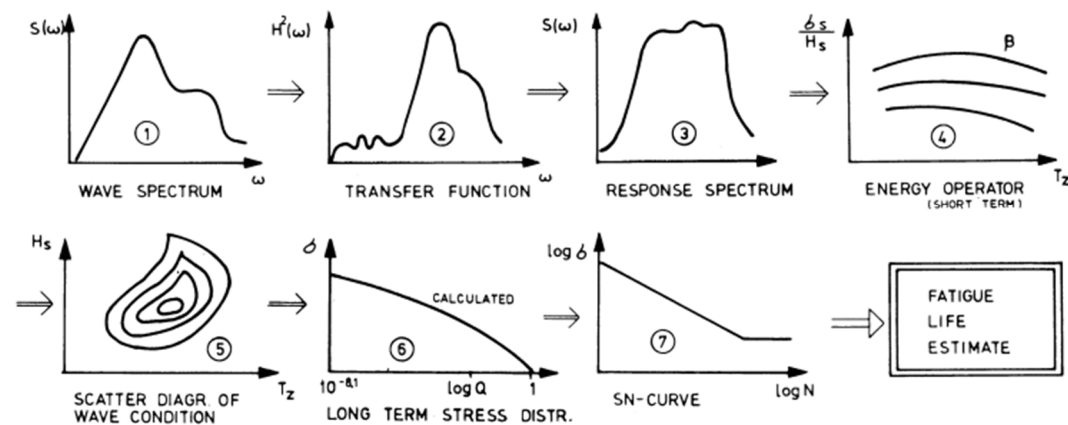


Figure 2.16 Steps in the stochastic fatigue analysis, (DNV, 2012).

The analysis considers 16 different wave headings with a step of 22.5 degrees and 36 wave periods and identifies critical locations where the fatigue damage is high. The semi-submersible is to operate in the Gulf of Mexico, for which reason a scatter diagram for this area is used (DNV, 2007). The accumulated fatigue damage is presented in contour plots.

3 Analysis of reference case - a cast integral

This chapter describes the reference cast integral, see Figure 3.1, and analyses it following the methodology described in Section 1.2. The geometry of the cast integral is a typical design used in the centre bulkhead connection between column and deck-box. The standardized design is normally implemented in GVA designed semi-submersibles.

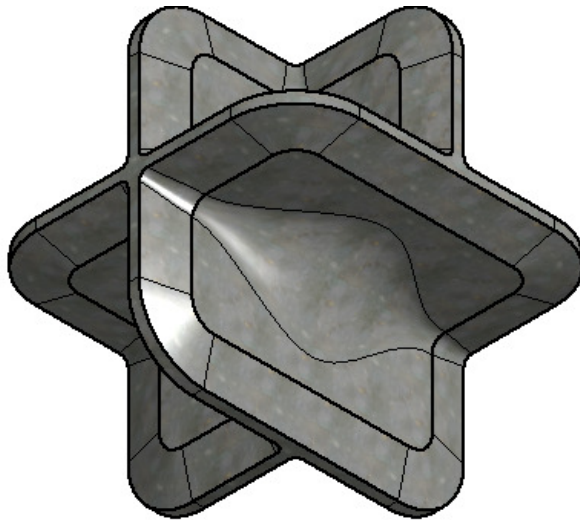


Figure 3.1 Solid model of the cast integral in isometric view used in the centre bulkhead connection in the intersection column/deck-box.

The cast integral analysed in this thesis is implemented in the connection highlighted in Figure 3.2 in a given semi-submersible production platform from previous GVA calculations. The South-West centre bulkhead in the column/deck-box connection is analysed. The cast integral is investigated in ULS, FLS, weight and cost in accordance to Section 2.1.

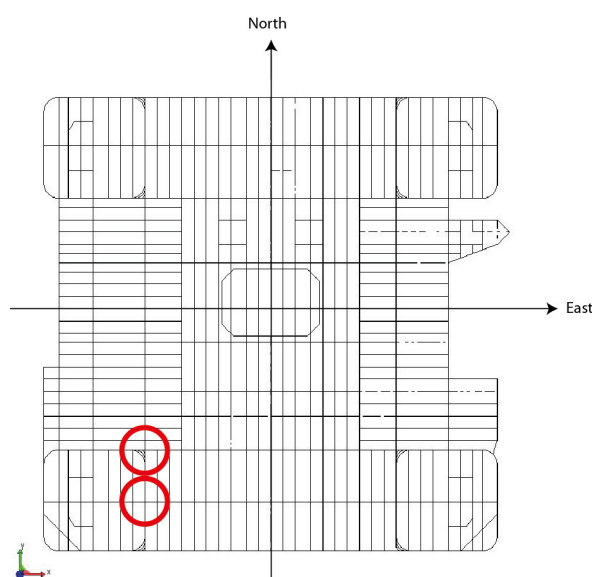


Figure 3.2 Coordinate system of the semi-submersible platform. Top view with analysed node connection and adjacent corner highlighted.

The hydrodynamic analysis, following the “Design wave approach” described in Section 2.1, is performed in a previous GVA project and therefore only applied in this thesis. A finite element analysis is conducted in order to calculate resulting stresses in the structure. The stresses are compared with the WSD for yielding and the simplified fatigue method for fatigue damage calculations. A fatigue damage calculation using a stochastic approach is also implemented to validate the results from the simplified method. Material properties used in this thesis are presented in Table 3.1.

Table 3.1 Material properties used in this thesis.

Property	Value
Young’s modulus	206 GPa
Density	7850 kg/m ³
Poissons ratio	0.3

3.1 Geometry and mesh

The reference cast integral is analysed using the sub-modelling technique with DNV Submod (DNV, 2004). The procedure makes it possible to transfer displacements from a global model to a smaller sub-model to be investigated in detail. Further information about the technique and procedure is presented in Appendix A.

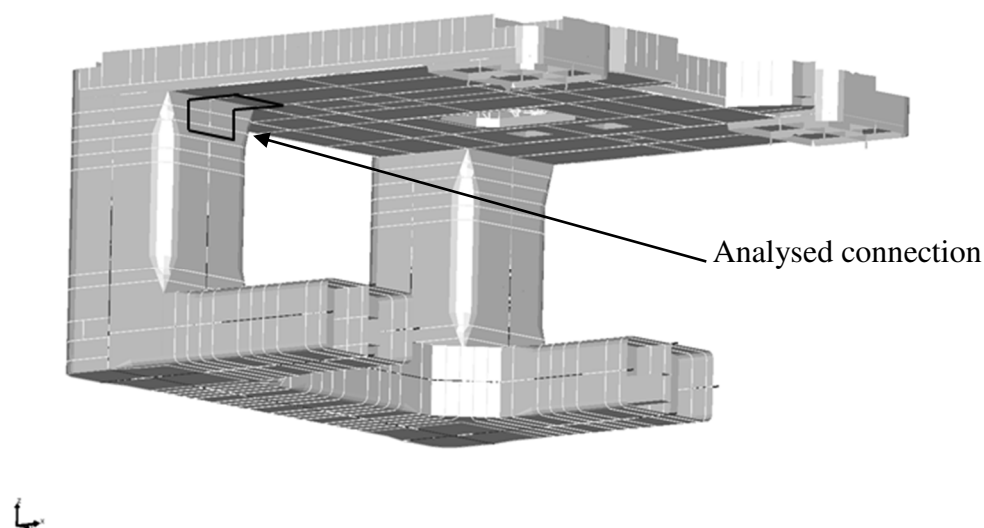


Figure 3.3 Section of the global model used in the case study with the sub-model area highlighted.

The global model is built of plates and beams to ensure the correct stiffness of the model and is analysed with a surface mesh containing 91644 4-node quadrilateral shell-elements for swift calculations. The global model used in the analysis is seen in Figure 3.3 with the smaller sub-model area highlighted. The sub-model is a small part of interest of the global model with similar plate thicknesses on the boundaries in order for the sub-modelling technique to work. The sub-model is meshed with quadrilateral

second order shell elements and modelled in DNV GeniE with prescribed boundary conditions as the boxes on the edges illustrate. The sub-model size is chosen so that local stresses on the boundaries, due to the sub-modelling technique, do not disturb the stresses in the area of interest, see Figure 3.6. The sub-model is approximately 5 m in all directions from the centre and is meshed with 41988 8-node quadrilateral surface elements. The different plate thicknesses in the sub-model can be seen in Figure 3.5. The thicker plating in the centre represents the cast integral in the sub-model.

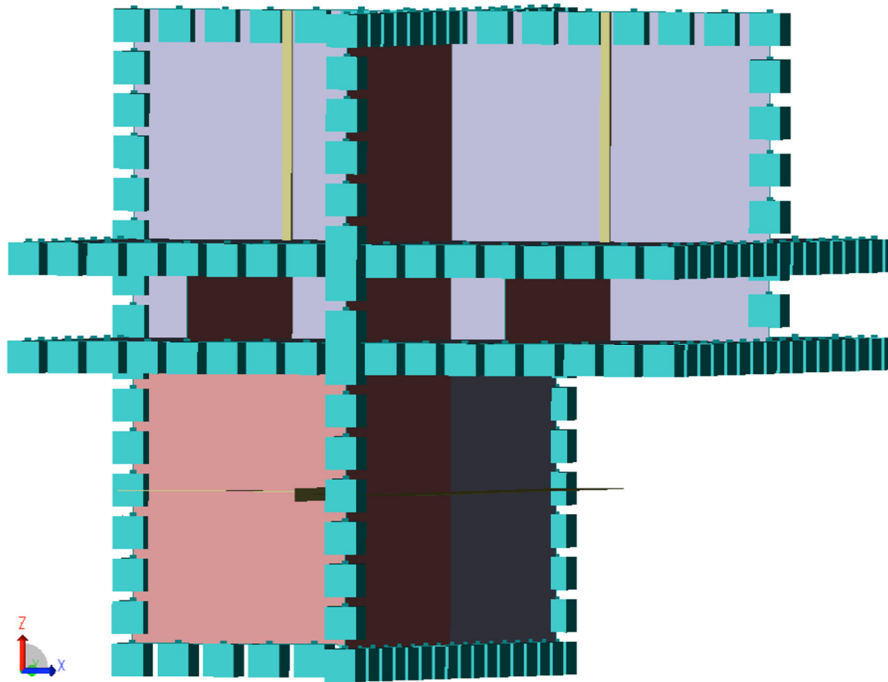


Figure 3.4 Sub-model created in GeniE with prescribed boundary conditions as the boxes on the edges illustrate.

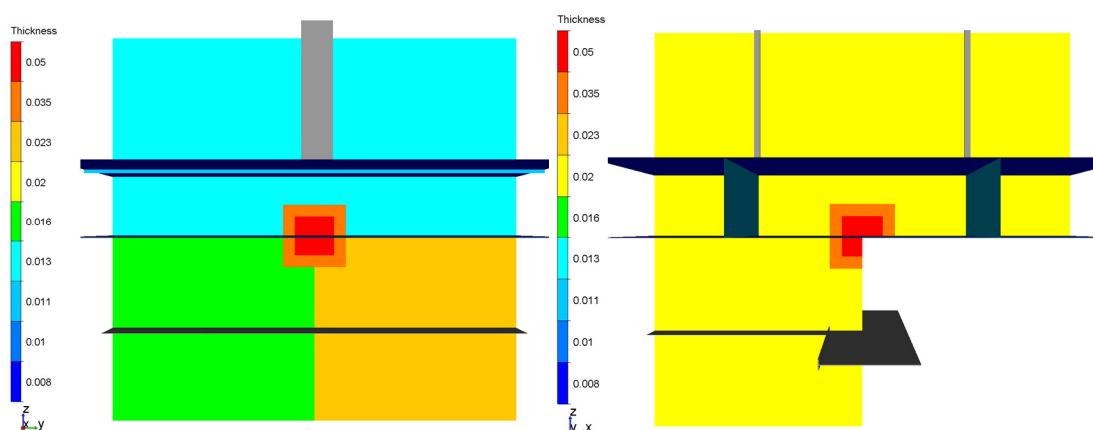


Figure 3.5 Plate thickness in sub-model YZ-view (left) and sideview (right).

The solid CAD-model in Figure 3.6 is created, for an even more detailed analysis in Autodesk Inventor and is approximately 1.5 metres in all directions from the centre. With the solid model the highest level of analysis is performed for the cast integral. The nominal plates have the same thickness as the plates in the sub-model for correct load transfer between the models.

The solid CAD-model is meshed with three-dimensional elements in Patran-Pre (DNV, 2010d) and properties and the prescribed boundary conditions are applied for the sub-modelling technique, see detailed information in Appendix A.

Both tetrahedron and hexahedron elements are considered suitable for the meshing. Hexahedron elements can often achieve good accuracy in slightly less computational time and have a good convergence rate. They can be used in complex 3D geometries with good results. Tetrahedron elements are, however, more geometrically flexible and also less sensitive to initial shape and distortion. First order elements cannot be used for stress analyses, due to the very slow convergence rate. It is concluded that second order 10-node tetrahedron elements must be used, or sometimes even the third-order 20-node elements. Both hexahedron and tetrahedron have pros and cons, but elements used in this assessment are chosen to be tetrahedron elements because of the geometrical benefits (Liu & Quek, 2013).

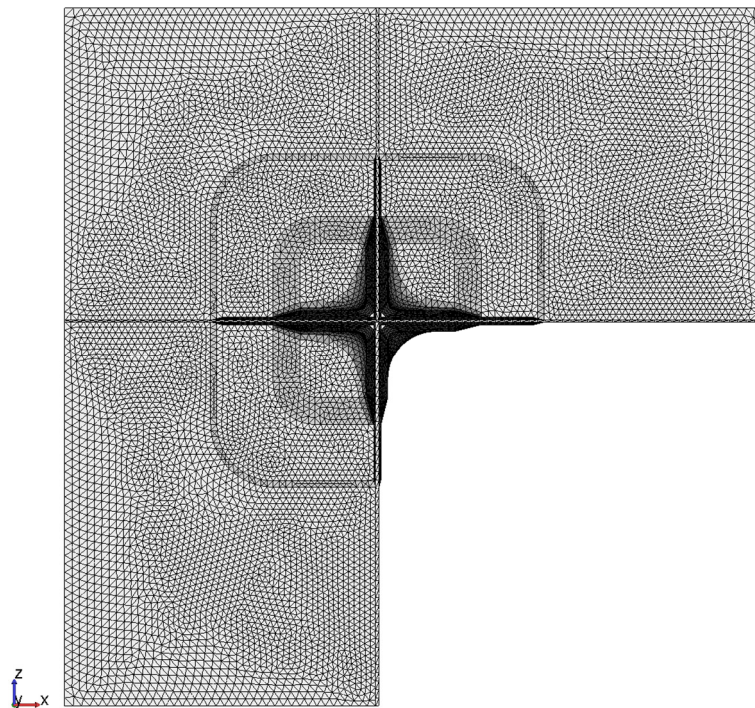


Figure 3.6 XZ-view of the solid model of analysed cast integral with mesh size 30 mm in the centre and 40 mm on the boundaries.

It is not only the element type that is of importance in a mesh but also the inspection of the element properties. Aspect ratio is of major importance for the accuracy of the element and is very important in high stress regions. The best aspect ratio is 1:1 but both Liu & Quek (2013) and DNV-GL (2014) recommend an aspect ratio of up to 1:5. For important regions DNV-GL recommends an aspect ratio of a maximum of 1:3 and for large regions with low stress gradients an aspect above 1:5 is possible to use. The skew angle is also an important parameter, and angles between 60°-120° are accepted.

To be able to choose and verify a suitable mesh size for the specific reference case a mesh convergence study is carried out. The mesh is investigated in the ULS condition described further in Section 3.2, and general von Mises stresses are used. To be able to perform a more dense mesh in the more central parts of the structure the boundary mesh density is fixed for all cases to 40 mm. An element size smaller than 20 mm is not achievable due to the limited computational power available. Three cases are studied and properties and results are listed in Table 3.2.

The calculation time increases dramatically with a smaller mesh size between the cases, although the stress results are quite similar and the accuracy and Case 2 is considered adequate in precision and used in the analyses. The model is meshed with 196932 second-order tetrahedral solid elements.

Table 3.2 Mesh convergence study of the solid model for three different mesh sizes with normalized maximum von Mises stresses in ULS.

	Case 1	Case 2	Case 3
Boundary mesh density	40 mm	40 mm	40 mm
Central mesh density	20 mm	30 mm	40 mm
Number of nodes	898 518	351 161	220 843
Calculation time	740 min	115 min	48 min
Nodal stress general von Mises	1.28	1.24	1.21
Element average general von Mises	1.25	1.17	1.16

3.2 ULS assessment

The general von Mises stresses for solid elements for all the loading conditions are plotted and shown in Figures 3.6 and 3.7. The highest stress in each element for each one of the 61 loading conditions, combined into one load case, contains the highest stresses for each instance. This is done to minimize the amount of stress plots. The maximum stress presented is calculated with the maximum stress from the static load cases added to the maximum cyclic stress.

3.2.1 Yield criterion

The maximum stresses are checked according to Section 2.2.2 against the allowable yield stress using the WSD approach and a usage factor $\eta_p = 0.80$. In Figure 3.6 (left)

the maximum stress in the cast integral is 0.84 and in Figure 3.6 (right) the maximum stress occur in the connection of the nominal plate and the tapering plate with a value of 0.99. In Figure 3.7 the maximum stress occurs in the connection of the nominal plate and the tapering plate with a value of 0.91.

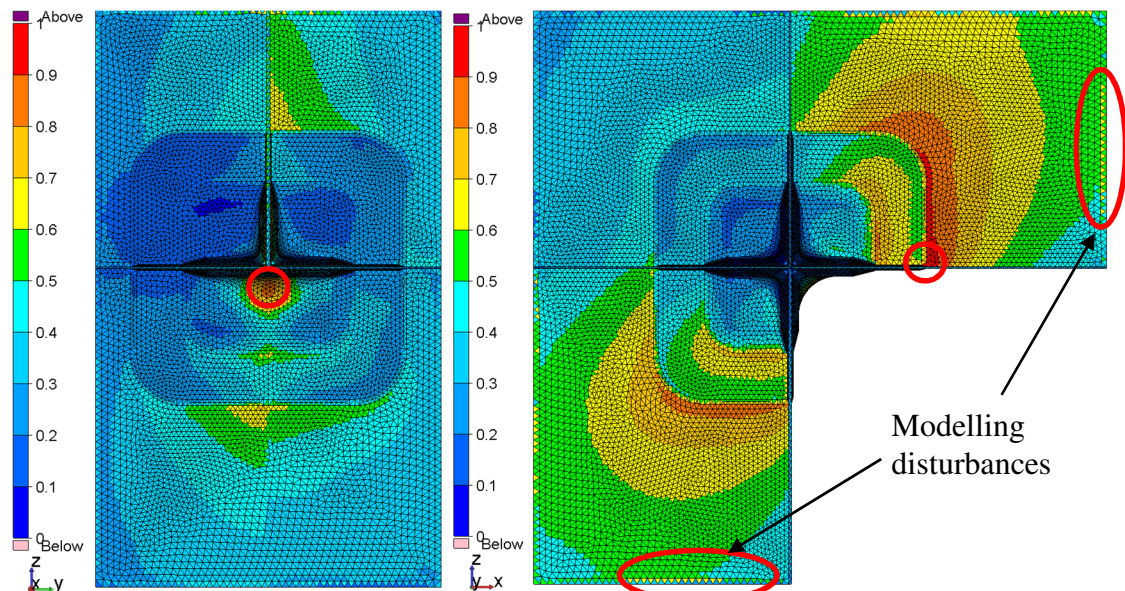


Figure 3.6 YZ-view (left) and XZ-view (right) for solid model of cast integral with mesh size 30 mm in the centre and 40 mm at the outer edges, normalized von Mises stresses, maximum stress (left) 0.84, maximum stress (right) 0.99.

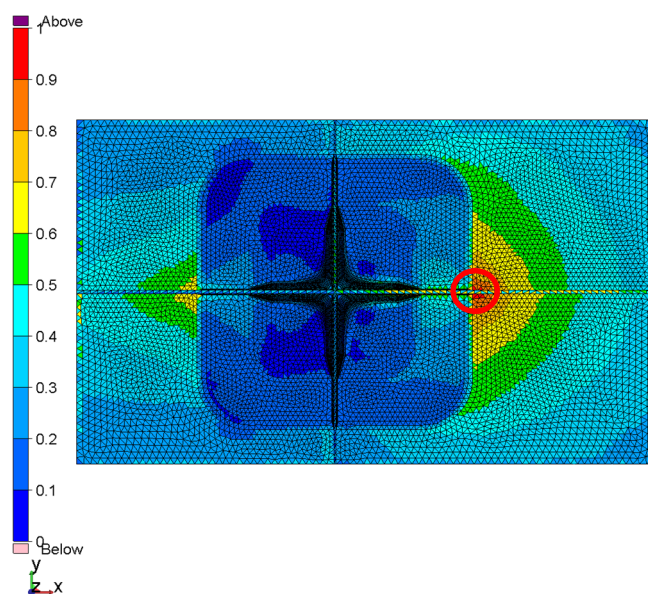


Figure 3.7 XY-view (top view) of solid model of cast integral with mesh size 30 mm in the centre and 40 mm at the outer edges, normalized von Mises stresses, maximum stress 0.91.

The column inner corner is also investigated for the un-modified (reference) structure, see Figure 3.8 and Figure 3.2 for the inner corner location. The stresses are distributed around the thicker plates added to represent the cast integral used in the corner.

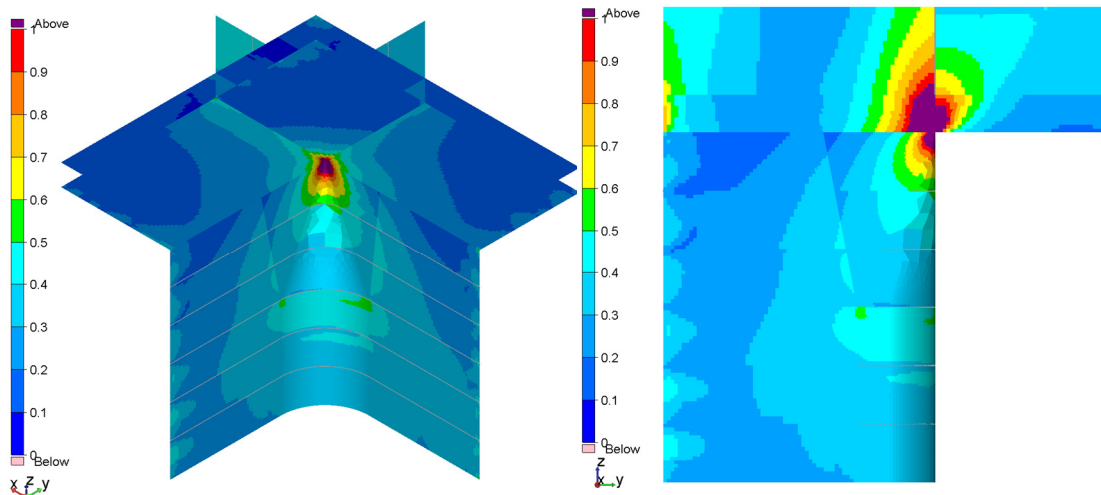


Figure 3.8 Isometric view (left) and XZ-view of the reference structure corner with maximum von Mises stresses.

3.2.2 Buckling analysis

To perform a buckling analysis of the centre bulkhead cast integral, the nominal plates are checked against buckling. The buckling analysis is performed in accordance with Section 2.2.2 and with the conservative assumption that the nominal plate will buckle before the thick cast integral. The cast integral is therefore not checked against buckling itself.

The maximum von Mises stress in the longitudinal and transverse directions and the highest shear stress is combined for the buckling analysis. The calculated usage factor of 0.67 shows that there is no risk of buckling for the cast integral.

3.3 FLS assessment

The maximum principal stress on the surface is evaluated according to Section 2.3.5. Fatigue class “C” can be used for the cast integral and due to the large stress gradient in the cast, a reduction of thickness is needed, see Section 2.3.3 (DNV-GL, 2014).

Due to the known sensitivity for fatigue damage in welds, they are considered in the assessment. The fatigue class “D” is investigated according to Section 2.3.2 with the hot spot method. The structure is located in air at all times, which is why S-N curves for air are used. A higher classification on the S-N curve may be used when the principal direction is different from the normal to the weld, see Figure 2.12. Following the procedure for welds classification, an even higher fatigue class can be allowed together with high demands on the production, but this is not investigated in this thesis (DNV-GL, 2014).

Due to the local design of the cast integral, fatigue stresses are calculated in the solid model. The correct geometry with plate alignments, etc., is modelled, and hence no stress concentration factor (SCF) needs to be applied to the stresses. The design fatigue factor is taken as “1” for semi-submersibles following normal inspections every 5th year (DNV, 2014c).

The geometry is evaluated for a fatigue life of 30 years in the Gulf of Mexico, which corresponds to $2 * 10^8$ load variations cycles. As described in Section 2.3.1, the fatigue stresses are scaled to the desired fatigue life, see Equation (2.14).

The results presented in Table 3.3 show that the damage due to fatigue is fairly low for all the welds. Figures 3.9 and 3.10 show the normalized principle stress used in the fatigue damage calculations. The weld with highest fatigue damage is found to be the connection between nominal and tapering plate, P7, see Figure 3.10. The fatigue damage of the cast integral is found to be very small.

Table 3.3 Fatigue damage of the cast integral.

ID	Location	Fatigue class	Damage
P1	Nominal (20 mm)/Tapering (35 mm)	D	0.14
P2	Tapering (35 mm)/Cast (100 mm)	D	0.48
P3	Cast center	C	Less than 0.1
P4	Tapering (35 mm)/Cast (100 mm)	D	Less than 0.1
P5	Nominal (16 mm)/Tapering (35 mm)	D	Less than 0.1
P6	Nominal (8 mm)/Tapering (35 mm)	D	0.30
P7	Nominal (10 mm)/Tapering (35 mm)	D	0.53

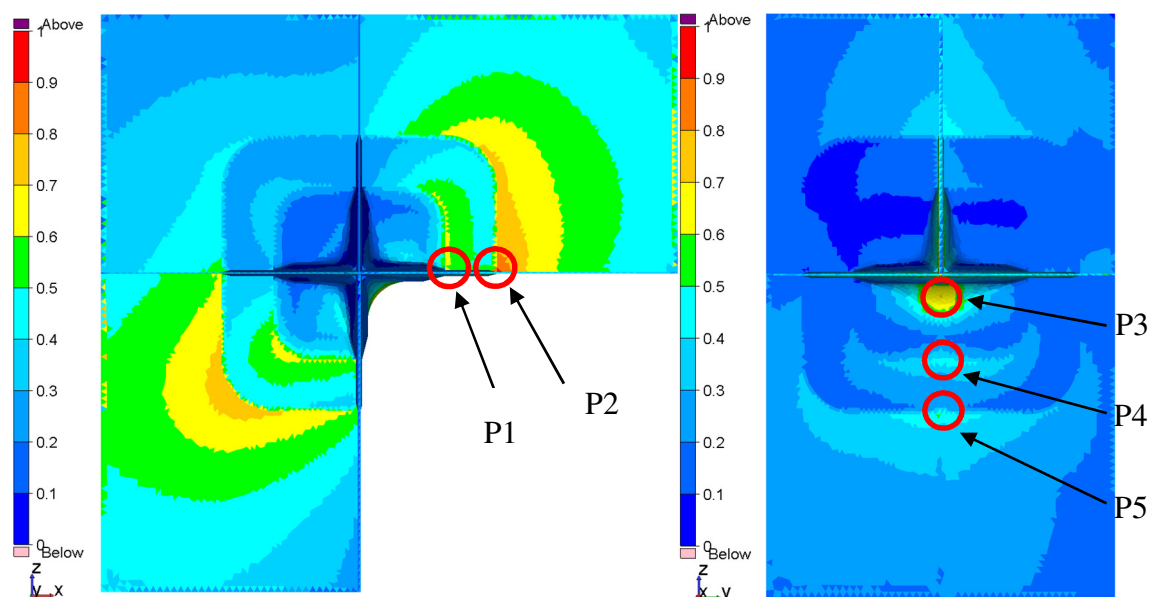


Figure 3.9 Fatigue locations with highest principal stresses, numbered for Table 3.3.

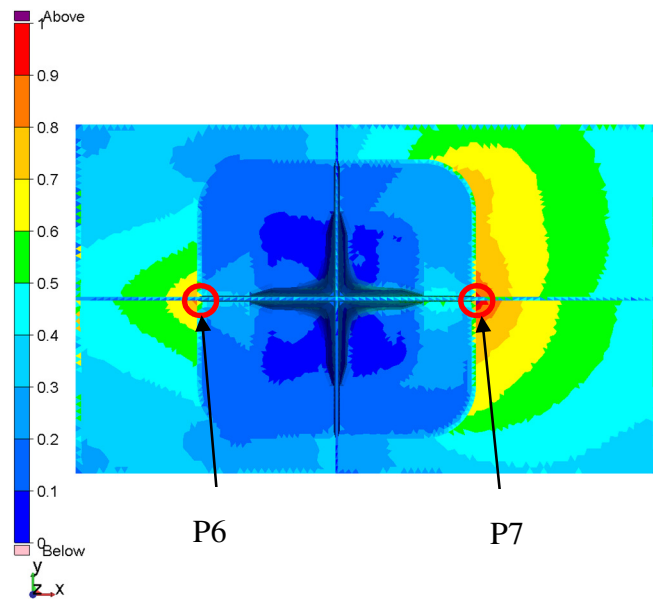


Figure 3.10 Fatigue locations with highest principal stresses, numbered for Table 3.3.

4 Investigation of possible cut-out designs

It is known that adding a fillet to sharp corners can lower stress concentrations and redistribute the stresses around the corner. Another technique is to add material to the areas of high stresses and thereby lower the stresses, with the effect that the detail is strengthened and stiffened (Kwok-Wai Chan, 1981). This may result in the detail becoming “too” stiff for the adjacent structure, and therefore increases the stresses in the connection between the stiff detail and soft surrounding. The investigated cast integral is an example, see Figure 4.1, where both a fillet and thicker plating is used.

Another common design is to use stress relieving notches or cut-outs, which are investigated in this thesis, to redistribute the stresses and therefore lower the stress concentration (Bijak-Zochowski et al., 1991). This type of design can be advantageous in the manufacturing process or when weight optimization is of concern.

The two principles are different in the fundamental design philosophy, either adding material to strengthen the detail or to change the stress flow in the detail by removing material with a cut-out or notch and therefore reduce the stiffness of the connection.

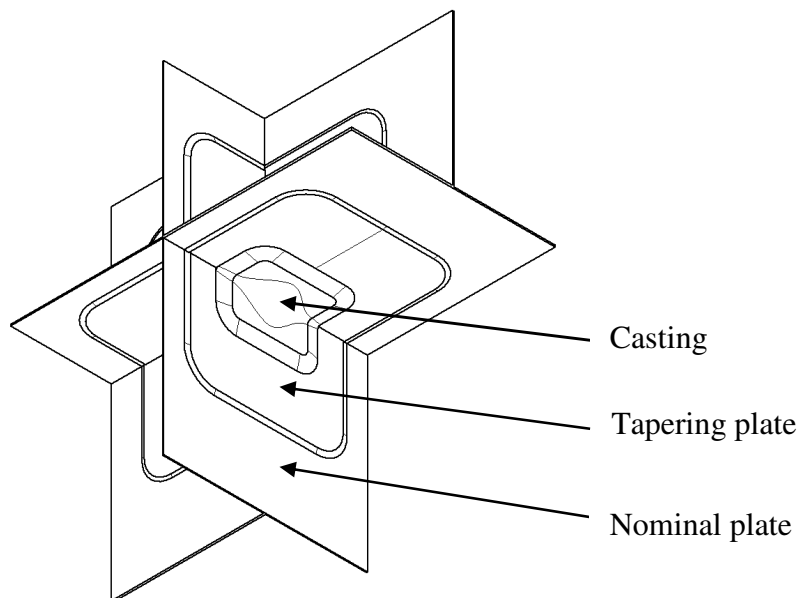


Figure 4.1 Isometric view of cast integral used in the column/deck-box connection together with tapering plates.

4.1 Consequences following a cut-out design

One of the main advantages using a cut-out design instead of a cast integral is the increased fatigue resistance. In the industry, notches have been widely used in order to reduce the risks of fatigue and are mostly used in small machined components where experimental charts describe the stress concentrations well. Even with smooth notches stress concentrations occur due to the change in geometry, but the stress can be redistributed to a known location in the detail. The best way of reducing the stress in the notch is to develop an alternative design where Lundh (2000) specifically suggests a large radius. Tabulated values imply that geometrical shape factors vary significantly for different radiuses (Institutionen för hållfasthetslära KTH, 2008). It should also be

noted that material fatigue resistance decrease with increasing material thickness, which is especially known for casted products (Lundh, 2000).

The potential use of a cut-out design would probably decrease the weight and lower the stress concentrations in the node connection. Various shapes and the direction of cut-outs have been studied in simplified load conditions in plates before, which are used as a basis for the cut-out design (Bijak-Zochowski et al., 1991).

The shape and bluntness of the cut-out must be investigated since corners and changes in the cut-out geometry give rise to stress concentrations (Kumar et al., 2013). The shape of the cut-out and adjacent structure needs to be investigated for the specific case due to the complex loading conditions. It is also shown that the cut-out geometry is dependent on the loading condition, bluntness and shape of the cut-out (Rezaeepazhand & Jafari, 2010). A variable notch radius could also be suitable for lowering the stress concentrations and improving the design (Mattheck, 2006) and (Taylor et al., 2011). A variable radius is, however, not applicable in the parametric study performed and is therefore regarded as future work.

4.2 Parametric study of a 2D geometry

To investigate different cut-out geometries and their stress distribution a simplified parametric study is performed. The connection between the horizontal centre bulkhead in the deck-box and the centre vertical bulkhead in the column, see Figure 4.2, have a simple geometry where a cut-out can be implemented. The purpose of the 2D analysis is to understand different geometric shapes and their responses in specific loading conditions. The different loads on the structure are illustrated with a 2D-model with simplified loading conditions and boundary conditions, see Figure 4.3.

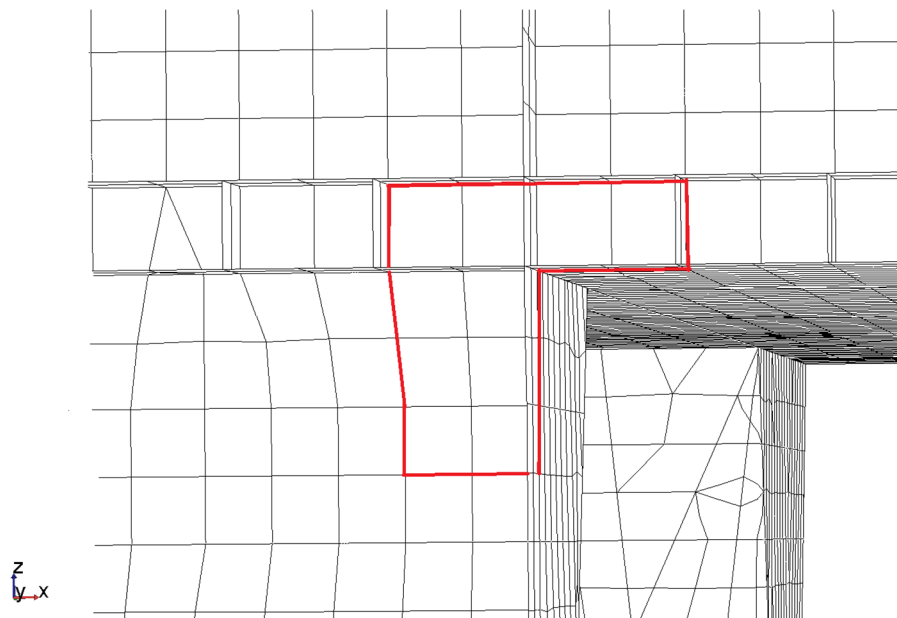


Figure 4.2 Section of the global model with the analysed node connection highlighted.

The global hydrodynamic responses from the loads acting on the semi-submersible can be divided into split forces between the pontoons, torsion moments, shear forces and

accelerations of deck mass, see Section 2.1 (DNV, 2012). It is noted that the longitudinal shear force will give a larger response than for split and torsion moments at the column/deck-box connection, but that the combination of shear forces and split forces also need to be investigated (Zhang et al., 2009). Symmetry conditions of the semi-submersible make the connection similar for all columns and a cut-out geometry and corresponding responses are therefore calculated in a simplified 2D-case and a principal geometry of a stress relieving cut-out is decided.

The boundary conditions and applied loads for the analysis are defined by Figure 4.3, which presents the three different loading conditions; tension, bending and shear. The material properties used are presented in Table 3.1. Load cases and support points are for the different cut-out geometries unchanged in the study. The loads represent the governing load cases for typical ring-pontoon semi-submersibles, but due to the simplification in 2D the transverse loads are not regarded. The transverse plating will also induce stiffness to the node connection that cannot be modelled in 2D, but is instead investigated in the 3D case study, see Chapter 5.

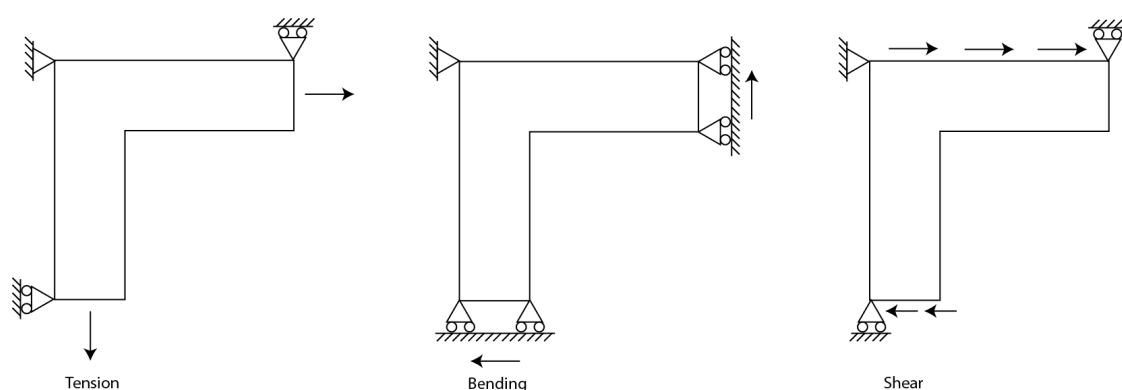


Figure 4.3 Sketch of boundary conditions and applied loads for the 2D parametric study for the results presented in Table 4.2.

A stress concentration factor (SCF) is defined as the maximum general von Mises stress in the geometry divided with the nominal stress for stress concentration comparison between different designs, see Equation (4.1). The nominal stress is calculated for the vertical plate, see Figure 4.4.

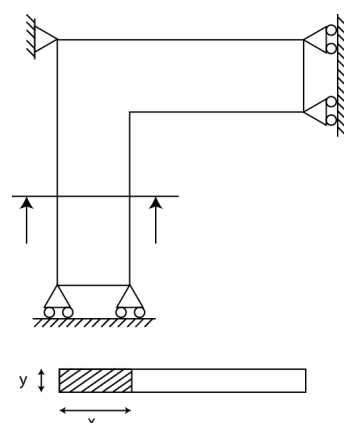







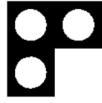


Figure 4.4 Area used for calculation of nominal stress.










$$SCF = \frac{\sigma_{max}}{\sigma_{nom}} \quad (4.1)$$

The different cases studied and the corresponding stress factors are listed in Table 4.1. The different geometries are tested to minimize the response in all three loading conditions. All cut-outs are designed with constant radii to simplify the modelling procedure and interpretation of responses. Case number 12 and 13 “butterfly cut-out” are reference designs used in semi-submersibles to increase fatigue resistance (Nygård, 2003). The cut-out design based on a large radius, case number 14, with an open corner is based on a previous GVA design.

A design with a 90° corner is used for reference and the test show that increasing the cut-out radii is a good way of lowering the SCF. In particular the SCF in shear and bending decrease with a larger radius. The parametric study shows that an open corner and a large radius decreases the stress response in all three loading conditions.

Table 4.1 Investigated cases of cut-out designs and corresponding SCF for the three different loading conditions in Figure 4.3; tension, bending and shear.

Case	Description	SCF		
		Tension	Bending	Shear
1 - 90° corner		6,4	31,15	14,47
2 - 40 mm tapering plate		3,73	19,8	8,22
3 - Undercut		5.29	15,19	8,95
4 - Hole radius 0.5 m		1,54	14,74	10,89
5 - Hole radius 1 m, 1.5 m from corner		10,91	35,29	17,14
6 - 3 holes		9,94	25,35	16,45
7 - Hole radius 1 m, 0.75 m from corner		21,88	77,64	43,26
8 - Circle radius 2 m		1,67	10,83	10,34

9 - Circle radius 2 m offset		0,85	8,55	6,6
10 - Radius 3.08 m		1,87	6,93	4,21
11 - Radius 6.43 m		3.67	5,74	3,72
12 - “Butterfly 1 cut-out”		3,69	16,25	10,87
13 - “Butterfly 2 cut-out”		29,18	12,78	8,42
14 - Radius 3.18 m		2,57	7.26	4,82
15 - Radius 4.81 m		2.52	6.30	3.95
16 - Radius 5.42 m		2.48	6.06	3.77
17 - Radius 6.25 m		2.52	5.80	3.58

The best overall design is found to be case 17 with a low SCF in all three load conditions, see Figure 4.5 for the bending condition. Keeping as much material as possible and at the same time having a large radius by adding a cut-out lowers the stress concentrations, which is also suggested by previous work on cut-outs (Kwok-Wai Chan, 1981). The shape of the cut-out design is smooth and no sudden geometrical changes are allowed to reduce stress concentrations.

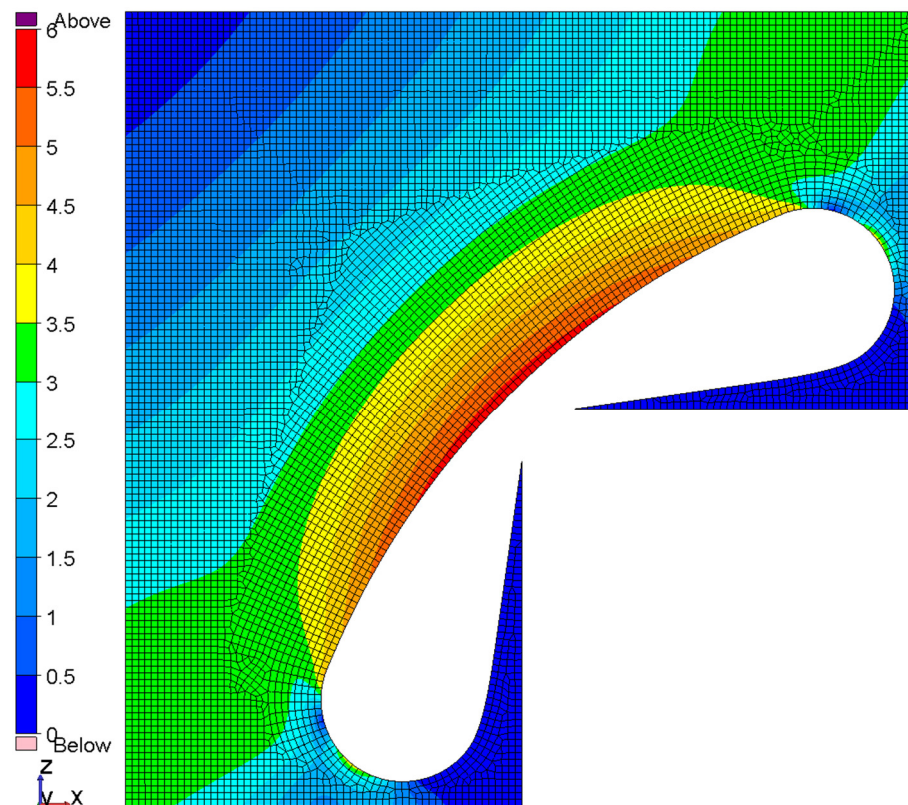


Figure 4.5 Case 17 from Table 4.2 in bending condition with a SCF and mesh size of 50 mm.

From the parametric study the conclusion is made that it could be possible to apply a cut-out design in the node connection and reduce the stresses. The cut-out must, however, be designed individually depending on stress direction and the surrounding structure in the specific area. The simplified load models and geometry of the cut-out must also be investigated for a complete semi-submersible to ensure correct results.

5 Analysis and assessment of a cut-out design

The case study in this chapter is based on the parametric study of a 2D geometry in Section 4.2. Designs 15, 16 and 17, see Table 4.2, and the corresponding SCF tend to converge and performs very well for the three load cases; bending, shear and tension. These cut-outs are the base for further investigation in the semi-submersible structure. The cut-outs are investigated in ULS, FLS and weight in accordance with Section 2.1.

5.1 Geometry and mesh

The same procedure as for the cast integral is used for analysing the cut-out design, see Section 3.1. The same sub-modelling technique is used and the sub-model of the cut-out with the prescribed boundary conditions on the edges is presented in Figure 5.1.

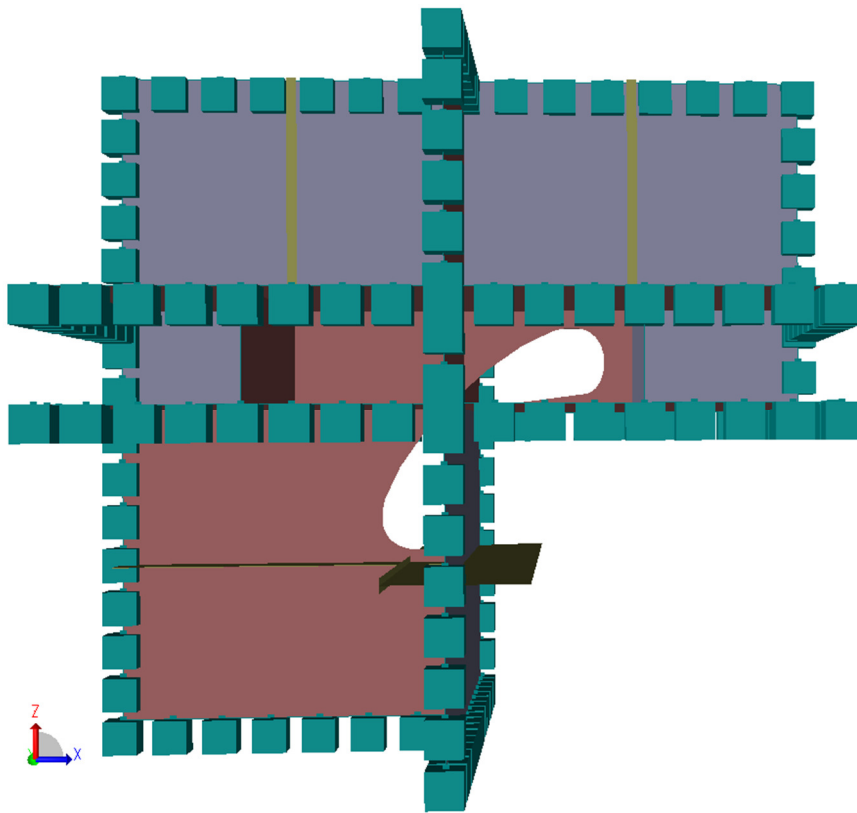


Figure 5.1 Sub-model in XZ-view used for the cut-out design with prescribed boundary conditions illustrated as boxes on the boundaries.

As described in Section 1.3, the main characteristics of the complete structure needs to be maintained and only minor changes are implemented. This involves the watertight plating in the corner; hence the cut-out design must not penetrate the vertical and horizontal outer plates in the structure.

When the cut-out design was applied to the sub-model it was found that due to the transverse plating in both vertical and horizontal direction, stress concentrations appeared in the corner connection, see Figure 5.2. For the cut-out design to work as intended, penetrating holes in the vertical and horizontal tapering plates, which the cut-out radii intersect, was used to create a free edge of the cut-out, see Figure 5.3.

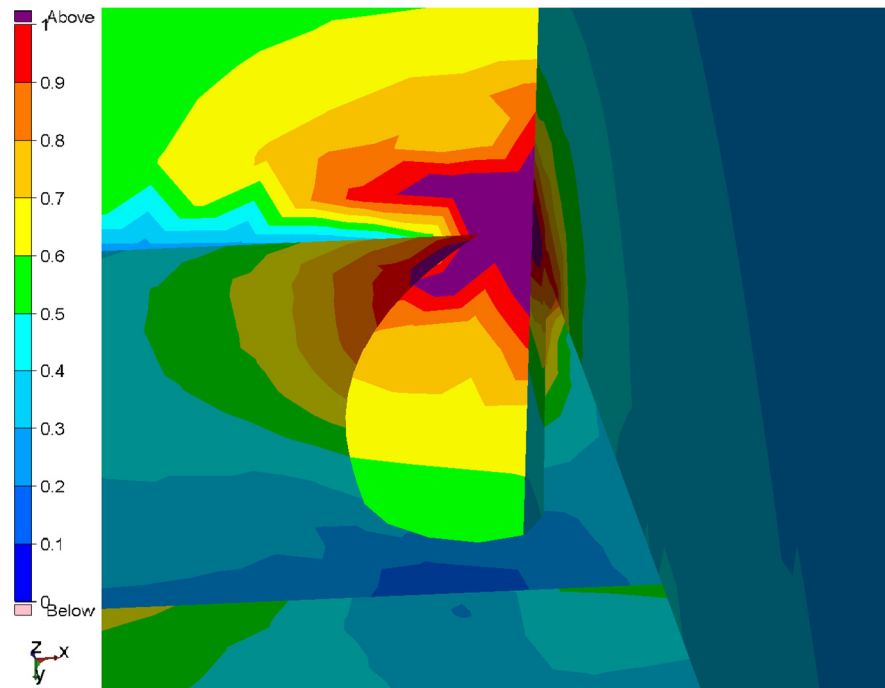


Figure 5.2 Zoomed view according to coordinate system, maximum von Mises stresses in the horizontal plate without hole.

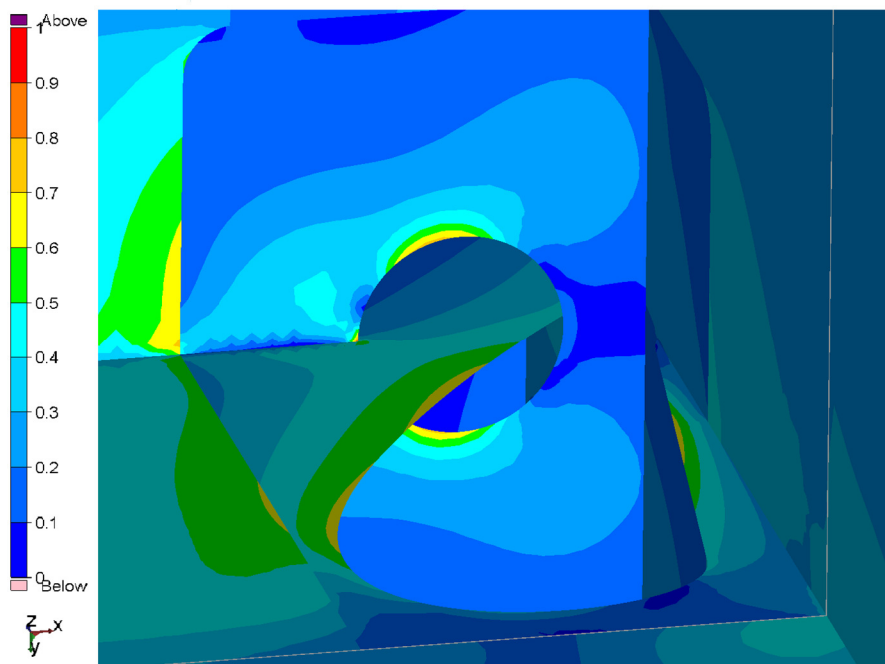


Figure 5.3 Zoomed view according to coordinate system, maximum von Mises stresses in the horizontal plate with hole.

Figure 5.4 present a drawing of the cut-out design in both XZ-view (left) and isometric-view (right), with the vertical and horizontal tapering plates and holes for the free edge of the cut-out radius to intersect. The three governing parameters recognized as the cut-out parameters recognized as the cut-out radius “ R ”, plate thickness “ t ” and tapering plate hole radius “ r ” which are important for the parametric study in Section 5.2 are also highlighted in Figure 5.4.

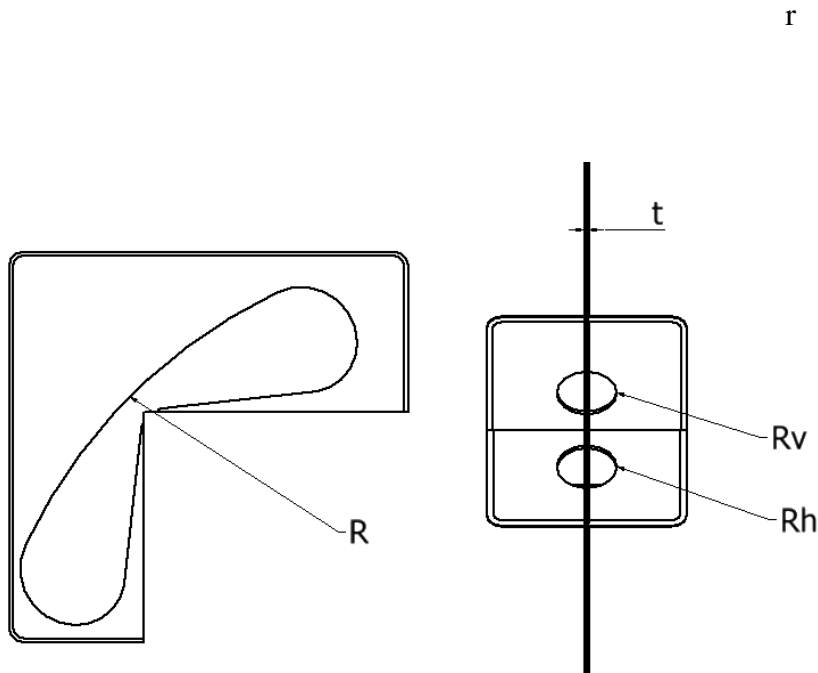


Figure 5.4 Governing dimensions of the cut-out design. XZ-view (left) with the cut-out radius R and isometric-view (right) with plate thickness t and both vertical and horizontal tapering plates with hole radius r .

A mesh comparison for the sub-model is performed in a similar way as for the cast integral. Four different mesh sizes are investigated as well as the corresponding stresses at four locations, see Appendix B for more details. The sub-models are investigated in ULS and the maximum von Mises stress in the different locations are noted. The element size together with a featured edge create a stretch function of the mesh, where a more dense mesh can be used in the areas of interest and a coarse mesh on the boundaries to reduce the computational time. A skew angle between 60° to 120° is accepted together with a Jacobian between 0.5 and 5 (Liu & Quek, 2013) and (DNV-GL, 2014). The mesh density is investigated for the sub-models, see Table 5.1, and found to have low influence of the measured stresses. The chosen mesh is 60 mm in the centre and 120 mm on the boundaries for the sub-model.

Table 5.1 Mesh comparison of four different mesh sizes for quadrilateral shell mesh, with normalised von Mises stresses.

	Case 1	Case 2	Case 3	Case 4
Boundary mesh	180 mm	120 mm	120 mm	120 mm
Central mesh	60 mm	60 mm	40 mm	30 mm

Number of nodes	69 000	112 000	135 000	174 000
Calculation time	14 min	53 min	74 min	126 min
Stress 1 (von Mises)	0.673	0.673	0.677	0.680
Stress 2 (von Mises)	0.843	0.845	0.853	0.873
Stress 3 (von Mises)	0.743	0.745	0.751	0.754
Stress 4 (von Mises)	0.620	0.622	0.650	0.652

The most detailed “solid model” is meshed with a more dense mesh, 30 mm in the centre and 40 mm on the outer edges, to fulfil requirements in the classification rules, see Figure 5.5.

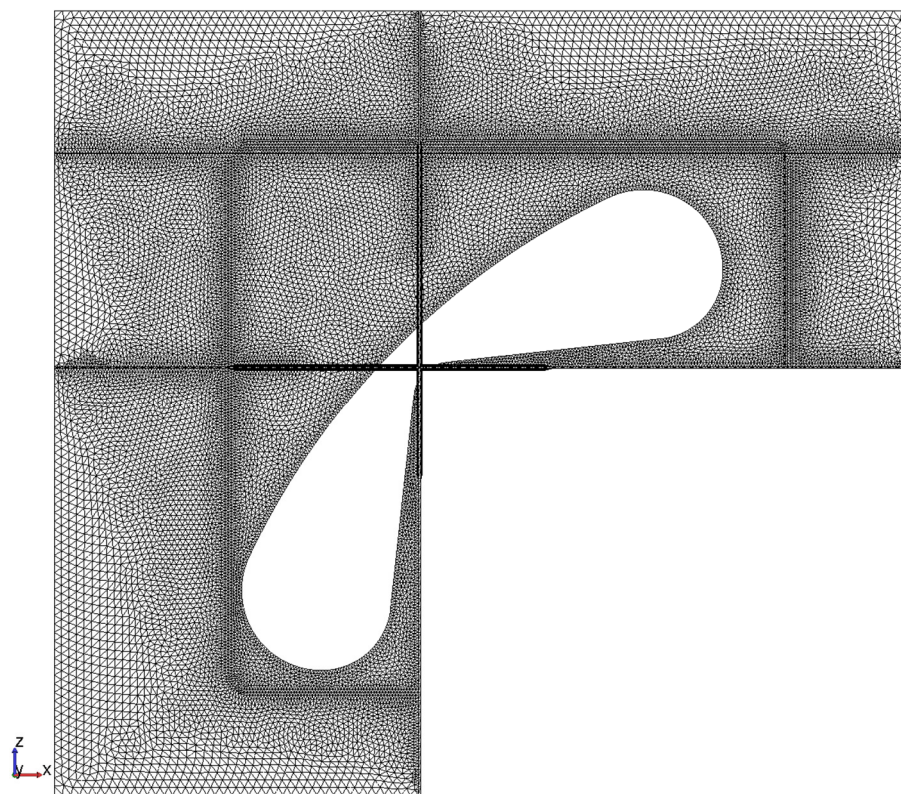


Figure 5.5 Solid model in XZ-view of a cut-out design with mesh size of 30 mm in the centre and 40 mm at the outer edges.

5.2 Parametric study of the cut-out geometry

To investigate and find a solution for the cut-out design, three major properties of the design are identified, see Figure 5.4. The holes in both vertical and horizontal tapering plates have the same dimension due to simplifications in the design stage.

To investigate how the parameters act together and associated responses in the semi-submersible, a parametric study is performed. The parametric assessment includes 45

different cases, see Table 5.2. Each cut-out radius is evaluated 9 times, due to the fact that each hole radius is tested with 3 different plate thicknesses. The parametric study is performed for the created sub-models and the final design is investigated in a solid model. The general von Mises stress is used in the design evaluation and the highest stresses for each loading condition are evaluated.

Table 5.2 Properties of the different cut-out designs; in total, 45 different designs are evaluated.

Cut-out radius, R [mm]	Hole radius, r [mm]			Plate thickness, t [mm]		
2190	200	300	400	20	30	40
2900	200	300	400	20	30	40
4080	200	300	400	20	30	40
5370	200	300	400	20	30	40
12500	200	300	400	20	30	40

Detailed information about the parametric evaluation is found in Appendix B. Figure 5.6 presents the combined average von Mises stress of four stress locations, depending on tapering plate hole radius and thickness of the plates for the cut-out radius of 5370 mm. These four stress locations are defined in Figure B.4 and the average evaluation is performed to identify with the best overall design. The cut-out design with a tapering plate hole radius of 300 mm and a plate thickness of 40 mm is found to be the best in the average evaluation.

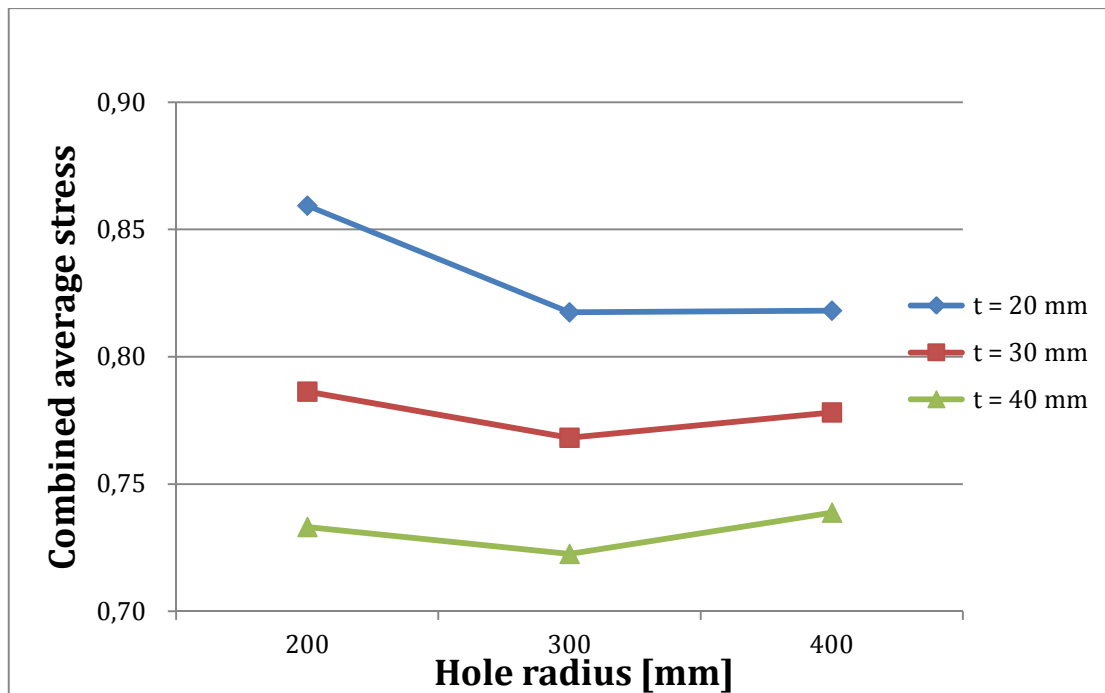


Figure 5.6 Cut-out radius of 5370 mm and varying tapering plate hole radius and plate thickness. Combined average stress of the four identified stress locations.

The results from the parametric study are presented in Appendix B, and the final design of the cut-out is shown in Section 5.3 and 5.4. The design with plate thickness 40 mm and hole radius 300 mm performed the lowest average stress in the structure and also the lowest weight of the different cut-out designs, see Figure 5.7.

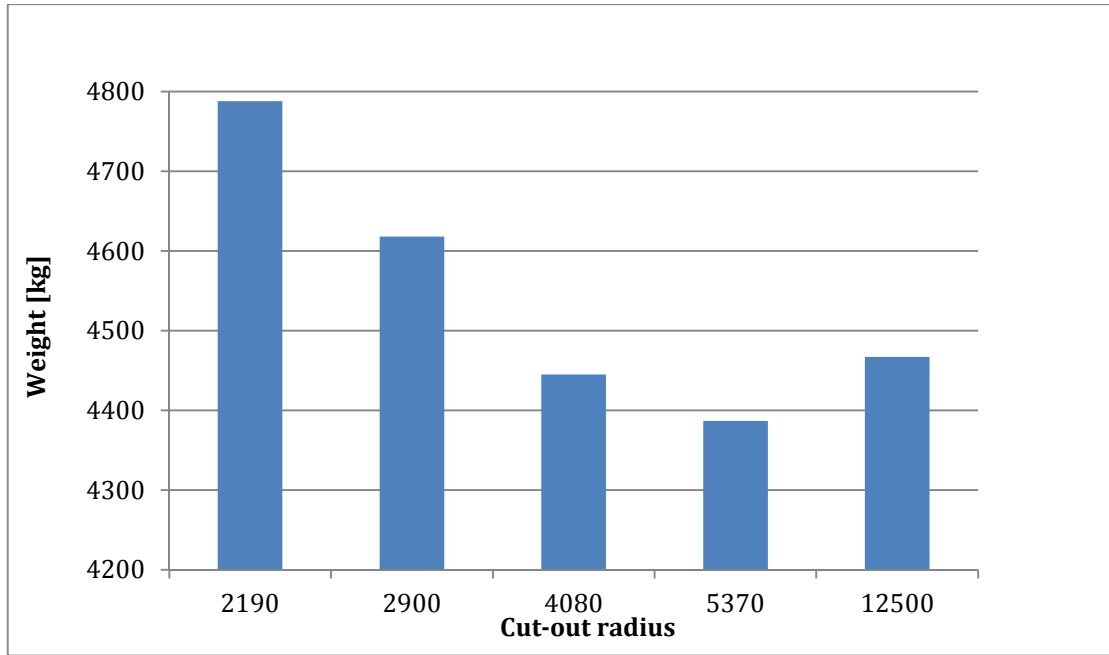


Figure 5.7 Weight for the different cut-out designs, with tapering plate hole radius 300 mm and plate thickness 40 mm.

5.3 ULS assessment

This section presents the final cut-out design for the case study. The solid model analysed is shown in contour plots with the highest normalized von Mises stresses in the ULS condition. The stresses presented are the highest stresses for each element in all 61 loading conditions combined into one stress plot for easier comparison and handling of stress plots. This is possible due to the comparison of maximum stress compared to the permissible stress in the local design, see Section 2.2.1.

5.3.1 Yield criterion

The maximum stresses are checked according to Section 2.2.1 against the allowable yield stress using the WSD approach and a usage factor $\eta_p = 0.80$. As is presented in Figures 5.8 to 5.10, the highest stress concentration on the radii is 0.69 of the normalized stress value. The highest stress on the vertical hole is 1.01 and 0.92 at the horizontal hole.

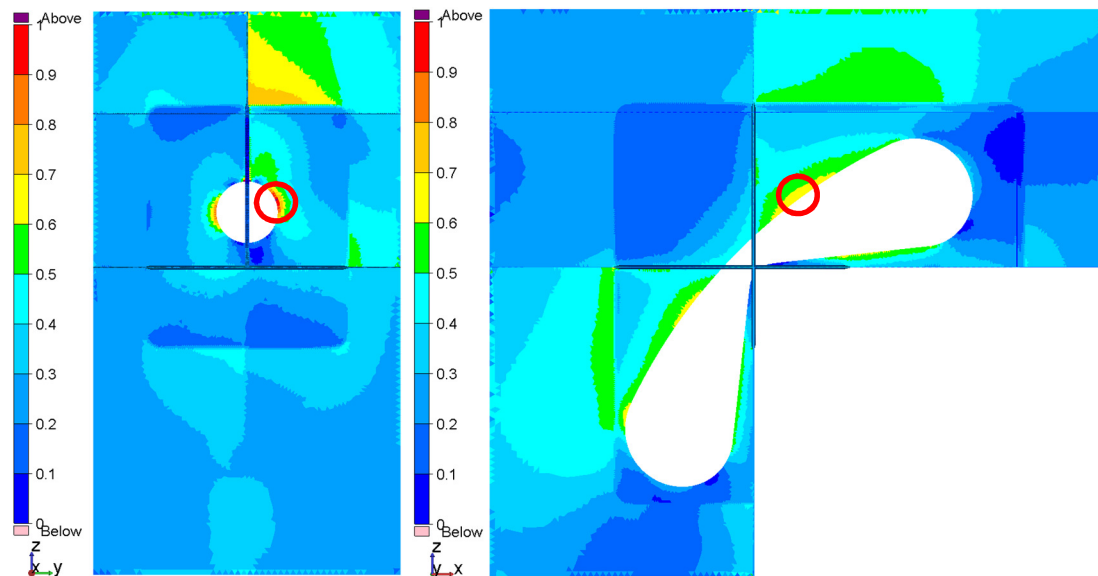


Figure 5.8 *YZ-view (left) and XZ-view (right) of solid model with the maximum von Mises stress of 1.01 at the vertical tapering plate hole radius (left) and 0.69 on the edge of the cut-out radius (right).*

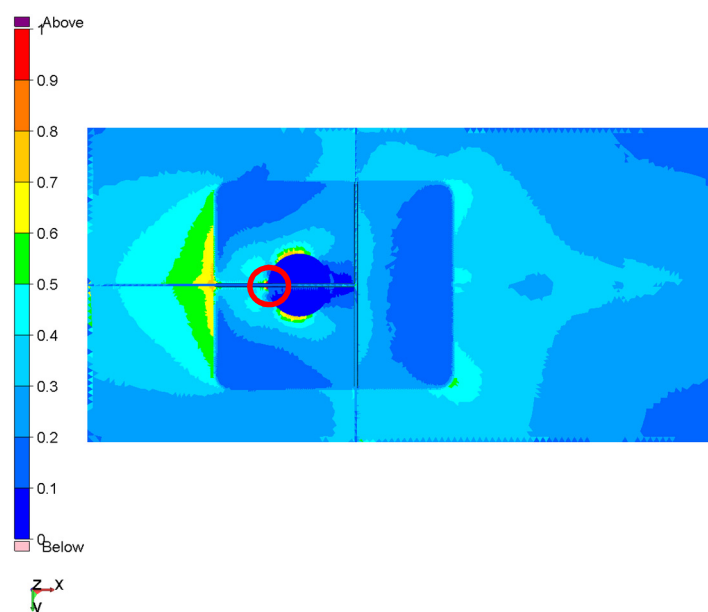


Figure 5.9 *XY-view of the solid model from below with maximum von Mises stress 0.92 on the horizontal tapering plate hole radius.*

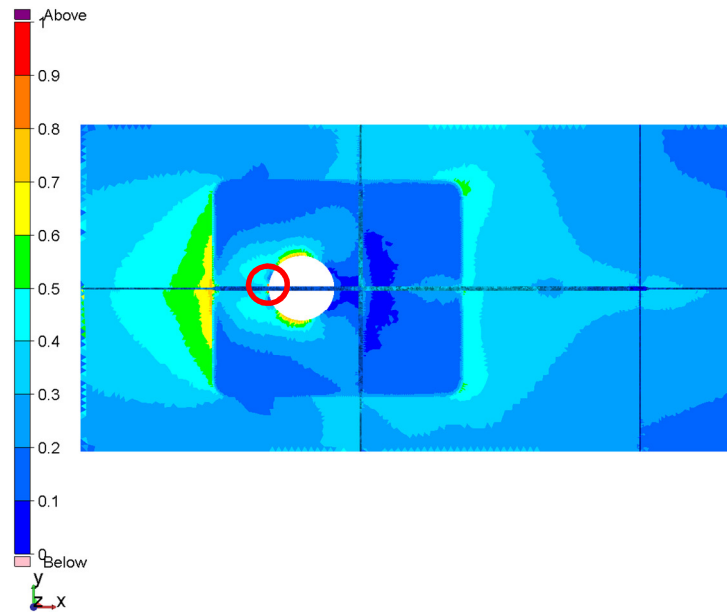


Figure 5.10 XY-view solid model from above with maximum von Mises stress 0.92 on the horizontal tapering plate hole radius.

The adjacent corner is also investigated with the cut-out added to the structure. Figure 5.11 illustrate von Mises stress in ULS with the final cut-out design added to the centre bulkhead connection in both longitudinal and transverse direction. The structure of the corner is unchanged. As shown in the stress plot, the highest stresses occur in the intersecting corner and the stresses are distributed around the thicker plating in the corner.

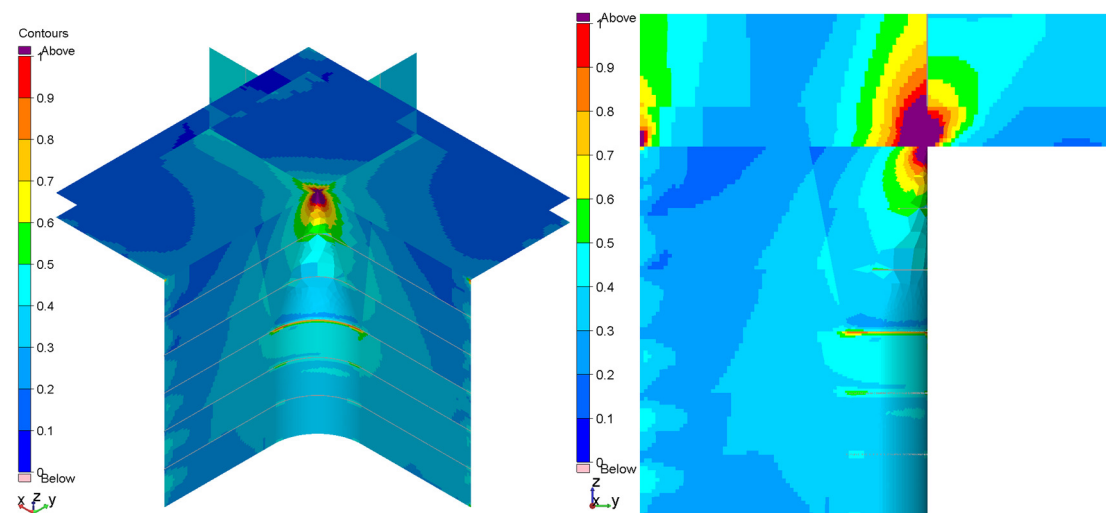


Figure 5.11 Isometric view (left) and XZ-view (right) of the column corner with the influence of cut-out design with maximum von Mises stress.

5.3.2 Buckling analysis

The buckling analysis follows the simplified procedure presented in Section 2.2.2. Figure 5.12 visualizes the cut-out design and its measurements. For the cut-out design the aspect ratio is not used due to the conservative use of Bijlaard's plate factor used in

the buckling analysis. The buckling check is made from the identified maximum von Mises stress in axial load with the highest stress in compression and the highest identified shear stress.

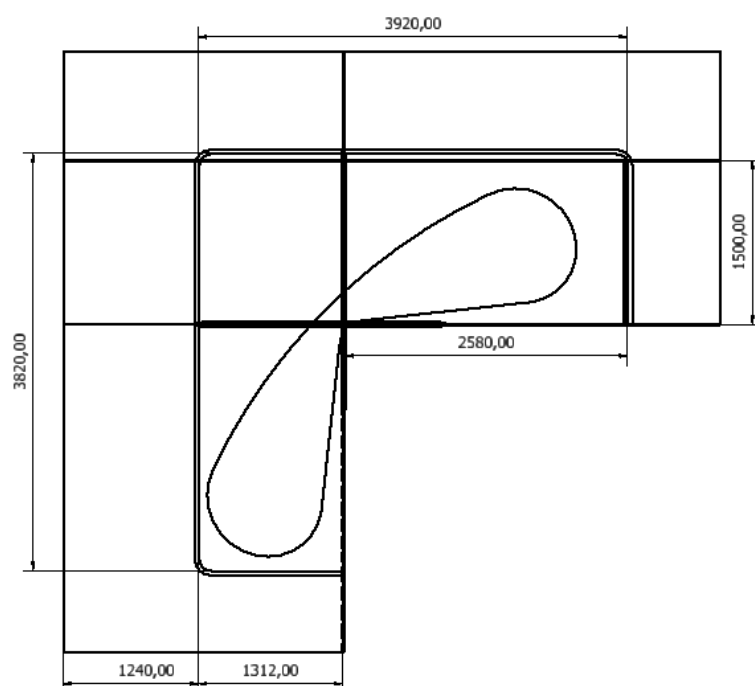


Figure 5.14 Drawing with dimensions for cut-out design for buckling analysis.

The critical stress for buckling deformation varies between authors. However, to be conservative, the plate factor of (Bijlaard, 1957) is used in this thesis. The critical stress is corrected with Johnson-Ostenfeld's criterion, see Equation (2.8).

The plate factor for combined compression and shear force is with the use of Equation (2.12).

$$k = k_{\infty} + \frac{\alpha_1 r + \alpha_2}{\alpha_3 r + \alpha_4 + \beta^{\alpha_5}} = 0.51$$

The usage factor from Equation (2.9) is applied to illustrate how close to the actual stress the critical stress is.

$$\eta = \frac{\text{Actual stress}}{\text{Critical stress}} = \frac{\sigma_{\text{applied}}}{\sigma_{\text{critical}}} < 1$$

The highest calculated value in the buckling analysis with highest stress in compression is $= 0.49$, which is below the critical value. Hence, the structure runs no risk of buckling.

5.4 FLS assessment

The stress plots from the simplified fatigue analysis of the cut-out are shown in Figures 5.13 to 5.15. The maximum principal stresses are used in the fatigue damage calculation, see Section 2.3.2.

Weld classification “D” is used for the plate connections in accordance with the hot spot method, and for the complicated geometry around the horizontal and vertical hole fatigue class “F” is used. The selection of weld class is made with regard to geometry and acting loads (DNV-GL, 2014). The accumulated fatigue damage from the simplified and stochastic fatigue analysis is listed in Table 5.3. The results show low fatigue damage and the relationship between stochastic and simplified assessment is as expected, see Section 2.3.

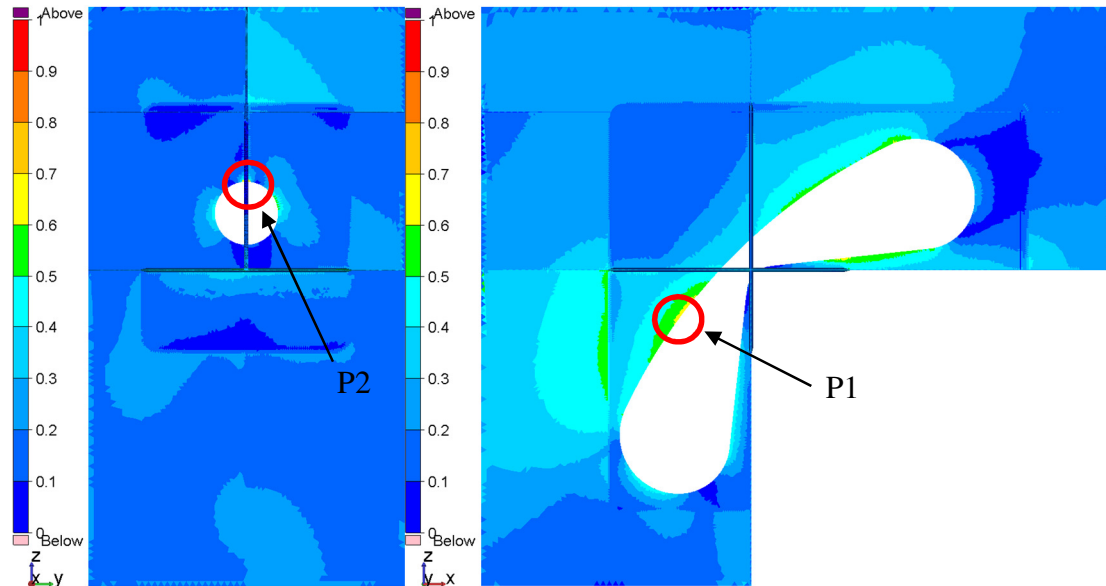


Figure 5.13 YZ-view (left) and XZ-view (right) of the solid model of cut-out design with FLS analysis, presenting the locations of fatigue analysis.

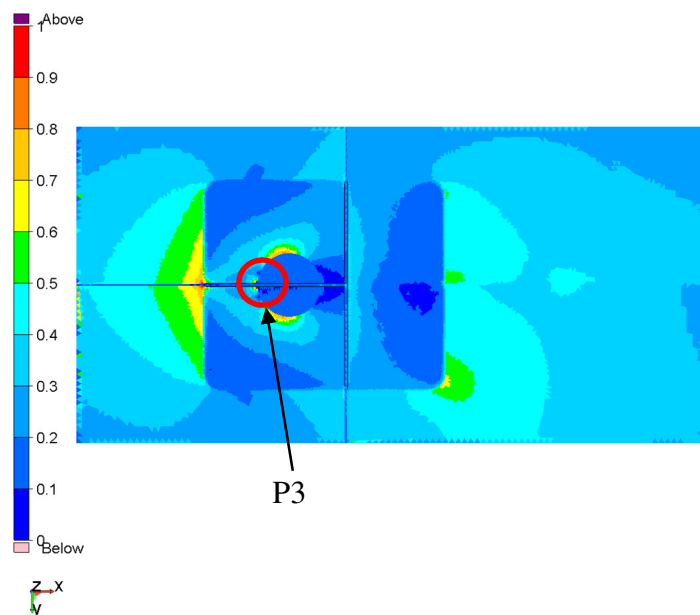


Figure 5.14 XY-view (seen from below) of the solid model of cut-out design with FLS analysis, presenting the locations of fatigue analysis.

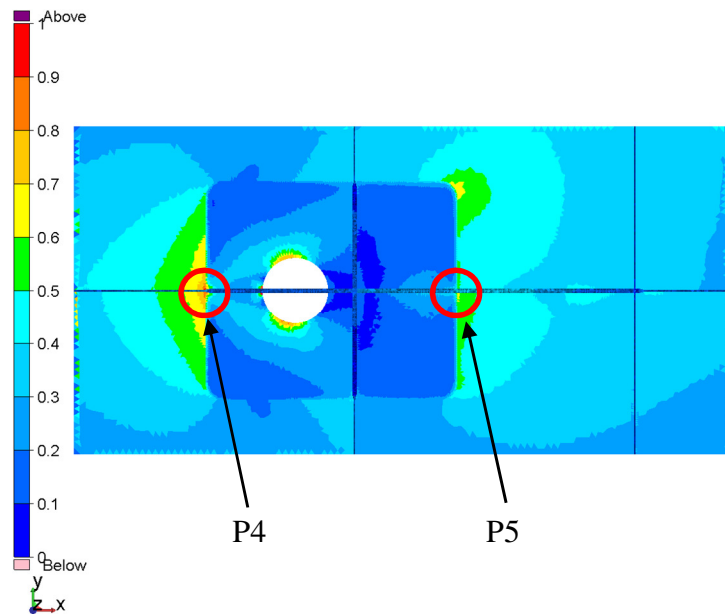


Figure 5.15 XY-view (seen from above) of the solid model of cut-out design with FLS analysis, presenting the locations of fatigue analysis.

Table 5.3 Fatigue damage from the simplified and stochastic fatigue analysis.

ID	Location	Fatigue class	Fatigue Damage	
			Simplified	Stochastic
P1	Free edge	C	Less than 0.1	Less than 0.1
P2	Vertical hole	F	0.66	0.45
P3	Horizontal hole	F	0.74	0.6
P4	Nominal to tapering back	D	0.42	0.2
P5	Nominal to tapering front	D	Less than 0.1	Less than 0.1

The stochastic fatigue analysis is based on the same loading conditions as the simplified method, but uses scatter diagrams of wave data from the location the semi-submersible will operate in. The analysis is made using the program DNV Stofat, which calculates the fatigue damage and presents it as a usage factor. Figure 5.17 shows the highest damage from the stochastic analysis, which occurs at the horizontal tapering plate.

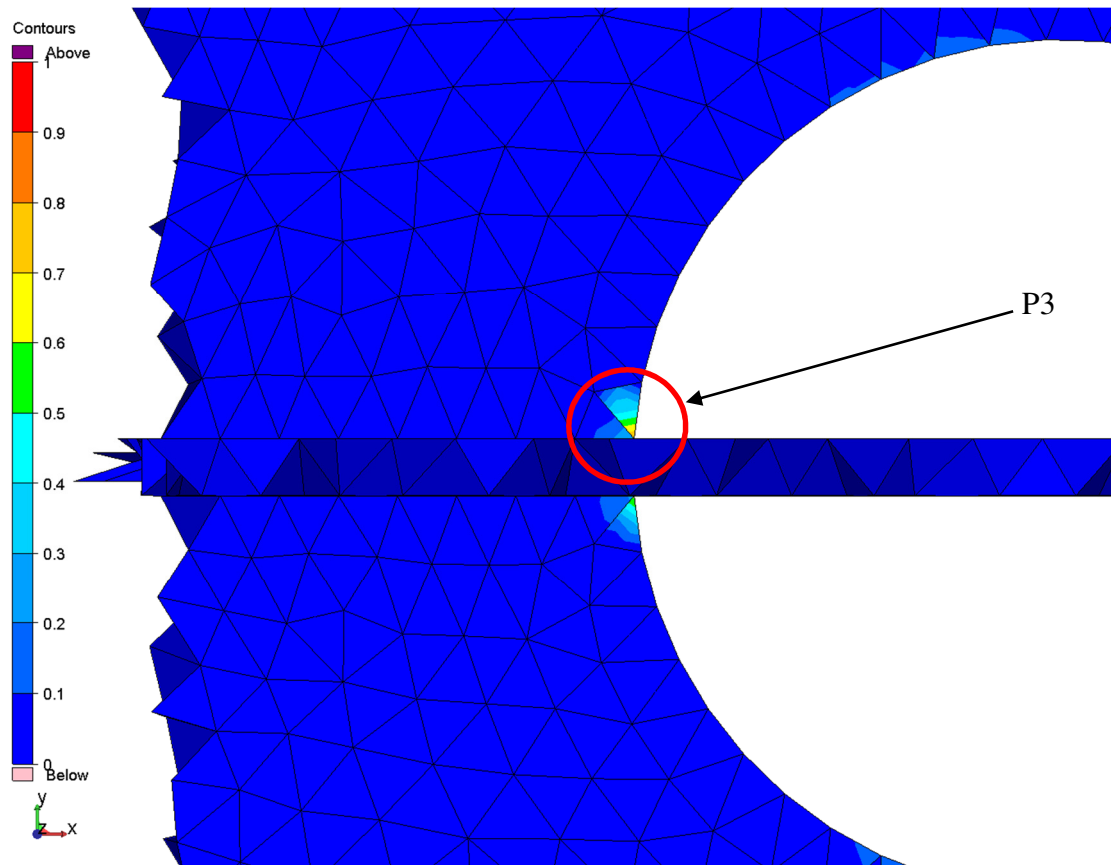


Figure 5.16 Accumulated fatigue damage in the stochastic analysis. The highest fatigue damage occurs at the horizontal tapering plate.

6 Design comparison

In this chapter a comparison of the cut-out and cast integral designs are presented. The different designs are compared in yield stresses for the ULS investigation and in fatigue damage for the fatigue limit state. The final cut-out design is also compared to the cast integral in a simplified cost and weight analysis. The buckling criterion is only used for control of the structure and not considered in the design comparison.

6.1 Concept evaluation

The results from the ULS calculations of both the cut-out and cast integral show that the calculated yield stresses are on approximately the same level. The cast integral have the highest normalized stress of 0.99 at the nominal/tapering plate weld and the cut-out have a maximum stress of 1.01 in the vertical hole of the tapering plate. The highest peak stress is slightly higher for the cut-out design, while the overall stress levels are lower, see Figure 4.8 and 5.5.

In order to see the effects from the introduced cut-out in the surrounding structure, and especially the adjacent inner corner, the cut-out is applied to the global model. The corner is investigated for the highest yield stresses, see Figures 3.8 and 5.11. The contour plots show that no drastic change in stress levels or distribution occurs when the cut-out is implemented. Adjacent plates show as difference in the stress flow, but peak stresses and overall stress distribution are kept stable. The cut-out design is thus considered to only have local influence. The inner corner is, however, recommended to be further examined in future work, see Chapter 9.

For the FLS evaluation of the designs, the cast integral show good results. The highest fatigue damage for the cast integral is 0.53 at the nominal/tapering plate weld. For the cut-out design the fatigue damage from the simplified fatigue analysis is 0.74 at the horizontal hole in the tapering plate. The stochastic fatigue analysis verifies the location of the highest fatigue damage to the transverse and longitudinal holes.

Due to the design with vertical and horizontal holes, the cut-out design performs similar to the cast integral in the examined load cases. Stress concentrations and fatigue damage is present in the connection between the tapering plate and nominal plate. High stress concentrations are also present on the horizontal hole in the cut-out design. The introduction of a fillet to the hole could potentially and probably decrease both stresses and fatigue damage, which is regarded as future work, see Chapter 9.

A cut-out in a thick plate is a simple geometry which can be manufactured directly by the shipyard. The cast integral is often manufactured by third-party companies and transported to the structure and thus risk and costs can be reduced.

6.2 Cost and weight analysis

Cost is always a governing factor in design and manufacturing, and due to the large steel weight for semi-submersibles the lightweight optimization is of interest. The cost comparison is also a way of assessing the feasibility of the structure and the different designs.

The cost analysis performed is based on the comparison of the cast integral and cut-out design where the cast integral is considered as the reference case. The total construction cost for structures this size can often be evenly divided into working costs and material costs, which is obviously an empirical estimation and differs between shipyards and countries. However, the detailed geometry and manufacturing of the cast integral is a

complicated process, which is why the manufacturing cost needs to be accounted for in a detailed analysis.

Due to the large variation in size between the cast integral and the cut-out design, a reference model including nominal plating is chosen, see Figure 6.1. The same size of the nominal plates is used for the cut-out design.

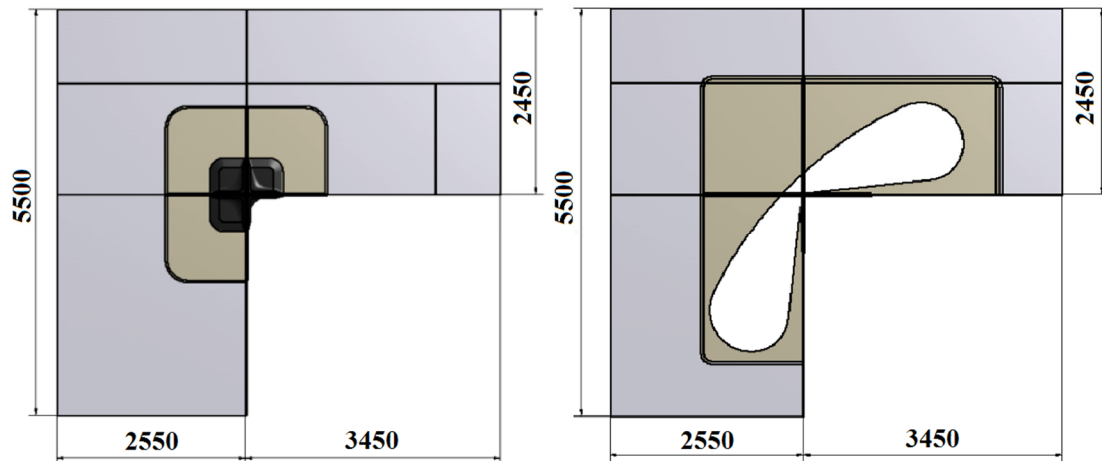


Figure 6.1 Dimensions for cast integral (left) and the cut-out design (right) used in the weight and cost comparison.

In order to calculate the manufacturing cost for the cut-out design, a general calculation method for shipbuilding is used. For large structures built in shipyards, cost estimations are often based on Equation (6.1).

$$C_C = W_S (H_T C_L + C_M) \quad (6.1)$$

C_C = Total manufacturing cost [USD]

W_S = Weight structural steel [ton]

H_T = Man-hour per ton [hour/ton]

C_L = Labour cost per hour [USD/hour]

C_M = Material cost [USD/ton]

The construction cost and the parameters listed in Table 6.1 are valid for an experienced South Korean shipyard that GVA has used for previous projects. Here the combination of man-hour per ton and the labour costs are about four times the material cost per ton.

Table 6.1 Cut-out design construction cost.

Design	W_S [ton]	H_T [h/ton]	C_L [USD/h]	C_M [USD/ton]	C_C [USD]
Nominal plates	4.400	125	75	2000	50050
Cut-out design	6.200	55	75	1100	32395

The cut-out design is divided into two parts, nominal plates and cut-out plates. This is due to the expected higher construction cost for the cut-out part of the structure together with the increased thickness of the cut-out tapering plate.

The cast integral is also divided into two parts as presented in Table 6.2. This is to achieve an equal comparison between nominal plates for the casting and cut-out. The cast integral construction cost is high and requires special knowledge and hence the cost of the cast integral is the expected and estimated manufacturing cost of the cast integral, based on previous designs.

Table 6.2 Cast integral construction costs.

Design	W_S [ton]	H_T [h/ton]	C_L [USD/h]	C_M [USD/ton]	C_c [USD]
Nominal plates	9.400	55	75	1100	49115
Cast integral	1.700	-	-	24700	42000

A complete comparison of the designs is presented in Table 6.3. The cut-out design is approximately 500 kg lighter and the cost about USD 8670 lower per unit, resulting in a decrease of 4.5% in weight and 9.5% in cost for the cut-out reference structure. The relatively small difference in weight suggests that the cut-out design can be used with good results, but require further investigations and comparisons to be verified.

Table 6.3 Weight and cost comparison between designs, positive % difference equals a reduction for the cut-out design.

	Cut-out design	Cast integral	Difference	Diff. [%]
Weight [kg]	10600	11100	500	4.5%
Cost [USD]	82445	91115	8670	9.5%

7 Discussion

Stress relieving cut-outs are a known design feature that can be used in various situations and applications. The developed cut-out design for the semi-submersible is found to be a viable alternative to the cast integral in the case study performed. The cut-out is found to decrease both weight and cost for the specific centre bulkhead connection, while the overall structure is found not to be affected by the change. The design assessment was made by a FEA in both the ULS and FLS for different geometries in a parametric study.

Today, the marine industry is growing at a fast pace and with it also increasing depths and the need for larger structures. Larger semi-submersibles also use larger components and the cast integral analysed in this thesis is one of them. Larger castings cost more, and are also a challenge to manufacture, why alternative designs are of interests. Weight optimization of the semi-submersibles is of concern due to the increased load carrying capacity and efficiency of the semi-submersible. Light weight optimization without compromising the structural strength or stability is therefore highly prioritized in the industry.

The initial parametric study of different 2D cut-outs in simplified loading conditions was based on the governing responses for the chosen node connection and calculated for the von Mises yield stress criteria (DNV, 2014c). The principal geometry of the cut-out was established and tested in a simplified study; however, the 2D study does not consider the transverse plating which is present in the real structure. Therefore, a parametric study with more variables was conducted in the case study of a previously designed semi-submersible by GVA.

The loads acting on the semi-submersible were taken from a previous case study for an in-house project at GVA and responses were calculated in ULS and FLS, which are considered governing in the analysis. The hydrodynamic analyses were made for the Gulf of Mexico, where the semi-submersible was to operate. An investigation of other weather conditions is necessary due to the change in loads and stress responses. However, the Weibull shape parameter, $h = 1.1$, which is used in this thesis, can be considered conservative and is approved for worldwide operations of the semi-submersible structure (DNV-GL, 2014).

The Serviceability and Accidental limit states were not investigated in the thesis. However, ALS could need further investigation due to the softening of the centre bulkhead connection. Accidents such as explosions in the deck-box need further investigation in order to understand the influence of the cut-out and to insure structural stability of the semi-submersible.

The WSD method was used for the calculation of yield stresses, since the load analysis was already performed. The stresses presented in the result plots are the highest stresses from each of the analysed 61 loading conditions for each element or node, combined into one plot. This can be done due to the calculation of maximum stress compared to the permissible stress. Due to the selection of the highest results in each node or element, the stresses may be unevenly distributed, which makes the response and deformation behaviour hard to interpret.

The hot spot method was used for the calculation of fatigue damage with the simplified fatigue assessment, due to the difficulties extracting the nominal stress for the local details. The comparison of fatigue damage is dependent on the choice of weld class, why the recommendations for weld classification and mesh size in the hot spot method

have been followed. The fatigue damage value depends on the weld class and applied load, which is why it is hard to compare the different designs in accumulated fatigue damage. The same fatigue class was used for both the cast integral and the cut-out to make it possible to compare the created damage. Improving the fatigue classification would decrease the accumulated fatigue damage.

The stochastic fatigue assessments used for comparison of the simplified method suggest that the fatigue damage is lower than the calculated values for the simplified fatigue analysis. This is an expected result, due to the level of conservatism of the simplified method (Seung Min Park, 2014). However, the stresses used in the simplified method are calculated with the suggested hot spot method and the fatigue damage given for the stochastic analysis are given for nodal stresses that may influence the results.

The cast integral used for the analysis is of a standardized type often used for the centre bulkhead connections. The cast integral was therefore not optimized in the same way as the node cut-out, but taken as a reference case for comparison. It can be noted that increasing the size of the cast integral and tapering plates would lower the stresses for the reference case, but would at the same time increase the weight and cost and are therefore not investigated.

The investigation of effects on the adjacent structure when introducing the cut-out was made by adding the cut-out to the global model and sub-model. The corner structure was therefore not changed in the comparison. The cast integral used in the corner connection therefore requires further analysis in order to verify the structural strength and stability. Due to the local changes implemented in the design, it could prove efficient to investigate a larger part of the structure and in that way improve the cut-out design further.

The cut-out design depends on several different geometric parameters, for example thickness, radius of the cut-out, holes in the horizontal and vertical tapering plates and overall length of the cut-out. The holes in the tapering plates were designed to create a free edge for the cut-out radii, which would otherwise stiffen the node connection. The governing stresses were located on the holes and from the fatigue damage calculation it was found that the holes need further investigation. The circular shape of the holes was determined after a shape evaluation of the holes. Due to loads occurring in different directions through the structure, the circular shape was established as the best solution. Adding a fillet to the connection in the hole would decrease both the fatigue damage and yield stresses which leave room for improvement of the cut-out design. The cut-out design is thus considered as an advantageous design in the studied case. Lowering the stresses in the considered hole would potentially make room for a decrease in thickness of the adjacent plating and therefore also weight/cost improvements.

The simplified cost analysis shows that the cost, depending on weight, is not drastically changed when introducing a cut-out. From a production point of view, it can, however, be efficient to exchange the cast integral with a cut-out design. The risk of cast defects in the integral and post-production processing is a risk that can be considered in the manufacturing and cost of the cast integral. The cut-out can be implemented directly in a thick plate and can therefore be manufactured at the shipyard, lowering expenses for third-party manufacturing and shipping costs. The same material can thus be used in the whole node connection.

8 Conclusions

The objective of this thesis is to investigate and evaluate an alternative cut-out design instead of the cast integral used today in GVA-designed semi-submersibles. The two solutions are compared regarding yield stresses, fatigue damage, weight and cost.

The cast integral is analysed as a reference case and the design is a standardized type used in GVA-designed semi-submersibles. The cast integral is analysed in the centre bulkhead connection on a typical semi-submersible, also designed by GVA. Yield stresses on the cast are found to be almost 1 in the connection between tapering plate and nominal plate, see Figure 3.6. The high stresses can be explained with the cast integral not being optimized for the geometry, but is of a typical design used by GVA. Buckling check of the cast is performed for an adjacent plate field and found to be 0.67. The buckling is, however, not regarded as a comparison parameter and only checked for verifying the design in ULS. The fatigue life of the cast integral is also investigated with a simplified fatigue method. The result shows that the highest fatigue damage, 0.53, will occur in the weld between tapering and nominal plate, see Figure 3.10.

An alternative design with a cut-out is implemented in the same structure as the cast integral. The cut-out design is achievable due to the simple geometry in the chosen node connection, and no large structural change in the geometry is needed for the implementation of the cut-out. A parametric study with simplified boundary conditions and loads is used for initial design of the cut-out. It is found that a large radius of the cut-out close to the corner decreases the stresses in bending, tension and shear. The best performing design in the simplified study is implemented in the complete semi-submersible structure and investigated further.

The maximum yield stress is 1.01 on the introduced hole in the horizontal tapering plate. The local peak of yielding is considered acceptable due to the large change in geometry (DNV, 2012). A buckling check from a simplified load model of the cut-out gives the usage factor to be 0.51, see Section 5.3. The fatigue damage is calculated with both the simplified fatigue method and a stochastic method to verify the results from the simplified method. The results show that the highest fatigue damage, 0.74, occurs on the horizontal hole and that the simplified fatigue method tends to overestimate the accumulated damage.

Yield stresses are also calculated for the adjacent inner corner in ULS and the distribution and peak stresses are investigated. The responses are kept on the same level with both the cast integral and the cut-out implemented in the global model, hence the conclusion is drawn that the cut-out design does not affect the adjacent structure. The design can therefore be seen as a local design and no major changes in the structure are needed for the cut-out design.

The cut-out design is evaluated for a typical semi-submersible and found to be a valid design suggestion. It should, however, be noted that only the specified loads are investigated for the reference structure, which is why the cut-out must be further evaluated and verified in other structures.

A simplified weight and cost analysis shows that the cut-out design would decrease the weight of the reference structure by 4.8 % and the cost would decrease by 9.5 %. The cut-out is therefore the recommended solution for the centre bulkhead connection on this specific semi-submersible, and future work can prove the design advantageous.

9 Future work

For future work and further evaluation of the cut-out design some important factors are here mentioned from experience gained from our work. For a complete analysis of the cut-out design, the following aspects are recommended.

A modal analysis is necessary to perform for the new cut-out design. One effect from the softening cut-out design that is not investigated in this report is the possible change in natural global frequency of the structure. The modal response and investigation of free-vibration frequencies are often forgotten in offshore structures and need to be further examined. The procedure suggested with a simple beam model for the calculation of modes may not be sufficient due to the way of modelling the corners very stiff to “*obtain mode accurate flexural beam lengths*” (Ringsberg et al., 2013). A full modal analysis should therefore be performed in order to verify the free-vibration frequencies of the structure. The modal analysis can also be used for performing a detailed buckling check of the cut-out design.

The cut-out design in this thesis is only implemented in one centre bulkhead connection between column and deck-box. Further studies of the global effects of the cut-out design need to be performed. To perform a final design of the cut-out for one column, a bigger part of the structure should be considered and analysed to be improved together with the cut-out design. A more lightweight cut-out design and more evenly distributed stress field could be accomplished if the adjacent structure is improved with different plate thicknesses.

An investigation as to whether the cut-out can be used for the centre connection between column and pontoon can be useful for reducing the number of castings used. It could also prove possible to apply the cut-out in the inner corner, but requires structural stability assessment of the complete semi-submersible. The structural design of the corner leaves no room for a stress relieving cut-out without great changes to the structure and the conical shape of the column therefore needs to be re-designed.

The cut-out design is only evaluated for the specific semi-submersible platform used in this thesis. Depending on semi-submersible platform design and applied loads, the cut-out may not be a valid design for other semi-submersibles. The design therefore needs to be evaluated for each specific semi-submersible and in various weather conditions to be able to draw conclusions about the general design and implementations.

The corrosion margin is not included in the calculations of the semi-submersible in this thesis. Consideration of the margin would increase the plate thicknesses for which reason an investigation of the corrosion protection of the local design is recommended in future work. However, due to the similar stress levels in both the cast integral and the cut-out, the corrosion margin would only affect the cost and weight estimation.

10 References

- Bambach, M. R., & Rasmussen, K. J. (2004). Effects of anchoring tensile stresses in axially loaded plates and sections. *Thin-Walled Structures*, Vol.42(Issue 10), 1465-1479.
- Bijak-Zochowski, M., Waas, A., Anderson, W., & Miniatt, C. (1991). Reduction of Contact Stress by Use of Relief Notches. *Experimental Mechanics*, Vol. 31(Issue 3), 271-275.
- Bijlaard, P. P. (1957). Buckling of Plates Under Nonhomogeneous Stress. *Journal of the Engineering Mechanics Division*, Vol.83(Issue 3), 1-31.
- Chakrabarti, S. K. (2005). *Handbook of Offshore Engineering* (Vol.2 ed.). Amsterdam: Elsevier.
- DNV. (2004). *SESAM User Manual Submod*. Hövik, Norway: Det Norske Veritas.
- DNV. (2007). *Environmental Conditions and Environmental Loads, Recommended Practice*, DNV-RP-C205. Hövik, Norway: Det Norske Veritas.
- DNV. (2010a). *SESAM User Manual Sestra*. Hövik, Norway: Det Norske Veritas.
- DNV. (2010b). *SESAM User Manual Wadam*. Hövik, Norway: Det Norske Veritas.
- DNV. (2010c). *Buckling strength of plated structures*. Hövik, Norway: Det Norske Veritas.
- DNV. (2010d). *SESAM User Manual Patran Pre*. Hövik, Norway: Det Norske Veritas.
- DNV. (2011a). *SESAM User Manual GeniE*. Hövik, Norway: Det Norske Veritas.
- DNV. (2011b). *SESAM User Manual Xtract*. Hövik, Norway: Det Norske Veritas.
- DNV. (2011c). *SESAM User Manual Stofat*. Hövik, Norway: Det Norske Veritas.
- DNV. (2012). *Recommended Practice Column-Stabilised Units*, DNV-RP-C103. Hövik, Norway: Det Norske Veritas.
- DNV. (2014a). *Design of Offshore Steel Structures, General (LRFD Method)*, DNV-OS-C101. Hövik, Norway: Det Norske Veritas.
- DNV. (2014b). *Structural Design of Offshore Units (WSD method)*, DNV-OS-C201. Hövik, Norway: Det Norske Veritas.
- DNV. (2014c). *Structural Design of Offshore Units (WSD Method)*. 2014: Det Norske Veritas.
- DNV-GL. (2014). *Recommended Practice: Fatigue design of offshore steel structures: DNVGL-RP-0005*. Hövik, Norway: Det Norske Veritas.
- Dowling, N. E. (2012). *Mechanical behaviour of materials*. Harlow, Essex, England: Pearson Education Limited.
- Ellobody, E., Feng, R., & Young, B. (2014). *Finite element analysis and design of metal structures*. Waltham, Massachusetts, USA: Elsevier Ltd.
- Health and Safety Executive (HSE). (2000). *Fatigue Reliability of Old Semi-Submersibles*. Det Norske Veritas.
- Institutionen för hållfasthetslära KTH. (2008). *Handbok och formelsamling i Hållfasthetslära*. Stockholm: E-PRINT AB.

- International Institute of Welding. (2008). *Recommendations for Fatigue Design of Welded Joints and Components*. Cambridge, UK: Abington Publishing.
- Kwok-Wai Chan, W. (1981). *Stress Relief by Using Notches*. El Paso, Texas: ETD Collection for University of Texas.
- Li, Z. (2013). *Fatigue Assessment of Container Ships - a Contribution to Direct Calculation Procedures*. Gothenburg, Sweden: Chalmers University of Technology, Department of Shipping and Marine Technology, Division of Marine Design.
- Liu, G., & Quek, S. (2013). *The finite element method: A practical course*. Waltman, Massachusetts, USA: Elsevier Ltd.
- Lizhong, C. (2013). In-place structural strength and fatigue analysis for floating platform topsides. *Engineering Sciences*, Vol. 11(Issue 4), 24-34.
- Lundh, H. (2000). *Grundläggande hållfasthetslära*. Stockholm: Instant Book AB.
- Mattheck, C. (2006). Teacher tree: The evolution of notch shape optimization from complex to simple. *Engineering fracture mechanics*, Vol. 73, 1732-1742.
- Mohan Kumar, M., Rajesh, S., Yogesh, H., & Yeshaswini, B. (2013). Study on the Effect of Stress Concentrations on Cutout Orientation of Plates with Various Cutouts and Bluntness. *International Journal of Modern Engineering Research (IJMER)*, Vol.3, Issue.3, May-June. 1295-1303.
- Nygård, M. (2003). Column Structure Design. *OGP Marine Risks Workshop Proceedings* (pp. 59-78). St Albans, UK: International Association of Oil & Gas Producers.
- Rezaeepazhand, J., & Jafari, M. (2010). Stress concentration in metallic plates with special shaped cutout. *International Journal of Mechanical Sciences*, Vol. 52(Issue 1), 96-102.
- Ringsberg, J. W. (2011). *Effective flange and buckling of bars, frames and stiffened plates*. Göteborg: Department of Shipping and Marine Technology, Chalmers University of Technology.
- Ringsberg, J. W., Ernholm, P., & Hagström, L. (2013). Procedure for identification and analysis of the vibration characteristics and the mode shapes of semi-submersible platforms. *Journal of Engineering for the Maritime Environment, Proceedings of the Institution of Mechanical*, Vol. 227 Issue 4, pp. 314-325.
- Ringsberg, J. W., Ernholm, P., & Hagström, L. (2013). Procedure for identification and analysis of the vibration characteristics and the mode shapes of semi-submersible platforms. *Journal of Engineering for the Maritime Environment*, 314-325.
- Saglam, H., & Lindekrantz, O. (2014). *Improved Column Design on a DP3 Semi-submersible unit*. Gothenburg, Sweden: Department of Shipping and Marine Technology, Chalmers University of Technology.
- Sandler Research. (2015). *Global Onshore Oil and Gas Market 2015-2019*. Dallas: Infiniti Research Limited.
- Seung Min Park, M. K. (2014). Fatigue Assessment on Cast Integral of Semisubmersible Rig. *Proceedings of the Twenty-fourth (2014) International*

- Ocean and Polar Engineering Conference* (pp. 205-210). Busan, Korea: International Society of Offshore and Polar Engineers (ISOPE).
- Taylor, D., Kelly, A., Toso, M., & Susmel, L. (2011). The variable-radius notch: Two new methods for reducing stress concentrations. *Engineering Failure Analysis* 18, Vol. 18(Issue 3), 1009-1017.
- World Resource Institute. (2000). *World Energy Assessment: Energy and the challenge of sustainability*. New York: United Nations Development Programme Bureau for Development Policy.
- Yu, C., & Schafer, B. W. (2007). Effect of Longitudinal Stress Gradients on Elastic Buckling of Thin Plates. *JOURNAL OF ENGINEERING MECHANICS*, 133(4), 452-463.
- Zhang, D., Yan, F., & Deng, Z. (2010). The Application of Lateral Braces in the Design of Floating Structures. *Proceedings of the Twentieth (2010) International Offshore and Polar Engineering Conference* (pp. 614-623). Beijing, China: The International Society of Offshore and Polar Engineers (ISOPE).
- Zhang, D.-g., Deng, Z.-c., & Yan, F.-s. (2009). An introduction to hull design practices for deepwater floating structures. *Journal of Marine Science and Application*, Vol. 8(Issue 2), 123-131.

Appendix A - Sub-modelling and computer software

The computer software used for calculations in this thesis is mainly DNV SESAM. It is a complete software package which can be used for finite element calculations on large ship and offshore structures. The program suite utilizes the sub-modelling technique which transfers displacements from a large model to a smaller, more detailed model.

The workflow of the parametric study of the design is repetitive, meaning that the different stages in the design evaluation must be conducted several times, as illustrated in Figure A.1. The software DNV SESAM is used for modelling and analysis of the shell models and Autodesk Inventor is used to model a detailed solid model.

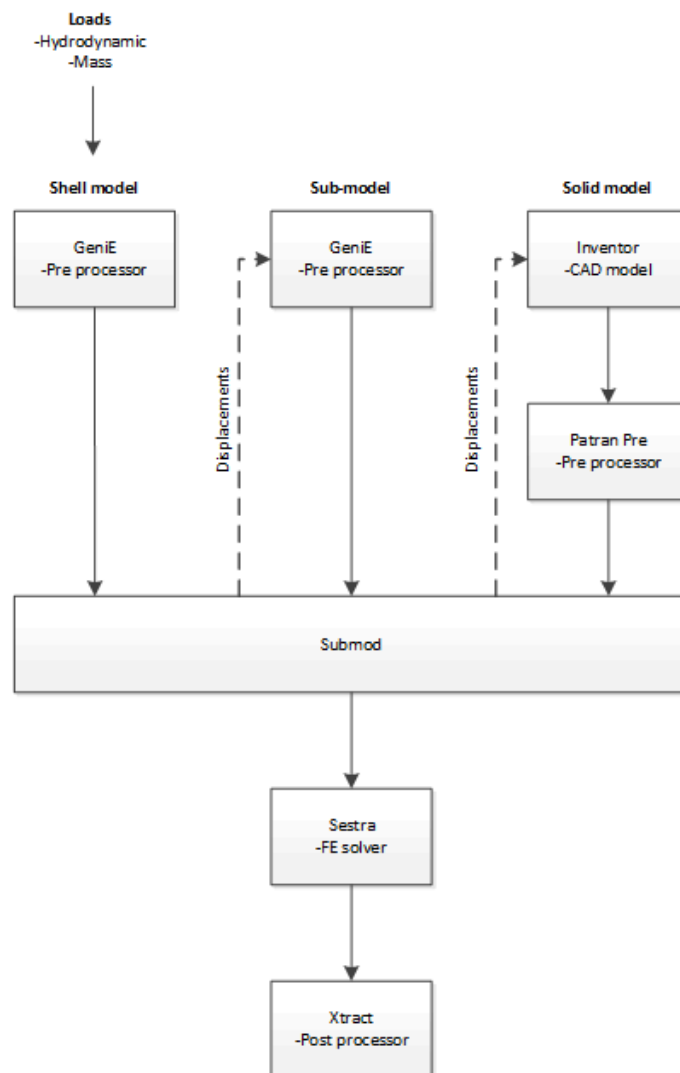


Figure A.1 The workflow with the software used in this thesis.

The initial design is evaluated with a “Global model” (Shell model in Figure A.1) that represents the entire structure built of shell elements. Both static and cyclic loads are applied to the shell structure and the areas of interest can then be further evaluated in a sub-model.

DNV Submod transfers node displacements from a large model to the boundaries of a smaller “sub-model”. The method makes a detailed analysis of a smaller area of interest possible. The method used in this thesis transfers the displacements from one large “global model” to a smaller sub-model. The final analysis is made on a solid model which is a smaller part of the sub-model. The finite element analysis is made using the linear FE-solver DNV Sestra and the results are visualized in the post-processor DNV Xtract.

The sub-model created in GeniE is a small section from the global model and a finer mesh is applied. It is important that the plate thickness of the boundaries are the same in the two models, otherwise Submod will not be able to transfer the correct displacements.

The “solid model” (volume model) is created in Autodesk Inventor and meshed in DNV Patran-Pre. The model is evaluated in the same way as described for the sub-model. In Patran-Pre the mesh properties are carefully investigated to create a proper mesh for the model at the important regions. The output from Patran-Pre is a solid mesh, material properties and input requirement of boundary displacements from a previous Submod file. The highest level of details and accuracy is obtained in the calculations of the solid model.

In order to verify the results from Submod and Sestra, the displacements from the global model to the sub-model, and the sub-model to the solid model are graphically compared. Individual stress components can also be investigated using the same methodology. An example of compared displacements is illustrated in Figure A.2, where the global model, the sub-model and the solid model is shown and compared. This verifies that the correct boundary conditions have been applied and that the geometry is correctly located in space.

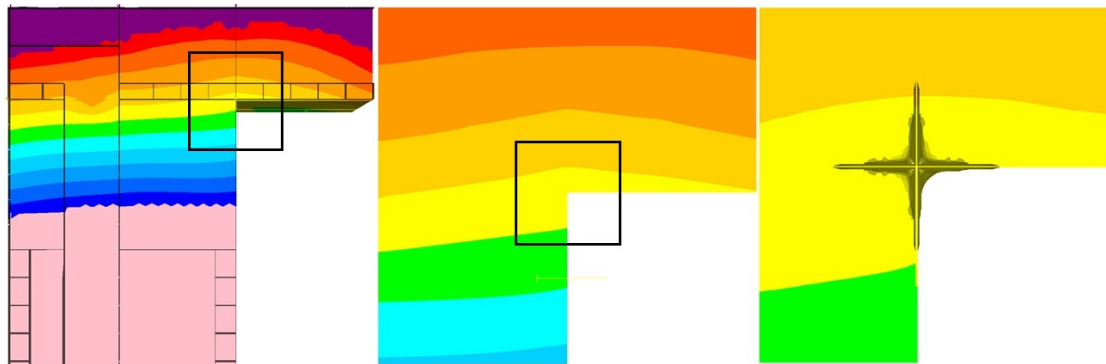


Figure A.2 Displacements are verified graphically between the global model (left), sub-model (middle) and solid model (right).

Appendix B - Cut-out design

For the evaluation of the cut-out designs a parametric study of 45 different design cases is performed. Three major parameters of the cut-out design are recognized:

1. Cut-out radius, R .
2. Radius of hole in tapering plate, r .
3. Plate thickness, t .

For the initial evaluation of the 45 cut-out designs the considered maximum von Mises stress is calculated on the edge of the cut-out radius, see Figure 5.4. Table B.1 show the parameters of the first 15 design cases.

Table B.1 The design parameters for the cut-out design with a hole radius of 200 mm and three different plate thicknesses for each cut-out radius.

Cut-out radius [mm]	Hole radius [mm]	Plate thickness [mm]		
2190	200	20	30	40
2900	200	20	30	40
4080	200	20	30	40
5370	200	20	30	40
12500	200	20	30	40

The circular holes in the vertical and horizontal tapering plates have a fixed radius of 200 mm and the stresses are presented in Figure B.1. The stress on the radii is found to decrease as the plate thickness increases. The increase in cut-out radii is also found to decrease the stress in the geometry to a certain point, see case “ $R=12500$ ” in Figure B.1. The different cut-out radii are presented depending on the normalized von Mises stress.

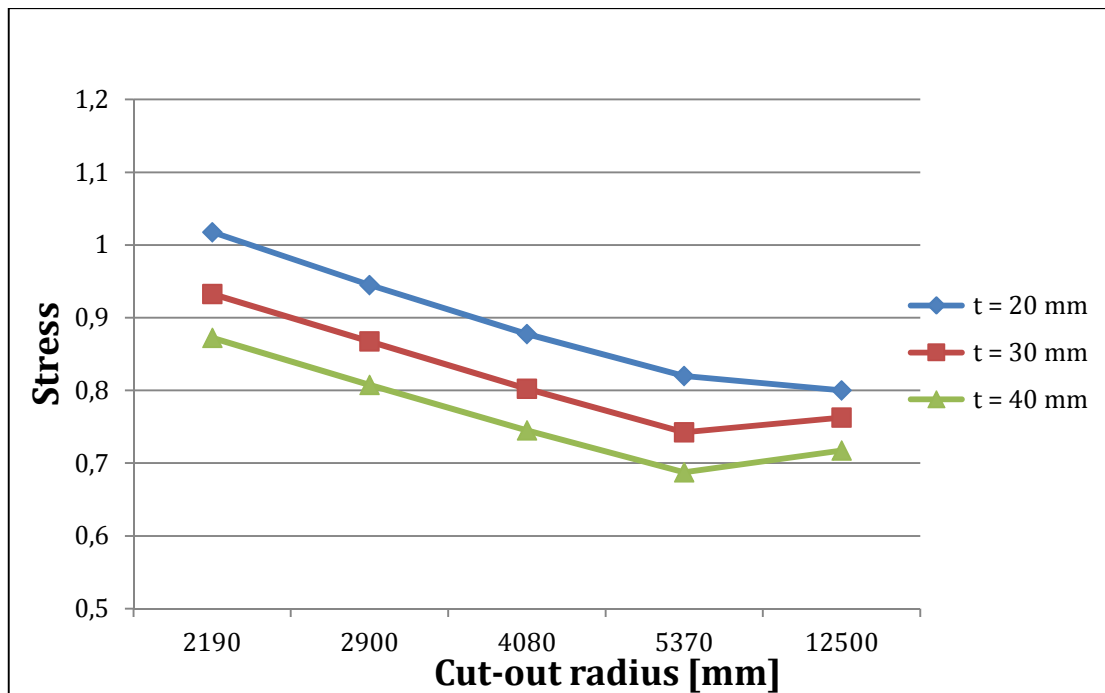


Figure B.1 Different cut-out radius and plate thickness with a constant tapering plate hole radius of 200 mm plotted against normalized von Mises stress on the cut-out radius.

The following 15 cut-out designs are evaluated in the same way as above but with a new constant tapering plate hole radius of 300 mm as in Table B.2.

Table B.2 The design parameters for the cut-out with a hole radius of 300 mm.

Cut-out radius [mm]	Hole radius [mm]	Plate thickness [mm]		
2190	300	20	30	40
2900	300	20	30	40
4080	300	20	30	40
5370	300	20	30	40
12500	300	20	30	40

The trend in Figure B.2 is similar to the trend in Figure B.1 but with an overall lower stress level. The cut-out design with a radius of 5370 mm has the lowest stress measured.

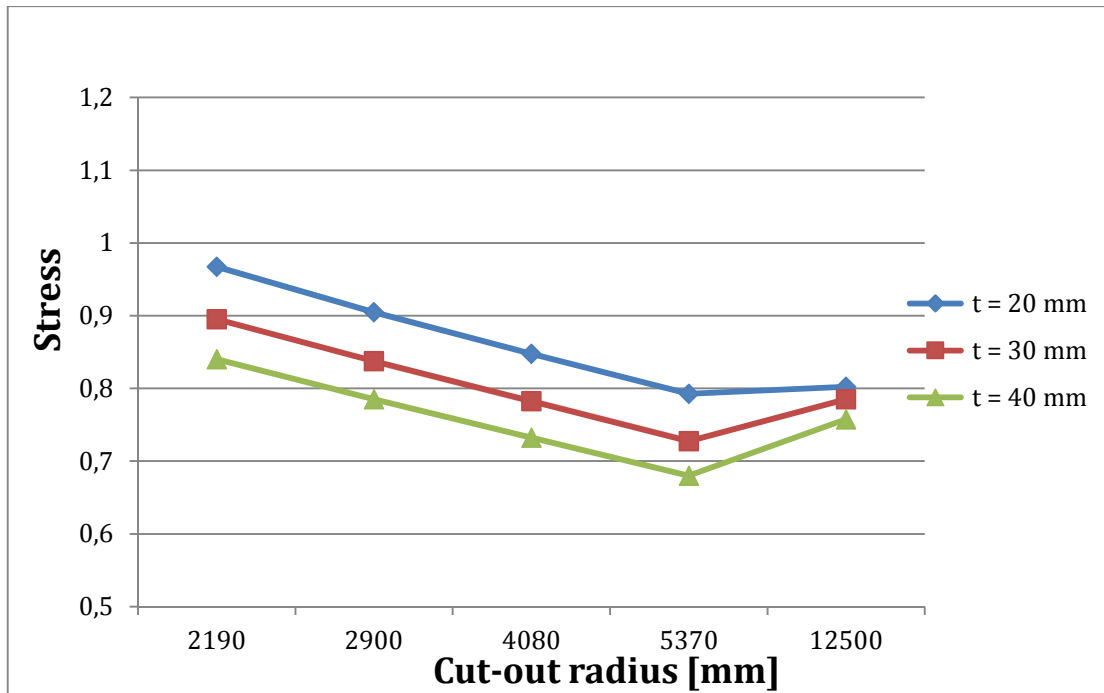


Figure B.2 Different cut-out radius and plate thickness with a constant tapering plate hole radius of 300 mm plotted against normalized von Mises stress on the cut-out radius.

The last 15 design cases with a constant tapering plate hole radius of 400 mm as in Table B.3.

Table B.3 The design parameters for the cut-out with hole radius of 400 mm.

Cut-out radius [mm]	Hole radius [mm]	Plate thickness [mm]		
2190	400	20	30	40
2900	400	20	30	40
4080	400	20	30	40
5370	400	20	30	40
12500	400	20	30	40

The trend is similar for these 15 design cases with an even lower overall stress. The cut-out design with a radius of 5370 mm and a plate thickness of 40 mm has the lowest stress as in Figure B.3.

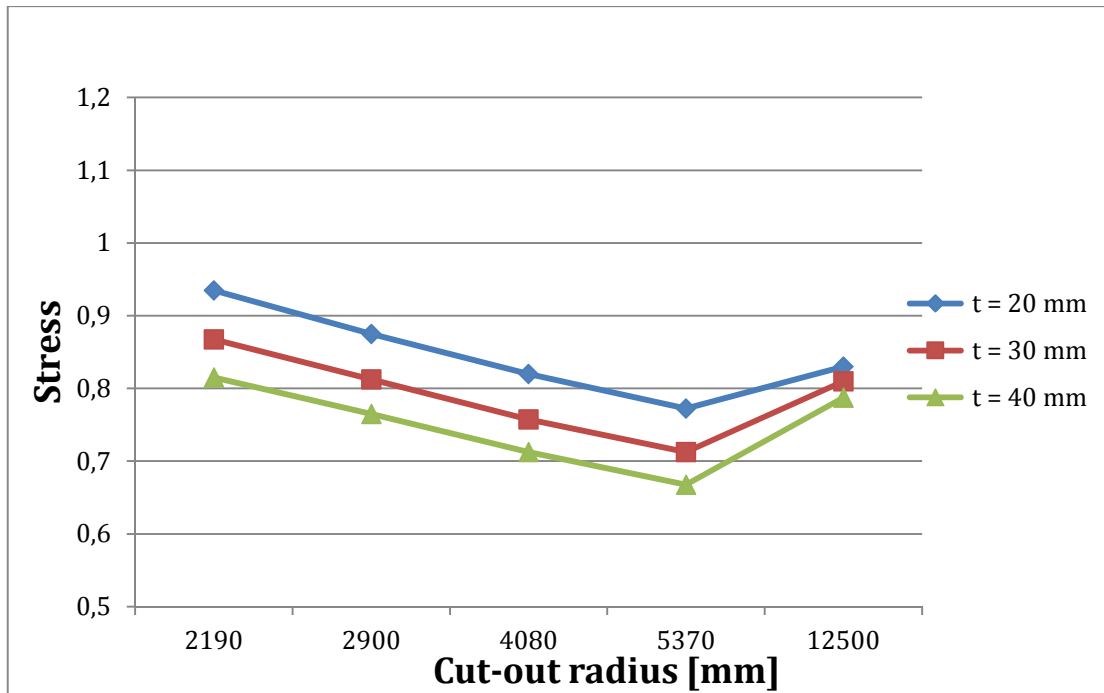


Figure B.3 Different cut-out radius and plate thickness with a constant tapering plate hole radius of 400 mm plotted against normalized von Mises stress on the cut-out radius.

To further evaluate the cut-out designs, additional important stress regions are analysed. The chosen regions are identified with local maximum von Mises stress in the specific geometry and Figure B.4 presents the four stress locations. This evaluation is performed to identify the best overall cut-out design.

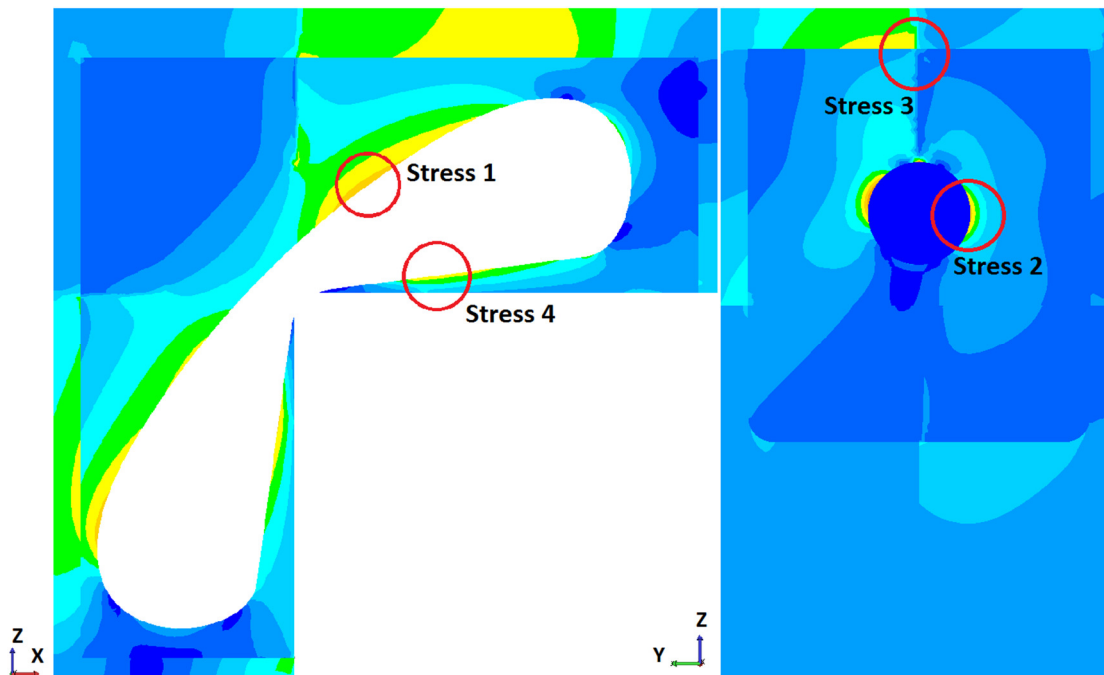


Figure B.4 Four locations with local maximum von Mises stress in the cut-out design.

These four regions were evaluated for all 45 different designs, but only the cut-out design with a radius of 5370 mm is presented in the following part. The evaluation are the same for all different designs but as illustrated in Figures B.1, B.2 and B.3 the cut-out radius of 5370 mm performs best.

Figure B.5 presents the stresses for the cut-out design with a tapering plate hole radius of 200 mm. Stress location 2 is found to be dependent on the plate thickness, which is the maximum normalized von Mises stress at the edge of the tapering plate hole.

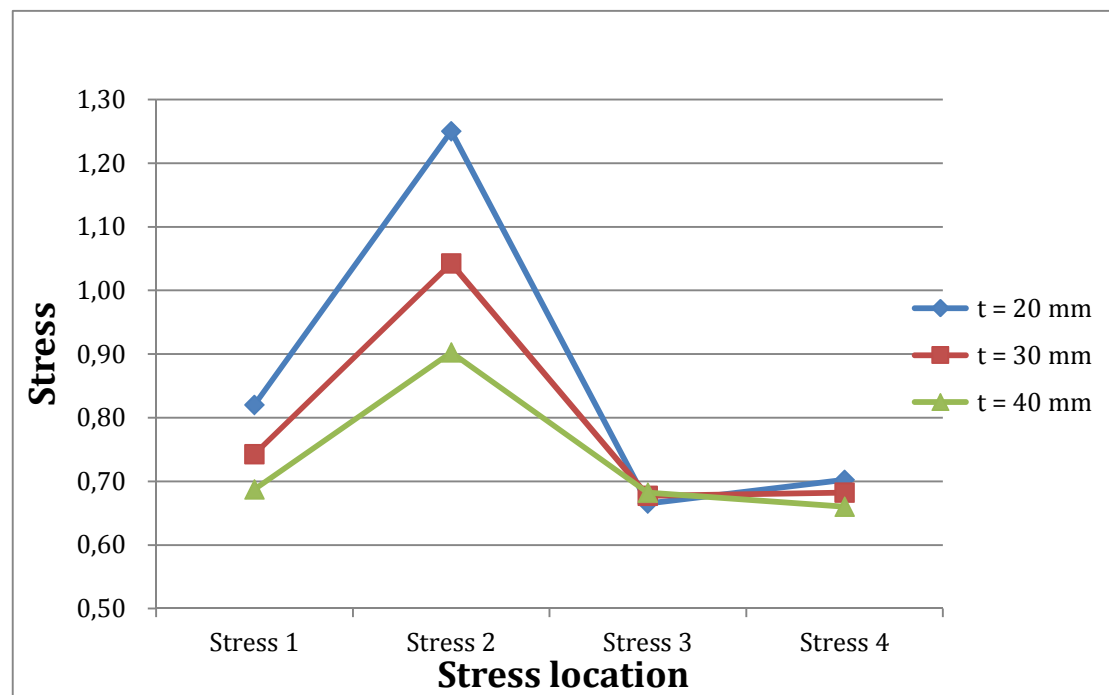


Figure B.5 Cut-out radius 5370 mm with four stress locations and stresses dependent on plate thickness for a constant tapering plate hole radius of 200 mm plotted against normalized von Mises stress.

The same evaluation is also shown in Figure B.6 for the tapering plate hole radius of 300 mm. However, the stress level at location 2 is slightly lower in this case, but, instead, the stress level at location 3 is increased. A bigger hole radius in the tapering plate distributes the stresses to the edge of the tapering plate, which c stress at location 3 shows.

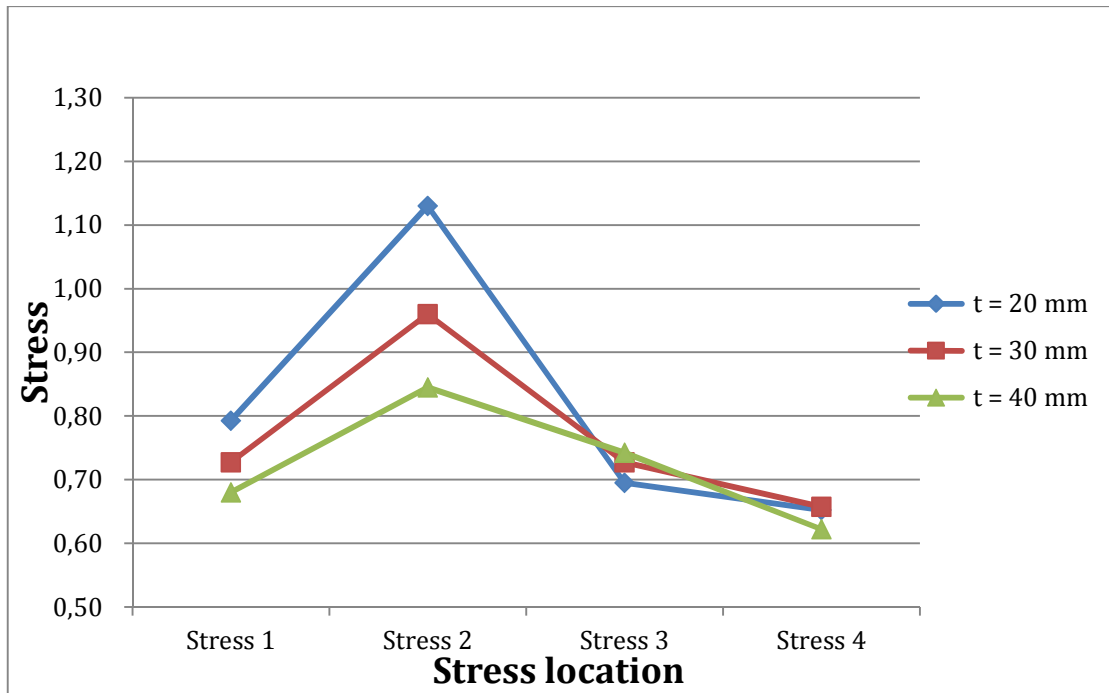


Figure B.6 Cut-out radius 5370 mm with four stress locations and stresses dependent on plate thickness for a constant tapering plate hole radius of 300 mm plotted against normalized von Mises stress.

In Figure B.7 the tapering plate hole radius is increased to 400 mm and the same trend occurred again. The stress level at location 2 decreases with an increasing hole radius but increases the stress level at location 3. Stress location 3 might also be a bad region to increase the stress too much due to the weld at the plate edge.

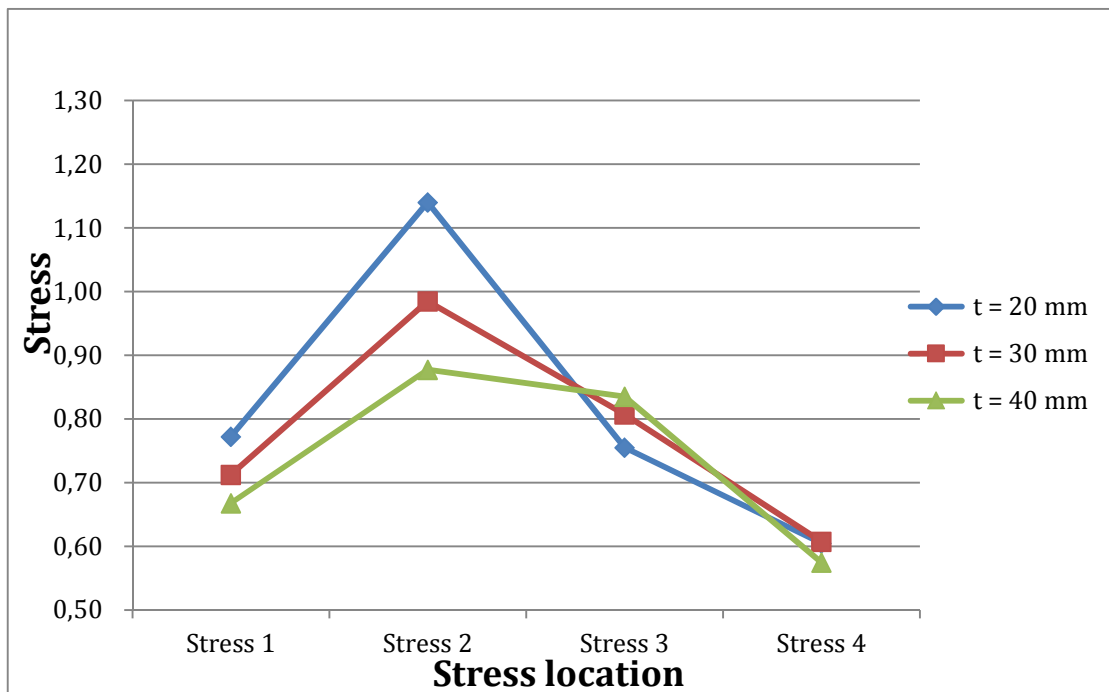


Figure B.7 Cut-out radius 5370 mm with four stress locations and stresses dependent on plate thickness for a constant tapering plate hole radius of 400 mm plotted against normalized von Mises stress.

The four stress regions are combined to calculate a combined average stress value of the maximum von Mises stress from each stress location, used for evaluation of the different designs. All five different cut-out radii were analysed with the three different tapering plate hole radii and with the three different plate thicknesses. The figures for the different cut-out radii are:

- Figure B.8 for cut-out radius = 2190 mm
- Figure B.9 for cut-out radius = 2900 mm
- Figure B.10 for cut-out radius = 4080 mm
- Figure B.11 for cut-out radius = 5370 mm
- Figure B.12 for cut-out radius = 12500 mm

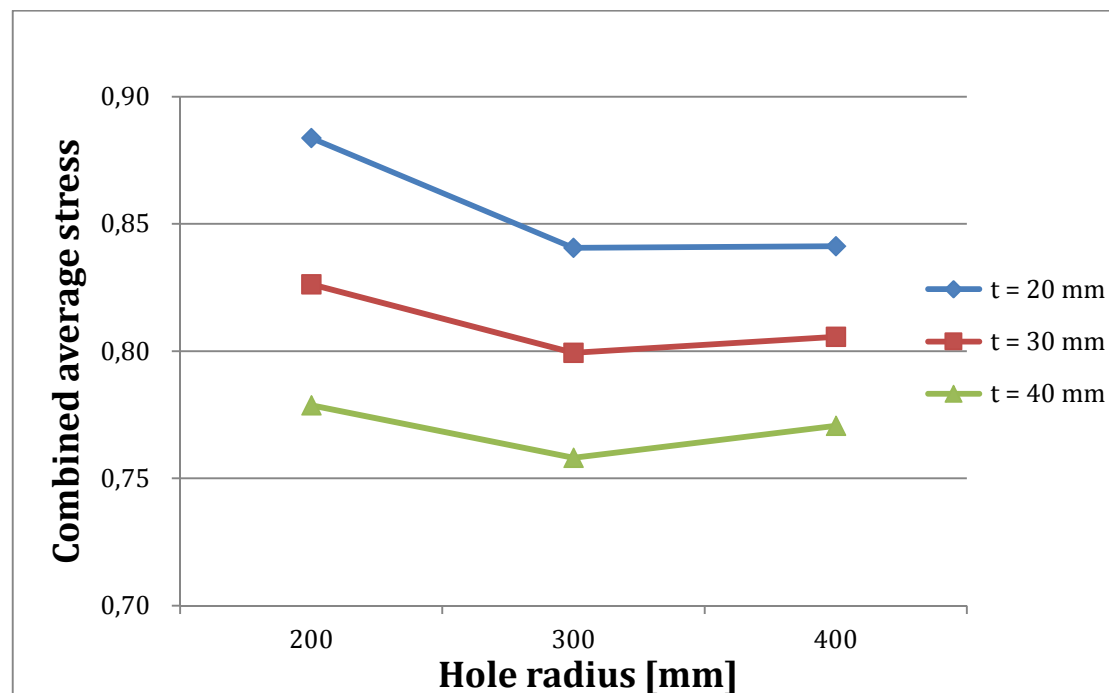


Figure B.8 Cut-out radius of 2190 mm and a varying tapering plate hole radius and plate thickness. Combined average von Mises stress of the four identified stress locations.

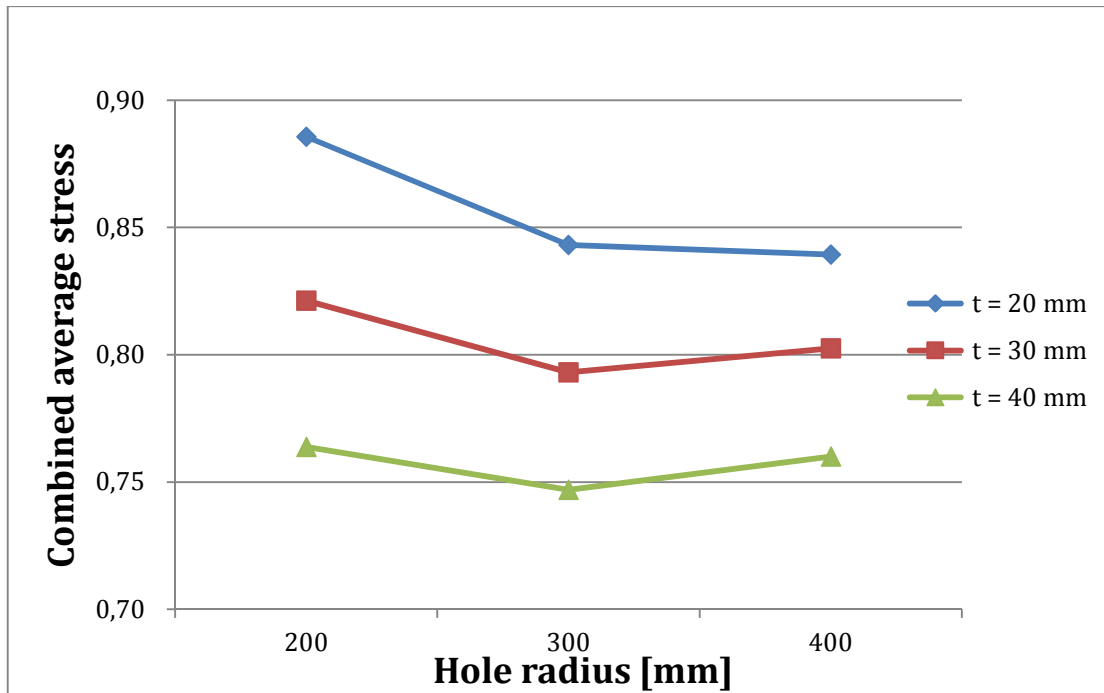


Figure B.9 Cut-out radius of 2900 mm and a varying tapering plate hole radius and plate thickness. Combined average von Mises stress of the four identified stress locations.

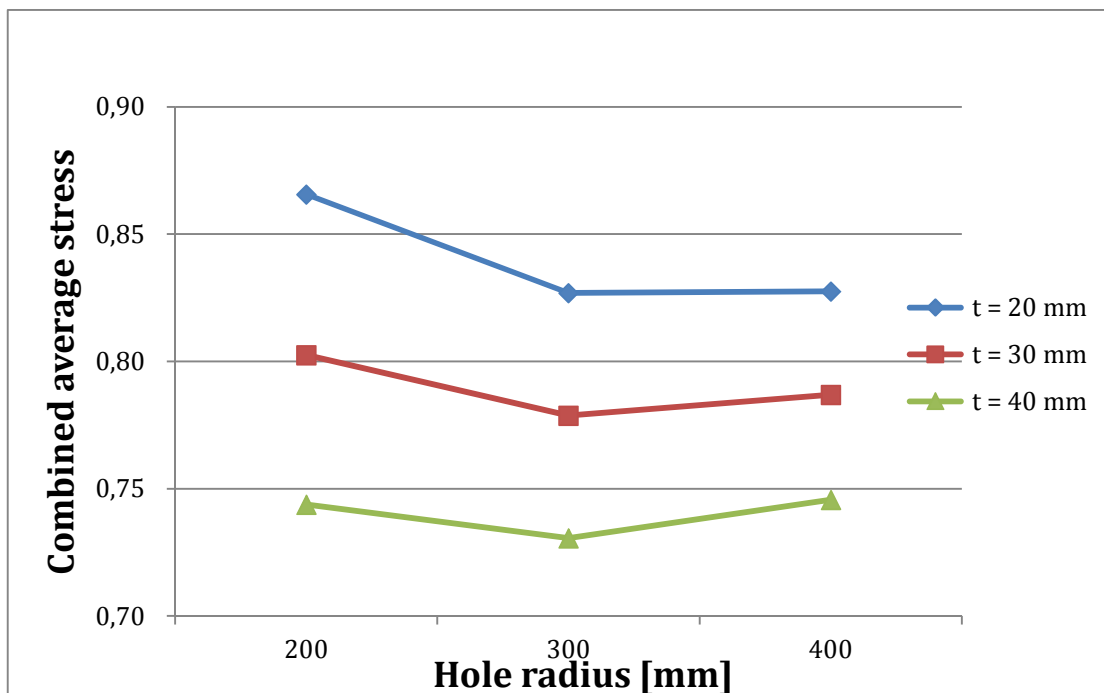


Figure B.10 Cut-out radius of 4080 mm and a varying tapering plate hole radius and plate thickness. Combined average von Mises stress of the four identified stress locations.

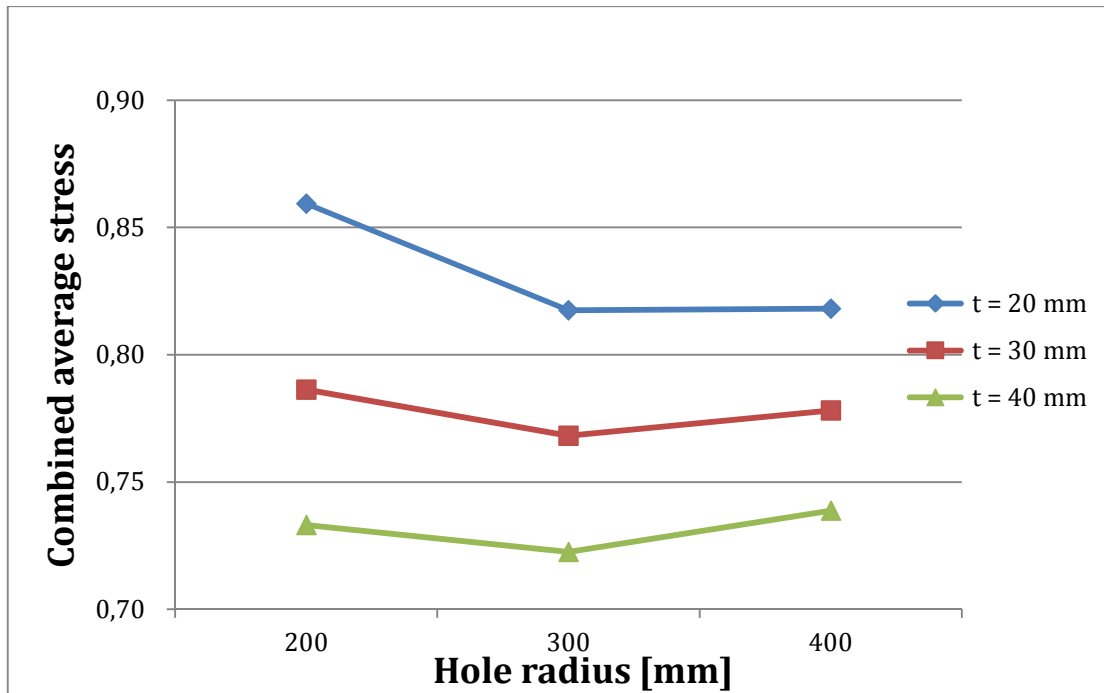


Figure B.11 Cut-out radius of 5370 mm and a varying tapering plate hole radius and plate thickness. Combined average von Mises stress of the four identified stress locations.

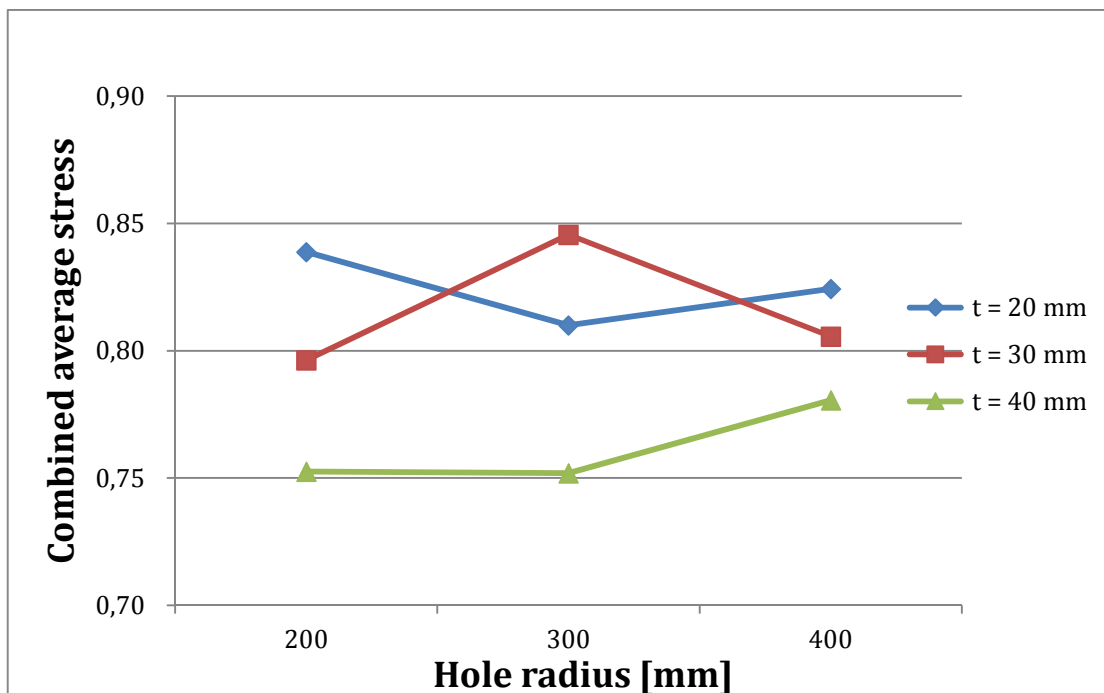


Figure B.12 Cut-out radius of 12500 mm and a varying tapering plate hole radius and plate thickness. Combined average von Mises stress of the four identified stress locations.

From this analysis it is easy to see that the best solution according to an average stress, is the cut-out design with a radius of 5370 mm, a tapering plate hole radius of 300 mm and plate thickness of 40 mm, which has the nominal stress of 0.73. This design is also the lightest of the different designs with the same hole radius and plate thickness, see

Figure B.13. This is the final cut-out design chosen in this thesis. This decision is based on the cut-out evaluation performed and the fact that this design has the lowest combined average stress, see Figure B.11. This cut-out design also has the lowest maximum von Mises stress at the governing stress location 2, see Figure B.6. With these results this cut-out design is chosen as the final design.

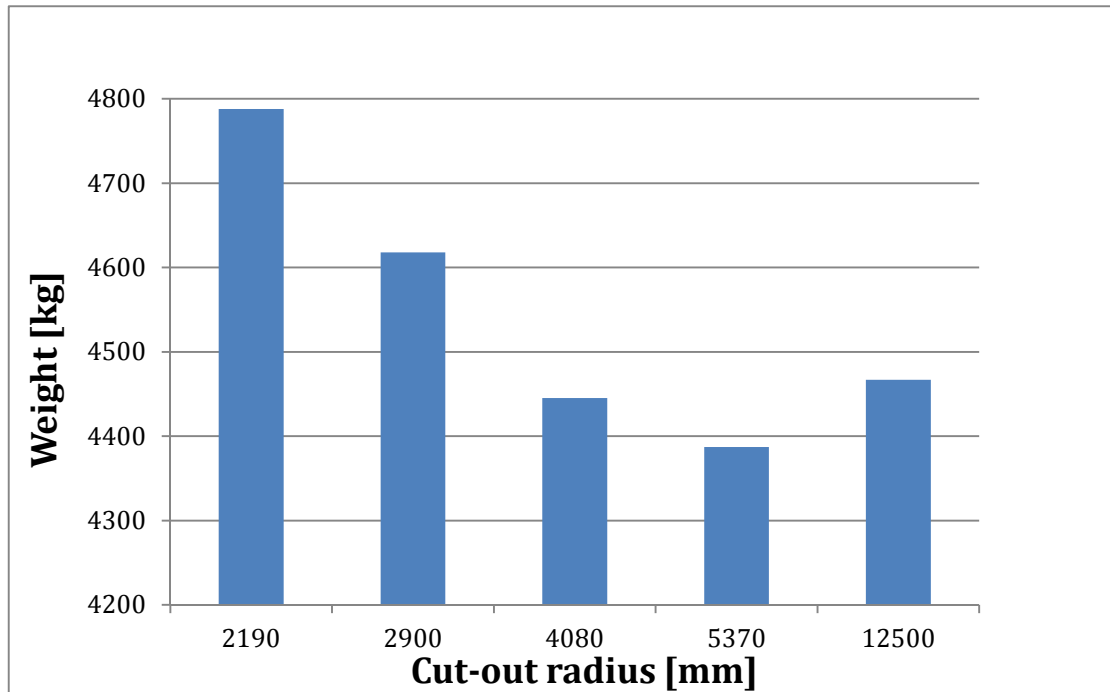


Figure B.13 Weight of the different cut-out designs with a tapering plate hole radius of 300 mm and plate thickness of 40 mm.